DURBAN UNIVERSITY of TECHNOLOGY

DEPARTMENT OF CHEMICAL ENGINEERING

SEPARATION PROCESSES FOR HIGH PURITY ETHANOL PRODUCTION

P. T. NGEMA

SEPARATION PROCESSES FOR HIGH PURITY ETHANOL PRODUCTION

By

Peterson Thokozani Ngema

(March 2010)

Research project submitted in fulfillment of the academic requirements for the Master's Degree in Technology: Chemical Engineering at Durban University of Technology (DUT).

DECLARATION

I, Peterson Thokozani Ngema, hereby declare that this project has been completed entirely by myself and this work has not submitted in whole or in part for a degree at another University

_____	DUT	11/03/10
P.T Ngema	**PLACE**	**DATE**

APPROVAL BY SUPERVISORS (DUT)

Name	**Mr Suresh Ramsuroop**	**Prof V. L Pillay**
Signature	_____	_____
Contact	**031 373 2362**	**031 373 2646**

APPROVAL BY CO-SUPERVISOR (UKZN)

Name	**Prof Deresh Ramjugernath**
Signature	_____
Contact	**031 260 3128**

ABSTRACT

Globally there is renewed interest in the production of alternate fuels in the form of bioethanol and biodiesel. This is mainly due to the realization that crude oil stocks are limited hence the swing towards more renewable sources of energy. Bioethanol and biodiesel have received increasing attention as excellent alternative fuels and have virtually limitless potential for growth. One of the key processing challenges in the manufacturing of biofuels is the production of high purity products. As bioethanol is the part of biofuels, the main challenge facing bioethanol production is the separation of high purity ethanol. The separation of ethanol from water is difficult because of the existence of an azeotrope in the mixture. However, the separation of the ethanol/water azeotropic system could be achieved by the addition of a suitable solvent, which influences the activity coefficient, relative volatility, flux and the separation factor or by physical separation based on molecular size. In this study, two methods of high purity ethanol separation are investigated: extractive distillation and pervaporation.

The objective of this project was to optimize and compare the performance of pervaporation and extraction distillation in order to produce high purity ethanol. The scopes of the investigation include:

- Study of effect of various parameters (i) operating pressure, (ii) operating temperature, and (iii) feed composition on the separation of ethanol-water system using pervaporation.
- Study the effect of using salt as a separating agent and the operating pressure in the extractive distillation process.

The pervaporation unit using a composite flat sheet membrane (hydrophilic membrane) produced a high purity ethanol, and also achieved an increase in water flux with increasing pressure and feed temperature. The pervaporation unit facilitated separation beyond the ethanol – water system azeotropic point. It is concluded that varying the feed temperature and the operating pressure, the performance of the pervaporation membrane can be optimised**.**

The extractive distillation study using salt as an extractive agent was performed using the low pressure vapour-liquid equilibrium (LPVLE) still, which was developed by (Raal and Mühlbauer, 1998) and later modified by (Joseph *et al.* 2001). The VLE study indicated an increase in relative volatility with increase in salt concentration and increase in pressure operating pressure. Salt concentration at 0.2 g/ml and 0.3 g/ml showed complete elimination of the azeotrope in ethanol-water system. The experimental VLE data were regressed using the combined method and Gibbs excess energy models, particular Wilson and NRTL. Both models have shown the best fit for the ethanol/water system with average absolute deviation (AAD) below 0.005.

The VLE data were subjected to consistency test and according to the Point test, were of high consistency with average absolute deviations between experimental and calculated vapour composition below 0.005.

Both extractive distillation using salt as an extractive agent and pervaporation are potential technologies that could be utilized for the production of high purity ethanol in boiethanol-production.

PREFACE

This project was carried out at the Durban University of Technology (DUT), Department of Chemical Engineering. The vapour liquid equilibrium (VLE) experiments were conducted at University of KwaZulu-Natal in the Chemical Engineering Thermodynamics Laboratory and pervaporation experiments were conducted at Durban University of Technology in Chemical Engineering Thermodynamics Laboratory. This project was supervised by Mr Suresh Ramsuroop and Professor V. L Pillay (DUT Supervisors) and Professor Deresh Ramjugernath (University of KwaZulu-Natal). The project was completed over a period of 24 months from January 2008 to December 2009.

ACKNOWLEDGEMENTS

I would like to acknowledge the following people for their support to this project:

- Project supervisors Mr Suresh Ramsuroop and Professor V. L Pillay at Durban University of Technology (DUT), Chemical Engineering Department
- Project co-supervisor Professor Deresh Ramjugernath at University of KwaZulu-Natal in the School Chemical Engineering.
- My family for their support and their passion for me to complete this project
- The supporters Zamandaba Ndaba, Manti Radiongoana, Nomaweza Mkhize and Londeka Nzimande
- The Laboratory Assistance Ayanda Khanyile and Linda Mkhize (University of KwaZulu-Natal in the Chemical Engineering Department)
- My friends Siyabonga Buthelezi and Patros Malusi Zwane
- My colleagues, Kumnandi Phikwa, Thulani Dlamini, Zwelidinga Regnald Fuzani and Mohammed Jaffar Bux (Masters students)
- The workshop Patrick Mncwabe (Durban University of Technology)
- The Master's student in the School of Chemistry who contributed to my project

TABLE OF CONTENT

LIST OF TABLES

LIST OF FIGURES

LIST OF PHOTOGRAPHS

ABBREVIATIONS

ACN	Acetonitrile
AD	Azeotropic Distillation
ASOG	Analytical Solution Of Group
DMF	Dimethethylformanide
ED	Extractive Distillation
EOS	Equation Of State
FID	Flame Ionization Detector
GC	Gas Chromatograph
G^E	Excess molar Gibbs free energy
HP	Hewlett Packard
LPVLE	Low Pressure Vapour Liquid Equilibrium
NFM	N-Formylmorpholine
NMP	N-Methylpyrrolidone
NRTL	Non-Random Two Liquids
TCD	Thermal Conductivity Detector
THF	Tetrahydrofuran
T-K Wilson	Tsuboka-Katayama Wilson activity coefficient model
UNIQUAC	UNIversal QUAsi-Chemical
UNIFAC	Universal quasi-chemical Functionally Group of Activity Coefficient
VLE	Vapour Liquid Equilibrium

NOMENCLATURE

A	Adjustable parameter in correlating equations, GC peak area, cubic EOS constant	-
B	Second viral coefficient	-
f	Fugacity	-
F	Difference between the number of variables	-
G	Gibbs energy	kJ/kg
G	Gibbs energy	kJ/kg
H	Enthalpy	kJ/kg
K	Distribution coefficient for component *i*	-
l	Membrane thickness	m
N	Number of component	-
P	Pressure	kPa
q	Parameter of the pure component molecular structure constants	-
r	Parameter of the pure component molecular structure constants	-
R	Universal gas constant	kJ/kg.K
T	Temperature	K
v	Specific volume	m^3/kg
V	Molar volume	m^3
x	Mole fraction of component *i* in liquid phase	-
y	Mole fraction of component *i* in vapour phase	-
Z	Compressibility	-

Greek symbols

α	Vapour pressure correlation for cubic EOS, parameter mixing rules, adjustable parameter in correlating equations
β	Constant or function in the T-K Wilson equations
γ	Activity coefficient
μ	Chemical potential
ϕ	Fugacity coefficient
Φ	Nonideality term in the LPVLE gamma-phi method, constant or function in the UNIQUAC equation, polarity factor in the Tarakad-Danner method
λ	Adjustable interaction parameter in the Wilson and T-K Wilson equations
κ	Parameter in the cubic EOS $\alpha(T_R, \omega)$ correlation
Λ	Constant or function in the Wilson and T-K Wilson equations
θ	Constant or function in the UNIQUAC and UNIFAC equations
ρ	Density
τ	Constant or function in the UNIQUAC and NRTL equations
π	Chemical species distributed at equilibrium
ω	Acentric factor
ψ	UNIFAC group interaction parameter
∞	Infinite dilution

Superscripts

calc	Calculated quantity
E	Excess quantity
G	Gas permeability
L	Liquid phase
sat	Saturation state pure component quantity

V	Vapour phase

Subscripts

c	Critical
i	Component identity
j	Component identity
l	Liquid through the membrane

CHAPTER 1

INTRODUCTION

Fuel grade bioethanol production has gained attention recently because of two main reasons. First, it is gradually/frequently being used as a fuel oxygenate in place of methyl t-butyl ether (MTBE). The second reason relates to its potential to be used as an alternate fuel. Bioethanol fuel is mainly produced by the sugar fermentation process; although it can also be manufactured by the chemical process or as a byproduct of some chemical processes (Vane, 2005a). The main sources of ethanol are sugar and crops. Crops are grown specifically for energy use and include corn, maize and wheat crops, waste straw, willow and popular tress, sawdust, reed canary grass, cord grasses, jerusalem artichoke, myscanthus and sorghum plants (O'Brien and Craig, 1996). There is also ongoing research into the use of municipal solid waste to produce ethanol fuel.

Ethanol or ethyl alcohol (C_2H_5OH) is a clear colourless liquid, which is biodegradable, low in toxicity and causes little environmental pollution if spilt (O'Brien and Craig, 1996). Ethanol burns to produce carbon dioxide and water. It reduces pollution associated

with petroleum products such as SO_x and NO_x. Ethanol is a high octane fuel and has replaced lead as an octane enhancer in petrol (Vane 2005a).

Bioethanol and biodiesel are the alternative fuels that can be used. The production of alternative fuel is due to the realization that crude oil stocks are limited, hence the swing towards more renewable sources of energy. Bioethanol and biodiesel have received increasing attention as excellent alternative fuels and have virtually limitless potential for growth. However, the main challenge facing bioethanol production is the separation of high purity bioethanol, because bioethanol contains water. The separation of ethanol from water is difficult because of the existence of an azeotrope in the mixture. The two traditional methods of high purity ethanol separation are:

- Extractive distillation
- Azeotropic distillation

Other three emerging techniques are:

- Salt distillation
- Pressure swing distillation
- Pervaporation

The purpose of this study is to explore the application of emerging technologies for the extractive distillation and pervaporation for high purity ethanol production manipulating the operation pressure and temperature to influence azeotropic point. In extractive distillation, salt is added as the third component and pervaporation is the direct separation, without salt addition.

The objective of this project was to optimize and compare the performance of pervaporation and extraction distillation in order to produce high purity ethanol:

- Study the effect of various parameters (i) operating pressure, (ii) operating temperature, and feed composition on pervaporation.
- Study the effect of salt as a separating agent and operating pressure in extractive distillation.

The research was undertaken in the Department of Chemical Engineering at the Durban University of Technology. The application of ($CaCl_2$) salt in the extractive distillation was investigated using the dynamic low pressure vapour-liquid equilibrium (VLE) still, which was designed by Raal (Raal and Mühlbauer, 1998). The application of pervaporation was investigated using a test unit built specifically for this study. In this study, high purity ethanol was diluted with distil water and used to represent the properties of bioethanol.

1.1 Extractive distillation

Extractive distillation is commonly applied in industry, and is becoming an important separation method in chemical engineering. In this study, extractive distillation was considered as a separation technique for ethanol-water system using a dissolved salt as a separating agent. The salt used was calcium chloride which has a high boiling point. Extractive distillation is the distillation in the presence of a component/solvent which is not volatile when compared to the separated components. The solvent is charged continuously near the top of the distilling column so that the concentration is maintained on all plates of the column (Hilmen, 2000). The main characteristic of extractive distillation is that the solvent with a high boiling point is charged to the components to be separated so as to increase the relative volatility of one component. The experimental vapour-liquid equilibrium (VLE) data obtained using the salt as a separating agent plays an important role in the design of extractive distillation columns.

Separation sequence of the columns combination with other separation processes, tray configuration and operation policy are described in full by Hilal *et al*., (2002). Since the solvent plays an important role in design of extractive distillation, such conventional and novel separating agents as solid salt, liquid solvent, the combination of liquid and solid salt, and ionic liquids are covered in this chapter. Selection of a suitable solvent/salt is fundamental to ensure an effective and economical design (Zhigang *et al*., 2005).

Ethanol forms minimum-boiling azeotropes with water at about 90 mol% ethanol. Extractive distillation is a technique used for the separation of minimum boiling binary

azeotropes by the use of a solvent/salt that has the heaviest species in the mixture and does not form any azeotropes with the original components. The solvent should be completely miscible with the original components.

A small concentration of salt is capable of increasing the relative volatility of the more volatile component of the solvent mixture to be distilled (Mario and Jamie, 2003). This is known as the salt effect which is due to preferential solvation of the ions (formed when the salt dissociates in solution) by the less volatile component of the solvent mixture (Mario and Jamie, 2003). Ethanol is a more volatile component. Ethanol is "salted out" from the liquid phase to the vapour phase.

Salt effects on vapour-liquid equilibria are important in extractive distillation (Lei *et al.*, 2002 and 2003) when the salt is used as a separating agent. However, the complex molecule-molecule, ion-molecule and ion-ion interactions in salt-water-alcohol systems pose a significant challenge to the development of a theoretical description of the system (Mario and Jamie, 2003). The effect of different salts on the relative volatility of ethanol and water was investigated (Duan *et al*., 1980 and Zhigang *et al*., 2005). It was found that some salts produce the large salt effect on the system and the results are tabulated in Table 2.2 Zhigang *et al*. (2005) arranged the order of salt effect: $AlCl_3 > CaCl_2 > NaCl_2$, $Al(NO_3)_3 > Cu(NO_3)_2 > KNO_3$. In this study, the choice of calcium chloride was reported by previous work such as that cited above, which indicates that calcium chloride provides the largest salting out effect on ethanol. In addition, it is also a cheap and common salt. In this study, calcium chloride is the salt chosen for further investigation because it has the large salting out effect, it is a common salt and it is cheap.

It was found that calcium chloride could completely eliminate the azeotrope at the high concentrations and increase the relative volatility. The system of ethanol/water/calcium chloride was generally regressed using Gibbs excess energy models in particular Wilson and NRTL. The benefits of the Wilson and NRTL parameters and consistent VLE data are indispensable to the process industry. In light of the current environmental regulations and given that energy efficiency and optimisation are the focus of the process industry, experimental VLE data and ongoing research in the analysis of the data are critical to both the improvement of current processes and the efficient design of future processes.

1.2 Pervaporation membrane

Pervaporation is a membrane separation process for liquid mixtures in which the initial solution comes in contact with the internal surface of a membrane module, permeate in the form of vapours with a low partial pressure was removed from its outer surface (Belyaev *et al.,* 2003). Pervaporation membrane separation can be considered as one effective method and energy-saving process for the separation of the ethanol/water azeotropic system (Huang *et al.,* 2008; Huang, 1991; Shao and Huang, 2006 and Wang *et al.,* 2007). Pervaporation through hydrophobic membranes is potentially economically competitive with distillation, especially for small to medium scale application (Vane, 2005a). In general, separation by pervaporation can be perfomed using membranes based on the solution-diffusion mechanism of transport. The mass transport through the permselective membranes involves three steps: (i) sorption of the penetrant from the feed to the membrane, (ii) diffusion of the penetrant in the membrane, and (iii) desorption of the penetrant from the membranes on the downstream side of the membrane (Xu *et al*., 2006). The pervaporation membrane has the added advantage in that it facilitates the direct separation of the azeotrope without the addition of the third component. Hence it reduces the capital and operating cost that may be associated with solvent recovery.

Pervaporation theory has advanced greatly since its introduction in the early 1950's, however it was only in recent years that research in this field have intensified. There has been a noticeable increase in the number of publications concerning membrane separation yet the technology is still far from perfect (Yampolskii and Volkov, 1991; Neel, 1991; Binning *et al.,* 1961 and Mulder *et al.,* 1985) are all prominent names in pervaporation and have written many papers of great significance. Pervaporation's potential versatility ensures its place in separation technology. It is only due to a lack of familiarity and poor knowledge of the weakness of pervaporation that inhibits its growth industrially. This should not be a problem in the future as new and improved membranes are constantly being produced, offering better selectivity and better resistance (chemically and thermally). Most of the liquid mixtures could be separated using pervaporation, yet research has concentrated on the separation of azeotropic and close

boiling mixtures due to difficulty in separating these mixture via conventional means (Driolli *et al.,* 1993).

By definition, the separation factor is equal to the ratio of the concentration of the permeant in the permeate to the concentration of the permeant in the feed, where the permeant is the component that is preferentially transported through the membrane. The separation of the ethanol/water system obtained by the researchers on the pervaporation is comparable to that obtainable in distillation systems though the transport rate of one $kg.m^{-2}.h^{-1}$ is far too low for industrial throughputs.

In this study, the recovery of pure ethanol from a feed stream of 90 – 99% wt% ethanol was studied. The pervaporation operating pressure and operating temperature were varied from 20 kPa to 80 kPa and 313.15 K to 343.15 K respectively.

1.3 Dissertation outline

Chapter 1

The introduction outlines the purpose of this study. It provides the background information on the utility of the extraction distillation using calcium chloride salt as a separating agent and the pervaporation process in order to recover high purity ethanol.

Chapter 2

This chapter reviews literature which deals with the application of emerging technologies of extractive distillation and pervaporation process for high purity ethanol production. Some concepts to understand and formation of destruction of azoetropes are also presented.

Chapter 3

Chapter 3 represents information about the thermodynamic fundamentals of the extractive distillation and pervaporation process. Data reduction schemes to predict the effect of salt on the behavior of the ethanol-water system are also presented.

Chapter 4

This chapter is devoted to the experimental and analysis procedures and methods used for the evaluation of salts as an extractive agent and the pervaporation studies. The analytical techniques used for both these studies are also presented in this chapter.

Chapter 5

This chapter contains the results and discussion obtained from:

- The study of the effect of salt in the separation of ethanol-water mixture.
- The pervaporation studies of ethanol and water mixture.
- The data reduction methods used in the vapour-liquid equilibrium studies.

Chapter 6

In chapter 6, conclusions and recommendations related to the effect of salt in the extractive distillation process, and direct separation of ethanol-water system using pervaporation to achieve high purity ethanol production are made.

CHAPTER 2

LITERATURE REVIEW

2.1 Introduction

To understand the separation difficulties associated with the ethanol-water system, it is necessary to outline the phenomenon that contributes to non-ideal VLE behavior, and how the non-ideal VLE behavior may be overcome. In this chapter a review is presented on:

- Azeotropy and its formation in the ethanol-water system.
- Brief overviews of methods to employ overcome the azeotropic behavior.
- Review of the use of salt as an extraction agent in extractive distillation and the use of pervaporation technology for high purity ethanol separation.

2.2 Description of azeotropic mixtures

The term azeotrope means “nonboiling by any means/way” (Greek: a – non, zeo – boil, tropos – means/way), and denotes a mixture of two components that at equilibrium, the vapour and liquid composition are equal at a given pressure and temperature. Azeotropic mixtures require special methods to facilitate their separation. There was a need to search for a separating agent other than different method that consumes a lot of energy. The separating agent might be a membrane material for pervaporation and either solvent or addition of salt in the extractive distillation. An introduction to the phenomena of azeotropy and non-ideal vapour-liquid equilibrium behavior will be given before considering the various methods to separate azeotropic mixtures. Separation of homogenous liquid mixtures (bioethanol and water) requires the creation or addition of another phase within the system (Smith, 1995). Separation of a liquid mixture by distillation is dependent on the partial vaporization of the liquid into a liquid and vapour samples in which their composition may differ. The vapour phase becomes enriched in the more volatile component. It was depleted in the less volatile components with respect to its equilibrium, liquid phase. An azeotrope could not be separated by ordinary distillation since no further enrichment of the vapour phase occurs. In most cases, azeotropic mixtures require special methods to facilitate their separation such method utilizes a mass separating agent other than energy that causes or enhances a selective mass transfer of the azeotropic forming component.

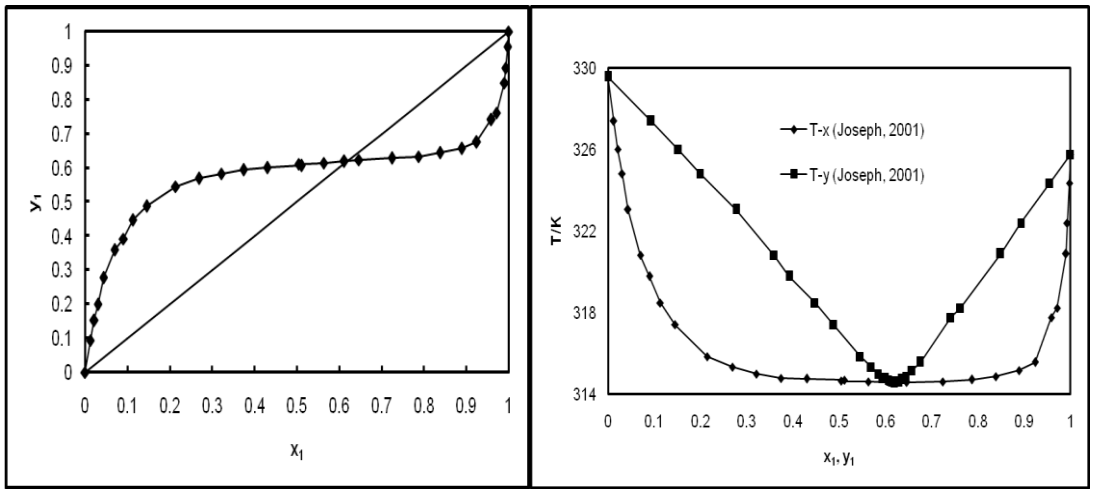

(a) (b)

Figure 2.1 Example of an azeotropic diagram for the ethanol (1)/cyclohexane (2) system at 40 kPa (a) x-y diagram and (b) T-x-y diagram (Joseph, 2001).

2.3 Formation of ethanol/water azeotrope

Ethanol and water produces a highly distorted curve with a maximum vapour pressure for a mixture containing 95.6% of ethanol by mass. At higher vapour pressure in ideal mixtures, the intermolecular forces between molecules break easily because they are fewer forces in the vapour phase than in the pure liquids. The ethanol and water system has a large positive deviation from Raoult's Law to produces a composition curve as shown in Figure 2.2. If the mixture has a high vapour pressure it means that it will have a low boiling point. The molecules are escaping easily and there is no need to heat the mixture too much to overcome the intermolecular attractions.

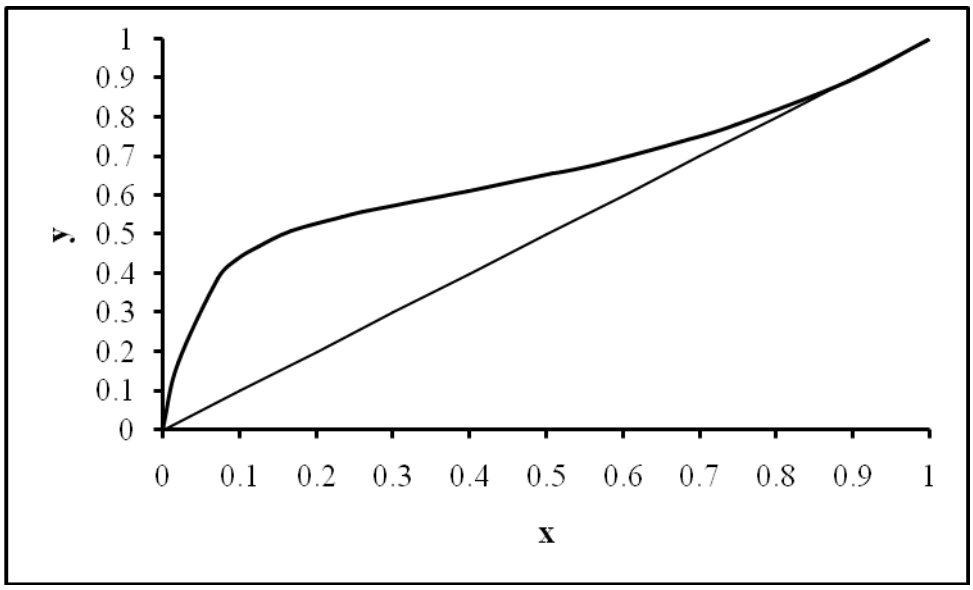

Figure 2.2: Ethanol (1)-water (2) composition curve (Ohe, 1991).

Figures 2.3 – 2.5 indicate the boiling point composition curve for the ethanol-water mixture. From the boiling point composition diagram it could be seen that a minimum value lower than the boiling points of either pure ethanol or pure water exists. The minimum azoetrope occurs at 95.6% by mass of ethanol in the mixture.

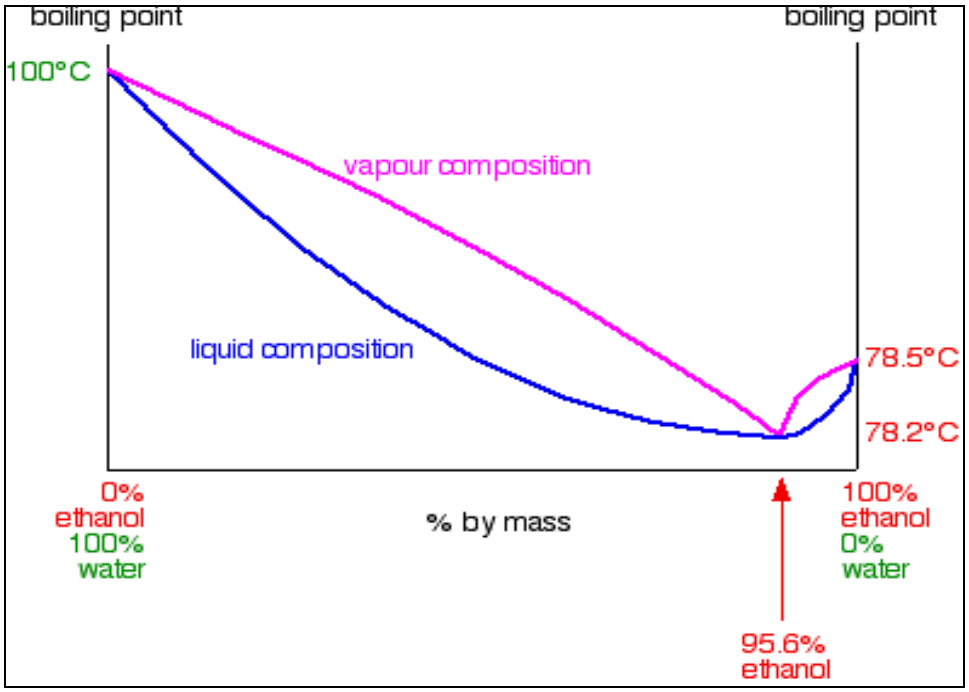

Figure 2.3: VLE plot for ethanol (1)/water (2) system showing composition curve for ethanol (1) and water (2) (Ohe, 1991).

By distilling a mixture of ethanol and water with composition C_1 as shown in Figure 2.4, it boils at certain temperature by the liquid curve and produces vapour with composition C_2.

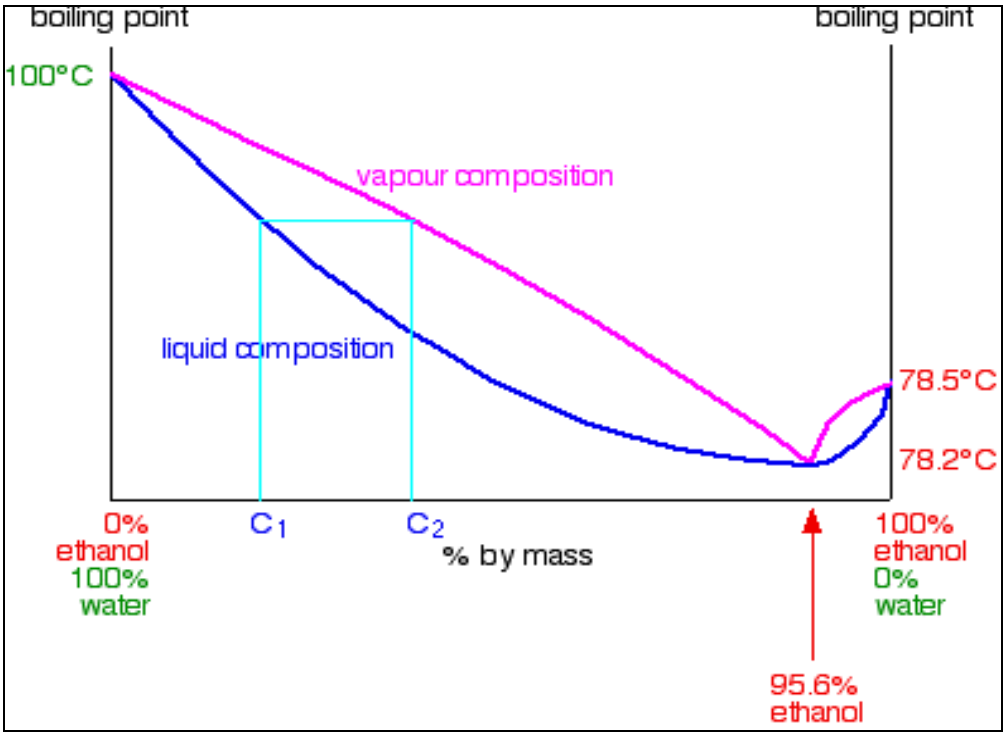

Figure 2.4: VLE plot for the ethanol (1)/water (2) system showing liquid composition C_1 produces and vapour composition C_2 (Ohe, 1991).

As the vapours are condensed, the composition of the vapour in the VLE still is C_2. By changing the composition C_2 in reboiler and recirculating in the VLE still, the composition are changing between C_2 and C_3 until the equilibrium is reached then a new vapour C_3 is formed as shown in Figure 2.5.

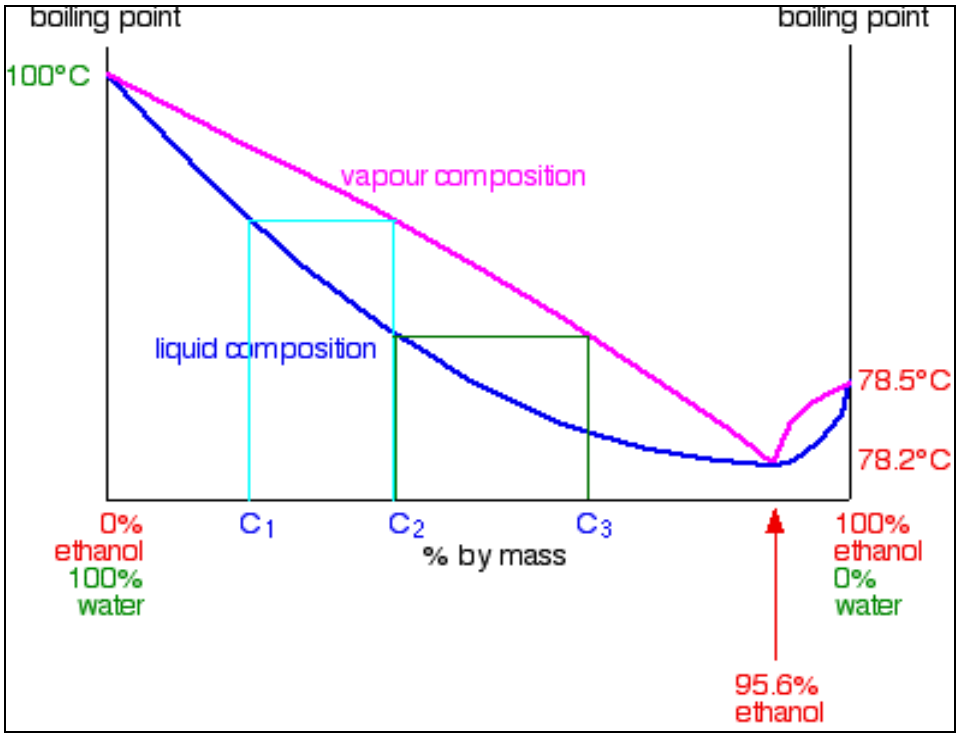

Figure 2.5: VLE plot for the ethanol (1)/water (2) system showing liquid composition C_2 produces and vapour composition C_3 (Ohe, 1991).

The sequence of boiling-condensing-reboiling the ethanol/water mixture continues until a vapour composition reaches 95.6% ethanol and the condensed vapours form the liquid composition with 95.6% ethanol (Ohe, 1991). The liquid curve and the vapour curve meet at that point. The vapour produced will have the same composition of 95.6% ethanol. If it condenses again, it will still have the same composition. At this point ethanol and water boils at a constant boiling point. This point is known as **azeotrope or azeotropic mixture (**Ohe, 1991). At this point, it is difficult to separate the mixture of ethanol and water. Minimum azeotrope is described later in this chapter. Usually azeotropes are formed by non-ideal mixtures.

2.4 Hydrogen bonding in ethanol and water

Hydrogen bonding is a term given to extremely strong polar molecular interactions (i.e ethanol and water). Any molecule which has a hydrogen atom attached directly to an

oxygen or nitrogen is capable of hydrogen bonding. These molecules have higher boiling points when compared to similar size of molecules which not have an –O-H or an –N-H group. The hydrogen bonding makes the molecules "stickier" and more heat is necessary to separate them (Ophardt, 2003). Solutions that exhibit hydrogen bonding generally exhibit azeotropic behavior. In this study of the ethanol/water mixture, ethanol has a hydrogen atom attached directly to oxygen and this oxygen still has exactly the same two lone pairs as in a water molecule. Hydrogen bonding can occur between ethanol molecules although not as effectively as in water (Ophardt, 2003). Mixing involves breaking hydrogen bonds between water molecules. Breaking hydrogen bonds between ethanol molecules makes a strong stickier hydrogen bond between water and ethanol molecules. This increases with increasing ethanol concentration hence the mixture becomes difficult to separate beyond a certain concentration (i.e at 90 mol% ethanol and 10 mol% water at which an azeotrope is formed).

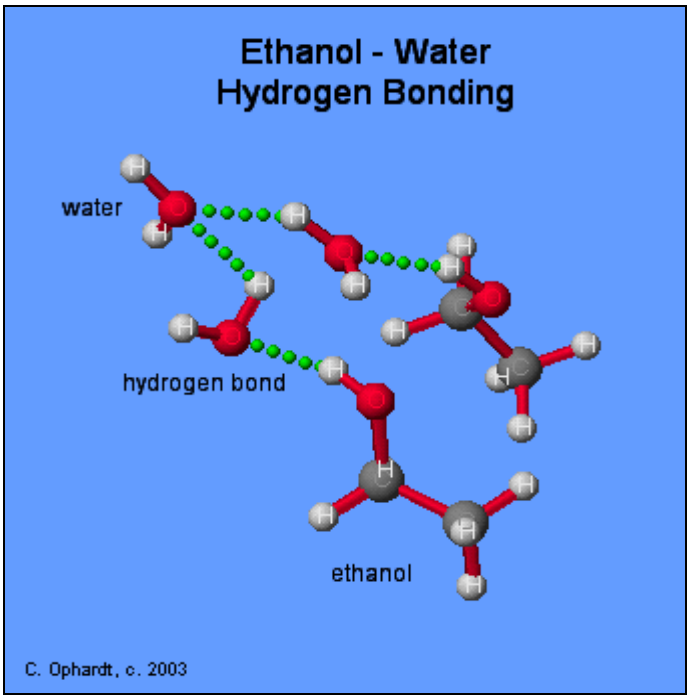

Figure 2.6: Ethanol-water hydrogen bonding (Ophardt, 2003).

2.5 Different types of distillation processes

The separation of azeotropic systems can be achieved by the addition of a suitable solvent, which influences the activity coefficient and relative volatility. Six methods for separating azeotropic mixtures as described by Stichimar *et al*. (1989) follow:

- Extractive distillation – a high boiling solvent is added near the top of the column to favourably alter the relative volatility in order to separate the components. A second column separates the bottom in order to recycle the solvent.
- Homogeneous azeotropic distillation – the liquid separating agent is completely miscible.
- Heterogeneous azeotropic distillation, more commonly, Azeotropic Distillation – where the liquid separating agent, called the entrainer or solvent, forms one or more azeotropes with the other components in the mixture and causes two liquid phases to exit over a wide range of compositions. This immiscibility is the key to making the distillation sequence work.
- Distillation using salts – the salts dissociates in the liquid mixture and alters the relative volatilities sufficiently that the separation becomes possible.
- Pressure swing distillation – a series of columns operating at different pressures are used to separate binary azeotropes which change appreciably in composition over a moderate pressure range or where a separating agent which forms a pressure-sensitive azeotrope is added to separate a pressure-insensitive azeotrope.
- Reactive distillation – the separating agent reacts preferentially and reversibly with one of the azeotropic constituents. The reaction product is then distilled from the non-reacting components and the reaction is reversed to recover the initial component.

Since the project focuses on two separation techniques namely extractive distillation with salt and pervaporation, both technologies are reviewed.

2.6 Process of extractive distillation

For the separation of a two component system in an extractive distillation process, two columns are generally used, i.e. an extractive column and a solvent recovery column. This two column process is shown in Figure 2.7, with this column arrangement, the two components A and B in the binary feed can be separated in the column. The product is obtained as high purity distillates stream from each column and the solvent S is finally recovered as bottoms product from the second column (Chen *et al.*, 2003). The solvent is not necessary vapourized in the extractive distillation process. The high boiling selective solvent is introduced not far from top of the extractive distillation column.

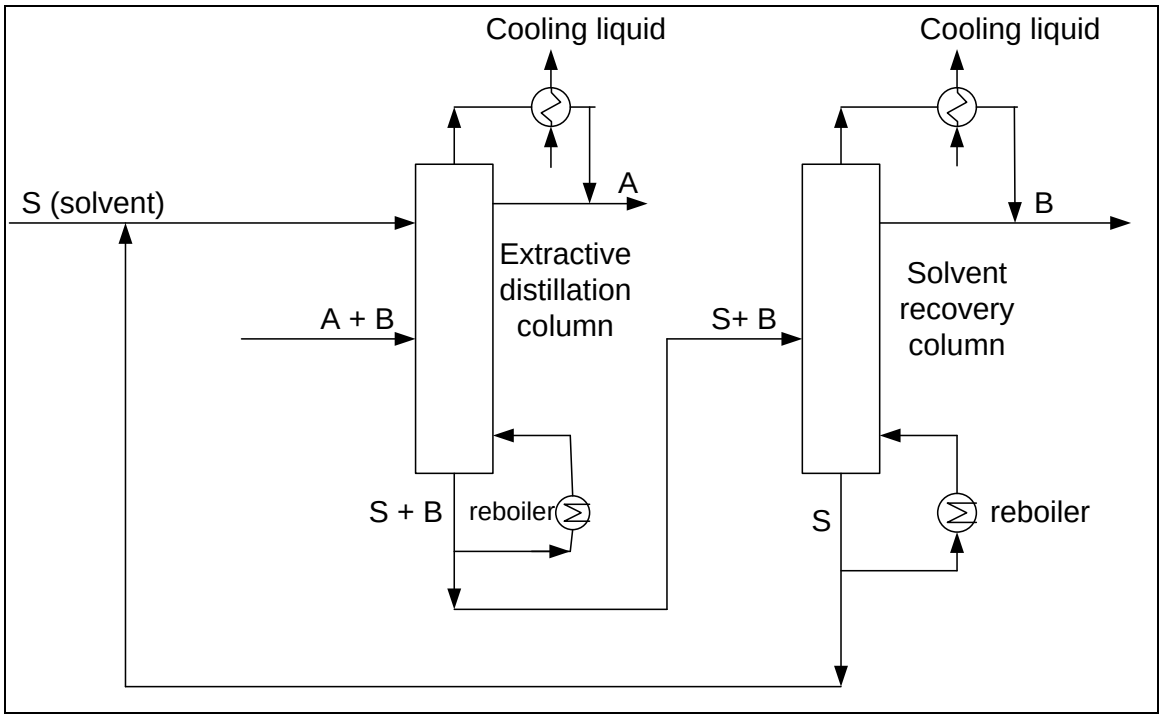

Figure 2.7: Two column for extractive distillation process (Zhigang *et al*., 2005).

The high purity of the products (ethanol) was mainly influenced by the number of theoretical stages in the column and the selectivity of the solvent. The purity of the ethanol depends on the saturation pressure of the solvent and the feed location. In azeotropic distillation a solvent is used which leads to the formation of a lower boiling azeotrope. Comparing azeotropic and extractive distillation, the azeotropic distillation has

the disadvantage that in contrast to solvents used for extractive distillation, the solvent has to be vaporized, which results in the higher energy consumption.

Liquid/solid as a separation agent in extractive distillation

In general organic compounds are used as selective solvents. For a safe and efficient operation, all selective solvents for separation process should have the following desired properties (Zhigang *et al*., 2005):

- High selectivity
- High capacity
- No separation problems in the required regeneration step
- High thermal and chemical stability
- Low melting point
- Non-toxic
- Low viscosity
- Negligible corrosivity
- Low price
- Simple purification

A high selectivity means a pure product and a higher distribution coefficient requires a lower solvent to feed ratio. In order to have little or no impurities in the distillate of the extractive distillation column and also to avoid separation problems in the regeneration column, the selective solvent for extractive distillation should have a higher boiling point than the components. High boiling point of solvent or separating agent means that at the top distillation column, only one component is more volatile.

2.7 Solvent for extractive distillation

Separation process and solvent selection (separation agent) are factors that influence the extractive distillation process. When a basic solvent is found, this solvent should be further optimized to improve the separation ability and decrease the solvent ratio and

liquid load of the extractive distillation column (Zhigang *et al*., 2005). The solvent is the core of extractive distillation. It is well known that selection of the most suitable solvent plays an important role in the economical design of extractive distillation. To date there are four kinds of solvents used in extractive distillation, i.e. solid salt, liquid solvent, the combination of liquid and solid salt, and ionic liquid (Zhigang *et al*., 2005).

Extractive distillation with solid salt

In the systems were solubility permits, it is feasible to use a solid salt dissolved in the liquid phase, rather than a liquid additive, as the separating agent for extractive distillation (Zhigang *et al*., 2005). The extractive distillation process in which the solid salt is used as the separating agent is called extractive distillation with solid salt. Ionic liquids are not included as solid salts although they are a kind of salt (Zhigang *et al*., 2005). Ionic liquids are described later in this chapter. Salt effect in the vapour liquid equilibrium (VLE) refer to the ability of a solid salt which has been dissolved in a liquid phase consisting of two or more volatile components to alter the composition of the equilibrium vapour without salt being present in the vapour. The feed component in which the equilibrium vapour is enhanced, is referred as "salting-out" by the salt, otherwise, if the equilibrium vapour is not reached then the component is known as "salting-in".

The process of extractive distillation with salt is different from the process shown in Figure 2.7, in that the salt is not recovered by means of distillation. The extractive distillation process can be taken as consisting of one extractive distillation column and one solvent recovery equipment. Figure 2.8 demonstrates a typical flow sheet for salt-effect extractive distillation. The solid salt which must be soluble to some extent in both feed components is fed at the top of the column by dissolving it at a steady state into the boiling reflux just prior to entering the column (Zhigang *et al*., 2005). The solid salt being non-volatile flows downwards in the column. One advantage of the process of extractive distillation with salt is that the salt is not difficult to recover, it is recovered by evaporation.

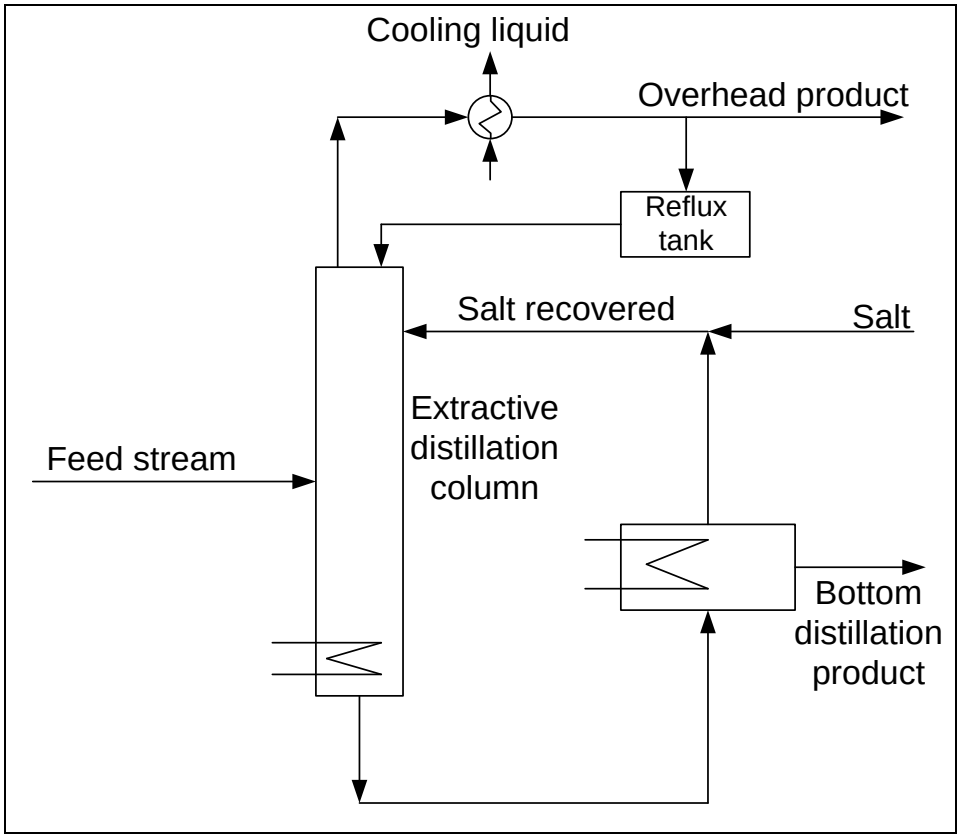

Figure 2.8: The process of extractive distillation with salt (Zhigang *et al*., 2005).

Extractive distillation with liquid solvent

This process is similar to the extractive distillation with solid salt. In certain systems where solubility permits it is feasible to use a liquid solvent dissolved in to the liquid phase, rather than salt, as the separating agent for extractive distillation. Therefore, the extractive distillation process in which the liquid solvent is used as the separating agent is called extractive distillation with liquid solvent. Note that, the ionic liquids are not included in the liquid solvents although they are in the liquid phase from room temperature to a higher temperature (Zhigang *et al*., 2005).

Increasing attention is given to the combination of solvents to enhance the extractive distillation process. The mixture using liquid solvents as the separating agent is

complicated and interesting. According to the aims of adding one solvent to another, it can be divided into two categories: increasing separation ability and decreasing the boiling point of the mixture (Zhigang *et al*., 2005).The most important factor in selecting the solvents is to improve the relative volatility. As a result, when one basic solvent is given, the key objective of adding a co-solvent to the mixture is to improve the relative volatility and to decreases the solvent ratio and liquid load of the extractive distillation column (Zhigang *et al*., 2005).

Table 2.1: Examples of the liquid solvents commonly used in the extractive distillation (Zhigang *et al*., 2005).

No.	Components to be separated	Solvents
1	alcohol (ethanol, isopropanol tert-butanol) and water	ethylene glycol and DMF
2	acetic acid and water	tribultylamine
3	acetone and methanol	water, ethylene glycol
4	methanol and methyl acetate	water
5	propylene and propane	acetonitrile (ACN)
6	aromatics and non-aromatics	DMF, NMP, NFM

Extractive distillation with the combination of liquid solvent and solid salt

This process is similar to the extractive distillation with solid salt or liquid solvent, in certain systems were solubility permits it is feasible to use a combination of liquid solvent and solid salt dissolved into the liquid phase, rather than only salt or liquid solvent, as the separating agent for extractive distillation. Therefore, the extractive distillation process in which the combination of liquid solvent and solid salts is used as the separating agent is called extractive distillation with the combination of liquid solvent and solid salt. Extractive distillation with the combination of liquid solvent and solid salt as the separating agent is a new process for production of high-purity products. This process integrates the advantages of liquid solvent (easy solvent) and solid salt (high

separation ability). The extractive distillation with the combination of liquid solvent and solid salt can be suitable either for the separation of polar systems or for the separation of non-polar systems respectively (Zhigang *et al*., 2005).

Extractive distillation with ionic liquid

This process is similar to the extractive distillation with solid salt or liquid solvent or the combination, in certain systems where solubility permits it is feasible to use an ionic liquid dissolved into the liquid phase, rather than only salt or liquid solvents, as the separating agent for extractive distillation. Therefore, the extractive distillation process where ionic liquid is used as the separating agent is called extractive distillation with ionic liquid. Ionic liquids are salts consisting entirely of ions. Ionic liquid are called "green" solvents. Most ionic liquids exhibit high thermal and chemical stability when compared to some of the commonly used high rated solvents such as acetonitrile (ACN), dimethethylformanide (DMF) and N-methyl-pyrrolidone (NMP), these solvents can decompose under their separation operating conditions (Zhigang *et al*., 2005).

Extractive distillation with ionic liquids can be suitable either for the separation of polar systems or for the separation of non-polar systems. According to Zhigang *et al*., (2005), the following polar and non-polar systems ethanol/water, acetone/methanol, water/ acetic acid, tetrahydrofuran (THF)/water and cyclohexane/benzene have been measured by Seiler *et al*. (2001). It was found that the separation effect was very apparent for these systems when certain ionic liquids were used. The challenge was to identify a suitable ionic liquid which displayed good solubility for the specific components of interest to be separated.

Some investigations on the use of ionic liquids as a solvent to separate ethanol-water have been done. Calvar *et al*. (2007) have conducted the study on isobaric vapour liquid equilibria for the ternary system of the ethanol + water + 1-hexyl-3-methylimidazolium chloride ([C_6mim][Cl]) and the binary systems containing the ionic liquid. These binary systems were ethanol + [C_6mim][Cl] and water + [C_6mim][Cl] carried out at 101.3 kPa. The VLE experimental data of binary and ternary systems were correlated using the NTRL equation. It was found that by adding different concentrations of ionic liquid from

10% (wt) to 50% (wt), **[C_6mim][Cl]** showed the negative effect in the system and it was difficult to eliminate the azeotrope of the ethanol/water mixture. In previous work of Calvar *et al*. (2006), the VLE of the ternary system of ethanol + water + 1-butyl-3-methylimidazolium chloride [C_4mim][Cl] was measured at 101.3 kPa. The study of **[C_4mim][Cl]** showed a positive effect and it was capable of eliminating the azeotrope of the ethanol/water mixture with the concentration of ionic solvent between 10% (wt%) and 50% (wt%).

2.8 Prediction of salt effects on VLE in alcohol/water/salt

Salt effect on the vapour-liquid equilibria is very important in extractive distillation (Furter, 1976) when the salt was used as a separating agent. However, the complex molecule-molecule, ion-molecule and ion-ion interactions in salt-water-alcohol systems pose a significant challenge to the development of the theoretical stages of extractive distillation. Many semi-empirical methods have been proposed to calculate VLE behavior in such system (Ohe, 1998). Most of these methods describe ternary VLE by extrapolation of constituent binary system data using binary interaction parameters. Binary salt-water and salt-alcohol systems are then described using methods such as those proposed by Pitzer (1973) and Chen *et al*. (2003) or using methods based on the mean spherical approximation (MSA). Binary alcohol-water systems are described using local composition models such as Wilson (1964); NRTL (Renon and Prausnitz, 1968) and UNIQUAC (Abrams and Prausnitz, 1975) models or by use of Equations of State.

A method for the prediction of the salting effecting effect on the vapour liquid equilibria of ternary alcohol-water-salt systems is proposed by Chou and Tanioka (1999). In this method, the nonidealities of the liquid phase were consider by employing Tan's modified Wilson model to describe the solvent-solvent interaction which can be obtained from the original Wilson model, and the solvent-salt interaction which could be obtained by the contribution of ion-ion and solvent-ion interaction. The estimation of the salt effect on the vapour-liquid equilibrium data of alcohol solutions plays an important role in the distillation process. The following models: Wilson, NRTL and UNIQUAC were verified and are successful in predicting VLE of non-electrolyte solution.

Tan (1987) modified the Wilson model to predict the salting effect on the VLE of alcohol aqueous solutions. More details will be presented in section 3.8**.** Tan (1987) measured two binary solvent-solvent interaction parameters and two binary solvent-salt interaction parameters; the solvent-solvent parameters were the same as those of the original Wilson model, and the solvent-salt parameter could be calculated from the vapour pressure data of the solvent-salt systems.

Kumar (1993) provides a review of theoretical and predictive models and correlation for estimating the salt effect. The models were classified into two categories depending whether the model is based on excess free energy or not. It was found that the models based on excess free energy were more realistic because of the pertinent interactions in the solution.

Table 2.2: Summary of the binary systems with different salts.

References	VLE system	Salt used	Conditions
Kato *et al.* (1971)	2-propanol + water	Calcium chloride	Atmospheric pressure
Sada *et al*, (1975)	2-propanol + water	Lithium chloride calcium chloride	Atmospheric pressure
Slusher *et al.* (1994)	2-propanol + water	Tetrabutylammonium bromide	Atmospheric pressure
Abu Al-Rub *et al.* (1999)	1-propanol+water	Calcium chloride Sodium chloride Ammonium chloride	333.15 K
Lee and Huand (2000)	Ethanol + water	Benzyltriethyl-ammonium chloride	Atmospheric pressure
Gu and Hou (2000)	(i)Acetone + water (ii) 2-propanol + water (iii) Ethyl acetate + ethanol (iv) acetone + carbon tetrachloride	Calcium chloride Potassium acetate and potassium bromide Calcium chloride Calcium chloride	Atmospheric pressure
Gao *et* al. (2003)	1-butanol + water	Penicil G potassium	2.67 kPa
Sevgili and Senol (2006)	2-propanol+water	Ammonium thiocyanate	Atmospheric pressure

Separation of 2-propanol and water

Marzal *et al*. (1996) measured isobaric vapour-liquid equilibrium data of the binary system of 2-propanol-water at 30 kPa, 60 kPa and 100 kPa. It was found that the system forms a minimum boiling azoetrope. It was found that the azoetropic water composition was shifted slightly lower as the pressure increases. The VLE data were collated with five liquid phase activity coefficient models (Margules, Van Laar, Wilson, NRTL and UNIQUAC).

Separation of ethanol and water

Ethanol is a basic chemical material and solvent used in the production of many chemicals and intermediates. Especially in the recent year, ethanol is paid more attention because it is an excellent alternative fuel and has a virtually limitless potential for growth. However, ethanol is usually diluted and required to be separated from water. It is known that ethanol forms azeotrope with water and can not be extracted to a high concentration from the aqueous solutions by ordinary distillation methods (Lei *et al.*, 2002). Extractive distillation using a 70/30 mixture of potassium and sodium acetate as the separating agent produces < 99.8% ethanol completely free of separating agent directly from the top of the column (Furter, 1992 and 1993). The separation of ethanol and water is the most important application of extractive distillation with solid salt. The influence of various salts on the relative volatility of ethanol and water was investigated (Duan *et al.*, 1980) and Zhigang *et al*., 2005) and the results are tabulated in Table 2.3 where the volume ratio of the azetropic ethanol-water solution and the separating is 1.0 and the concentration of salt is 0.2 g/ml. Zhigang *et al*., (2005) arranged the order of salt effect: $AlCl_3 > CaCl_2 > NaCl_2$, $Al(NO_3)_3 > Cu(NO_3)_2 > KNO_3$. It was concluded that the results in Table 2.3 revealed that the higher the valence of metal ion, the more salt effect.

Table 2.3: The influence of various solid salt and liquid solvents on the relative volatility of ethanol and water (Zhigang *et al*., 2005).

No.	Separating agent	Relative volatility
1	No separating agent	1.01
2	Ethylene glycol	1.85
3	Calcium chloride saturated	3.13
4	Ethylene glycol + NaCl	2.31
5	Ethylene glycol + $CaCl_2$	2.56
6	Ethylene glycol + $SrCl_2$	2.60
7	Ethylene glycol + $AlCl_3$	4.15
8	Ethylene glycol + KNO_3	1.90
9	Ethylene glycol + $Cu(NO_3)_2$	2.35
10	Ethylene glycol + $Al(NO_3)_2$	2.87
11	Ethylene glycol + CH_3COOK	2.40
12	Ethylene glycol + K_2CO_3	2.60
13	Potassium acetates	4.05

The advantages and disadvantages of extractive distillation with solid salts

In the systems where solubility considerations permit their use, solid salt as the separating agents have major advantages. The ions of a solid salt are typically capable of causing much large effects than the molecules of a liquid agent, both in the strength of attractive forces which they exert on feed component molecules and in the degree of selectivity exerted. This means that the salt provides good separation ability. In the extractive distillation process, the solvent ratio is much smaller than that of the liquid solvent, which leads to high production capacity and low energy consumption. Moreover, since solid salt is not volatile, it can not be entrained into product. No salt vapour is inhaled by operator and it is environmentally friendly (Zhigang *et al*., 2005). However, when solid salt is

used in industrial operation, dissolution reuse and transport of salt is a problem. The concurrent blockage and erosion limit the industrial value of extractive distillation with solid salt. That is why extractive distillation with solid salt is not widely used in industry.

2.9 Reduction of low pressure VLE data

It is very important to test experimental equilibrium data for thermodynamic consistency. According to Prausnitz *et al*. (1999) the Gibbs-Duhem equation could be used to interrelate activity coefficient of all components in a mixture. The experimental data should obey the Gibbs-Duhem equation, if they do not, the data cannot be correct. If they do obey the Gibbs-Duhem equation, the data is probably correct and can be used for designing distillation column (Prausnitz *et al*., 1999). There are simple models for VLE data reduction developed from excess Gibbs free energy. The choice of a correlating equation for the excess Gibbs free energy is an important decision in data reduction, and systems with complex behavior may require the testing of several equations before a suitable experimental fit is found (Raal and Mühlbauer, 1998). The search for an appropriate equation is complicated if there is much scatter in the data or if the data set is thermodynamically inconsistent. In that case it may be necessary to re-measure the data or to compute variables (for example, vapour composition) for which the accuracy is suspect.

All the calculations are based on modified Raoult's law described in Chapter 3. In this study, the gamma/phi method of VLE is used and includes the activity coefficient to account for liquid-phase nonidealities, but is limited by the assumption of vapour-phase ideality (Smith *et al*., 2001). Gamma/phi method of VLE, reduces to Raoult's law when $\Phi_i = \gamma_i = 1$, and to modified Raoult's law when $\Phi_i = 1$.

Dewpoint and Bubblepoint calculations

When a liquid at constant pressure is heated, at the certain temperature, the first bubble of vapour will form. This temperature in the bubble-point and it will have associated with it an equilibrium vapour composition, y_i. When the total pressure above a liquid composition x_i at constant temperature is reduced, a vapour bubble will form at a pressure equal to the bubble-point pressure. The dew-point is the temperature at which the first

droplet of liquid will condense when a vapour of composition y_i is cooled at constant pressure, or when the pressure is increased at constant temperature. In addition, dew-point and bubble point calculations may be required for process equipment design.

Bubble-point and dew-point calculations find greatest application in multi-component distillation, since for a known or specified liquid composition it is usually necessary to find the vapour composition and equilibrium temperature on each plate of the distillation column (Raal and Mühlbauer, 1998). The nature of dew-point and bubble-point calculation is evident of correct experimental data by applying Raoult's law and modified Raoult's law (Smith *et al*., 2001). All calculations making use of the gamma/phi approach require iteration because of its complex functionality:

$$\Phi_i = \Phi(T, P, y_1, y_2 ....., y_{N-1}) \tag{2.1}$$

$$\gamma_i = (T, x_1 x_2 ....., x_{N-1}) \tag{2.2}$$

$$P_i^{sat} = f(T) \tag{2.3}$$

At the moderate pressure where the gamma/phi approach to VLE is appropriate, activity coefficients (γ_i) were assumed independent of pressure (Smith *et al*., 2001).The need for the iteration was evident, for the BUBBLE P calculation of $\{y_i\}$ and P, which requires values of Φ_i that were functions of P and $\{y_i\}$. Simple iterative procedures are described in Chapter 3.

2.10 PERVAPORATION TECHNOLOGY

Table 2.4: Summary of pervaporation theorical development and application.

Description	**References**
Study of gas separation through thin plastic non-porous films and a rubber film.	Brubaker and Kammermeyer (1954); Binning *et al.* (1961)
Postulated "solution, diffusion and re-evaporation" mechanism and the investigation of the membrane process of the phase change across the membrane.	Neel (1991)
The potential economic viability of pervaporation during the 1950's via the examination of isopropanol drying and the separation of various hydrocarbon mixtures that placed pervaporation research the forefront.	Binning *et al*. (1961) and Fleming (1992)
Pervaporation was to undergo a dramatic change with the introduction of the asymmetric membranes for use in reverse osmosis systems because the benefits of asymmetric membranes (improved mass transfer and separation) pertained to pervaporation.	Loeb (1958); Rautenbach and Albrecht (1984)
The derivation and improvement of various mathematical models.	Fleming (1992)
In the late 1970s and early 1980s a few integrated distillation/pervaporation plants had been erected and were running fairly economically. However, capacities were low, varying from 1000 to 50 000 lpd. The ethanol dehydration plants were capable of obtaining an ethanol purity of 99.85%.	Redman (1990); Guerreri (1992) and Fleming (1992)

Table 2.4: Summary of pervaporation theorical development and application continued.

Description	References
In 1983, elastomeric membranes were tested in aqueous/organic as well as organic/organic liquid mixtures.	Koops and Smolders (1991)
The introduction of asymmetric-composite-polymer, flowing liquid and ceramic membranes technology had advanced to the stage that of economical, chemically and thermally stable membranes plants.	Fleming (1992)
In 1988, the pervaporation unit was constructed at Bethernville (France) in order to produces pure ethanol from an aqueous mixture for use in the upgrade of octane rating in lead-free petrol and to produce sugar from sugar beet. The dehydration of isopropanol mixtures was tested.	Redman (1990) and Fleming (1992)

In 1991, pervaporation companies moved away from the plate and frame module. This module has a low membrane area and limited plants in their capacity. The new modules: spiral wound and hollow fibre, were introduced in commercial plants in the few years and have proved to be extremely viable, resulting in higher output and lower costs.

The driving forces for the development of pervaporation have changed since those of the 1970s and today such factors as reduced energy costs, lower capital and operating and reduction in pollution as well as superior separation were high on the list of requirements of many companies. Today a number of commercial pervaporation plants have been erected for the recovery of solvents, the removal of organics from aqueous mixtures, including ethanol dehydration and dealcoholization of wines (Redman, 1990).

Pervaporation has only been around commercially for about 30 years, though there has not been a large upsurge in the number of pervaporation plants. In addition, there are few

companies involved in the production of the membranes themselves, but this will hopefully change in the future as the demand increases. Haggin (1988) predicted that membrane growth will be somewhere in the region of 12 to 14% annually as from 1990, however, the growth may be stifled if the technical and economic problems concerning membrane systems are not reduced. A factor affecting the successful introduction of pervaporation into industry is the low fluxes which are presently achieved. The low flux does not compare favourably with mass flow rates that alternative unit operations can produce. However, with the advent of high area/module volume ratio (high packing density) systems, pervaporation should find an increased usage within industrial applications. Generally industrial pervaporation plants require hollow fibre pervaporation modules for increased mass flow rate while laboratory scale units use plate and frame modules because of their ease of operation on a small scale.

The most advances in pervaporation researches have been done in the past 20 to 30 years as new polymers have been synthesized and as the theory of sorption and diffusion in polymers has been improved (Yamposki and Volkov, 1991). Improvement in both hydrophobic and hydrophilic membranes (Driolli, 1992) via cross linking using composite membranes makes pervaporation more inviting as time progresses. The future prospects for pervaporation, as well as with other membrane processes, rely on continued research into the chemistry of the polymer. The separation of organic mixtures and ethanol-water mixture using pervaporation looks set to be an important field of the future. The United States Department of Energy (DoE) ranks this particular pervaporation area as its top research priority (Haggin, 1990). Though there have been numerous investigations conducted on the pervaporative separations of organic/organic mixtures and liquid mixtures, there are no large scale pervaporation plants dealing with the separation of alcohol and water, only medium scale plants are in operation. It would appear that the current application of pervaporation industrially, that is the dehydration of alcohols, will continue increasing, using different types of pervaporation membranes.

Theory of pervaporation membrane

In principle, pervaporation is based on the solution-diffusion mechanism. Its driving force is the gradient of the chemical potential between the feed and the permeate sides of

the membrane. In general, there are two different types of pervaporation processes: pressure and sweep gas pervaporation. In the pressure pervaporation process shown in Figure 2.9, a solution to be separated contacts the pervaporation membrane at the feed side, where the retained retentate leaves the unit. On the permeate side, the partial pressure of pervaporated permeate is lowered by using a pressure pump. In the sweep gas pervaporation process shown in Figure 2.10, an inert sweep gas such as nitrogen (N_2) is used on the permeate side to reduce the permeate partial pressure (Huang *et al.*, 2008) and (Huang, 1991). Membranes used in pervaporation can be either hydrophilic or hydrophobic, i.e. either producing water or ethanol as the permeate stream. The hydrophilic pervaporation membranes would be generally used at high concentrations of ethanol.

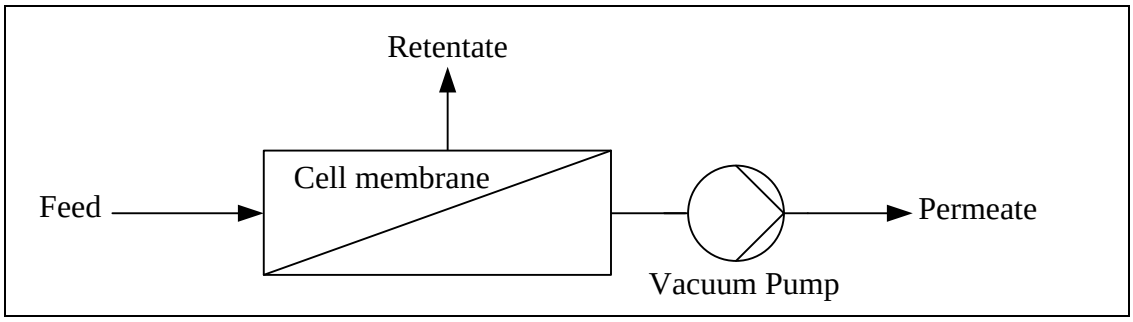

Figure 2.9: Pressure pervaporation process.

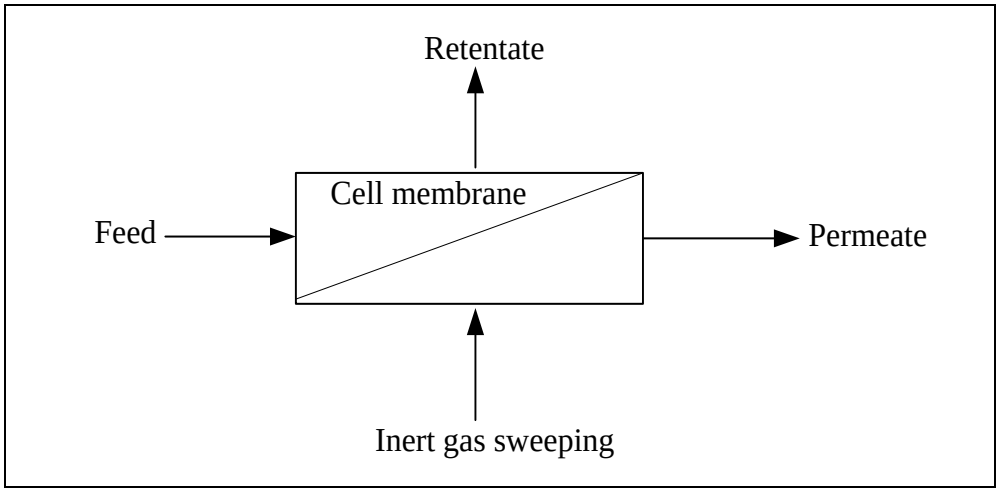

Figure 2.10: Sweep gas pervaporation process.

The hydrophilic membranes are available as inorganic membrane or polymeric membranes. Inorganic membranes exhibit greater temperature stability and mechanical strength and they are expensive. An expensive type of inorganic pervaporation membranes are tubular zeolite NaA and silica membrane. The tubular zeolite NaA membrane module, has a pervaporation flux of 2.35 kg/m^{2}h and the separation factor of above 5000 for the solution of 95 wt% ethanol at 368.15 K (Busca *et al.*, 2008). The NaA zeolite membrane showed high water selectivity permeation and high permeation flux (Busca *et al.*, 2008 and Huang *et al.*, 2008).

The polymeric membranes are commonly used materials for membranes. The advantages of polymeric pervaporation membranes are low energy and material consumption, the continuous character of the processes simplicity, and flexibility of control. However, upon wetting, they swell altering the structure of the membrane (Verhoef *et al*., 2008). Swelling occurs because a solvent enters and passes through the membrane, due to a chemical potential gradient. This increases the permeability. The advantage of combining inorganic membrane and polymeric membrane is to obtain the high ratio of membrane performance. A large number of polymeric pervaporation membranes, for example cellulose acetate butyrate membrane, polydimethylsiloxane (PDMS) membrane, polydimethysiloxane-polystyrene interpenetrating polymer network (PDMS-PS IPN) supported membranes, aromatic polyetherimide membranes have been investigated. According to Busca *et al.* (2008) and Huang *et al.* (2008) the preferable membrane is a PDMS membrane as a continuous fermentation/membrane pervaporation system to produce ethanol resulting in permeates of 20 – 23 wt% while 4 – 6 wt% level was retained in stirred tank fermentor. The selectivity ranged from 1.8 to 4.1 when using polydimethysiloxane-polystyrene interpenetrating polymer network supported membranes for pervaporation separation of ethanol from aqueous solutions (Huang *et al.*, 2008). For the feed having low ethanol concentration the membrane was more selective for ethanol, at high ethanol concentrations it was more selective for water. Huang *et al.* (2008) investigated the sorption, diffusion and pervaporation of ethanol solution in homogeneous and composite aromatic polyetherimide membranes. The performance of these membranes was found dependent on the permeate diffusivity rather than its solubility.

2.11 PERVAPORATION PROCESS

Characteristics of the pervaporation membrane

The pervaporation process offers several distinguishing characteristics:

- Direct separation of azeotropic and close boiling mixtures
- It has low energy consumption when compared to other liquid mixture separation techniques
- No solvent required, no contamination
- Permeate must be volatile at operating conditions
- Its functioning is independent of vapour-liquid equilibrium

Although pervaporation and vapour permeation are attractive membrane separation technologies, they are quite often combined with distillation, leading to unrivalled performance when compared to each respective technology alone.

Pervaporation membranes used for ethanol mixture

Based on the materials used for membrane production, there are three categories of membranes: inorganic, polymeric and composite membrane.

Inorganic membrane

Inorganic pervaporation membranes have more popular applications in chemical reaction, because of their superior temperature stability and mechanical strength (Sommer and Melin, 2000). For example, tubular zeolite NaA and silica membranes are still stable at temperature of above 573.15 K and feed pressures above 100 bar.

Polymeric membrane

According to O'Brien and Craig, (1996), the preferable membrane is PDMS membrane as a continuous fermentation/membrane pervaporation system to produce ethanol. It results in permeates of 20 – 23 wt% while 4 – 6 wt% level were retained in stirred tank fermentor. The selectivity ranged from 1.8 to 4.1. Schue *et al*. (1999) investigated the sorption, diffusion and pervaporation of the ethanol solution in homogeneous and

composite aromatic polyetherimide membranes. The performance of these membranes was found dependent on the permeate diffusivity rather than its solubility.

Composite or mixed membrane

To combine the advantages of inorganic membrane and polymeric membranes and obtain high ratio of membrane performance, various inorganic-polymer or polymer-polymer composite membranes such as polystyrenesulfonate/alumina, poly-electrolytes multi-layer mixed matrix membranes and poly-sodium alginate blend membranes have been studied for pervaporation separation of the ethanol/water mixture (Dong *et al*., 2006). They prepare a hollow fiber composite membrane PVA-SA blend, supported by a polysulfone (PS) hollow-fiber ultrafiltration membrane for pervaporation ethanol dehydration. With ethanol concentration at 90 wt% in the feed at 318.15 K the separation factors of 384 and permeation fluxes of 384 $g.m^{-2}.h^{-1}$ were obtained (Dong *et al*., 2006).

Pervaporation of aqueous organic mixtures

Pervaporation of aqueous mixtures is an extremely important research area in pervaporation technology as it is the most widely researched field (Dutta and Sikdar, 1991) and the only field to date that has been scaled successfully to industrial scale. Most of the mathematical models have been derived using these particular mixtures, and the mathematical models hold for under trial scale organic/organic pervaporation as well. The system of ethanol/water dehydration system has gained more attention in research.

The ethanol/water mixture was tested for its solubility and permeability characteristics in different membranes (Mulder *et al.*, 1985). One common feature, except in the water/ethanol/polysulfone data, is that sorption into the membrane is a rate controlling factor in the mechanism of these particular pervaporations. However, the polysulfone membrane shows the diffusion through the membrane to be rate controlling.

An integrated pervaporation/fractional distillation system was explored as a possible avenue for the purification of ethyl alcohol (Guerreri, 1992). It was found that pervaporation with a PVA/PAN composite membrane provided a high driving force for ethanol dehydration and that separation purities after the pervaporation step were well

above that of the azeotropic concentration of 95.57 wt% (at atmosphere pressure). In fact purities of 99.85 wt% were attainable. Guerreri (1992) believed that using an integrated pervaporation/distillation system, one could reduce capital and operating costs by approximately 25%. Guerreri (1992) also proposed a mathematical model similar to that derived by Rautenbach and Albrecht (1980).

Separation factors as high as 900 and flux of 1 $kg/m^2.h$ were reported (Nakane and Yanagishita, 1992) when using an asymmetric polyimide membrane to concentrate aqueous ethanol mixtures. The separation factor is an expression defined in a similar manner to the selectivity that describes the performance of the system in separating mixtures.

Four different membranes: silicone composite; polydimethylsiloxane (PDMS); polymethyoxysilone (PMS) and polyether block amide (PEBA), were used to concentrated acetone-water mixtures using the pervaporation process (Hollein *et al.*, 1993). Fluxes were generally low (less than one $kg/m^2.h$ and selectivities were higher (greater than 30) – expect for the PMS and PEBA membranes, where selectivities were below ten. The PEBA membrane, tested by Hollein *et al.* (1993), was inefficient for their particular system while the silicone composite gave the best results and was then used to test temperature and pressure effects.

Raghunath and Hwang (1992) looked at aqueous toluene and aqueous phenol separation through PDMS and PEBA membranes. Increasing membrane thickness had a pronounced effect on decreasing the flux of both aqueous mixtures as is expected when using Fick's law to describe the mass transport. Increases in membrane thickness also resulted in decreases in the selectivity of the organic component from water, though from the definition of selectivities, it is not obvious why there should be any effect of the membrane thickness on the selectivity.

Rautenbach and Albrecth (1984) studied the water/isopropanol/cellulose system. Both asymmetric and symmetric membranes were modeled mathematically. Flux increased with increasing water content in the feed while separation was achieved. The reduction in flux with increasing membrane thickness was also noted (Rautenbach and Albrecht,

1984). They also noted the presence of a temperature drop across the membrane and recorded the drops until the temperature reach 278.15 K. This temperature drop is often assumed negligible, yet for accurate modeling, it should be taken into account. The temperature drop cannot be predicted by the model unless heat transfer effects describing the loss of energy in vapourising component are included within the model.

Rautenbach *et al.* (1988) measured the water/isopropanol system using PVA/PAN membrane. Flux varied linearly with water concentration and followed Arrhenius law with respect to temperature. Excellent separation was achieved, decreasing with increasing water content and unaffected by temperature changes. These results were in agreement with those found by Mulder *et al.* (1985). `

Boddeker *et al.* (1990) selected the polyether-polyamide block copolymer (PEBA) via a screening process conducted with three different membranes, for separating various aqueous butanol isomers. Organic flux density through the PEBA membranes increased dramatically after 3 wt% butanol in the feed had been reached, however, for the butanol isomer, 2-methyl-2-propanol, a small increase in flux with increasing feed concentrated was noted. Increasing permeate pressure (downstream pressure) resulted in a decrease in flux as the saturation pressure had been reached.

Separation of alcohol and water by pervaporation membrane

Pervaporation is the recent technology used as the removal of organic from water (Peng *et al.*, 2003). Pervaporation membranes separate water at the feed side and a vapour at the permeate side, simultaneously evaporating the permeating compound. The polyether-polyamide block copolymer (PEBA) membrane is used for the separation of aromatics, and it was found that it was suitable for the separation of phenol and water (Kondo and Sato, 1994).

The separation of a phenol/water mixture using a polyurethane membrane by a pervaporation method was investigated by Hoshi *et al.* (1997). The polyurethane layer was sandwiched within a porous polypropylene membrane. Pervaporation measurement was carried out under pressure on the permeate side and the permeate vapour was collected with a liquid nitrogen trap. The phenol concentration in the permeate solution

increased from 0 to 65 wt% with increasing the feed concentration of phenol from 0 to 7 wt%. The total flux increased up to 930 g/m^2.h with increasing phenol partial flux. In the sorption membrane at 333.15 K, the concentration of phenol in the membrane was 68 wt% which was higher than that of the permeate solution. Therefore, it was considered that the phenol selectivity was based on high solubility in the polyurethane membranes.

Application of the pervaporation for the removal of phenol from water solutions modeling wastewater was investigated (Kujawski and Pozniak, 2004) using the following composite membranes: PEBA, polydimethylsiloxane (PDMS) and zeolite –filled PDMS pervaporation. It was found that the PEBA membrane achieved the best selectivity.

Field and Lobo (2002) have reported that the pollution control was achieved and waste minimised. It was found that pervaporation is more viable when operated as a pervaporation-decanter hybrid process than in a stand-alone mode.

Xu *et al*. (2006) studied twelve kinds of polyimide membranes for separation of ethanol and water mixtures for pervaporation properties. Twelve kinds of polyimide membranes using three dianhydrided (including 2,2-bis[4-(3,4-dicarbonxyphenoxy)phenyl]propane dianhydride (BPADA), 3,3,4,4-benzophenonetetracarboxylic dianhydride (BTDA), and 3,3,4,4-biphenyltetracarboxylic dianhdride (ODPA) and four diamines (including benzidine (BZD), bis(4-aminophenyl)phenyl phosphate (BAPP), 4,4-diaminodiphenylmethane (MDA), and 4,4- diaminodiphenylether (ODA) consist of two steps. The permeation experiments of water + ethanol mixtures through 12 polyimide membranes were carried out at 333.15 K. The temperature dependence of pervaporation performances on ODA-based polyimide membranes were investigated. The flux of ethanol + water mixtures through the polyimide membranes with the same dianhydrides increased following the order of BZD < ODA < MDA < BAPP. The permeation flux increases with an increase in temperature and the relationship between the flux and temperature can be described by the Arrhenius equation.

Hydrophobic membrane for the removal of ethanol

The most promising hydrophobic polymeric membranes are poly (1-trimethylsilyl-1-propene) (PTMSP), polydimethylsiloxne (PDMS) membranes, hydrophobic zeolite membranes and the potential composite membrane. According to Nomura *et al.* (2002) the ethanol-water separation factors of PDMS, PTMSP, composite membranes, and zeolite were reported to be in the range of (4.4 – 10.8), (9 – 26), (7 – 59) and (12 – 106) respectively. However, the ethanol – water separation factors, in some other cases, might exceed these ranges. In general, the ethanol/water separation factors are largely ranked in the following order: PDMS < PTMSP < composite membranes < zeolite membranes. The hydrophobic zeolite membranes are commercially available, while polymeric membranes (PDMS, PTMSP) and composite membrane are still under investigation. The zeolite membranes are more expensive than polymer membranes, but zeolite membranes have higher separation factors and flux than polymer membranes. Therefore, zeolite-membranes may be more cost effective on per unit ethanol basis (Vane, 2005b).

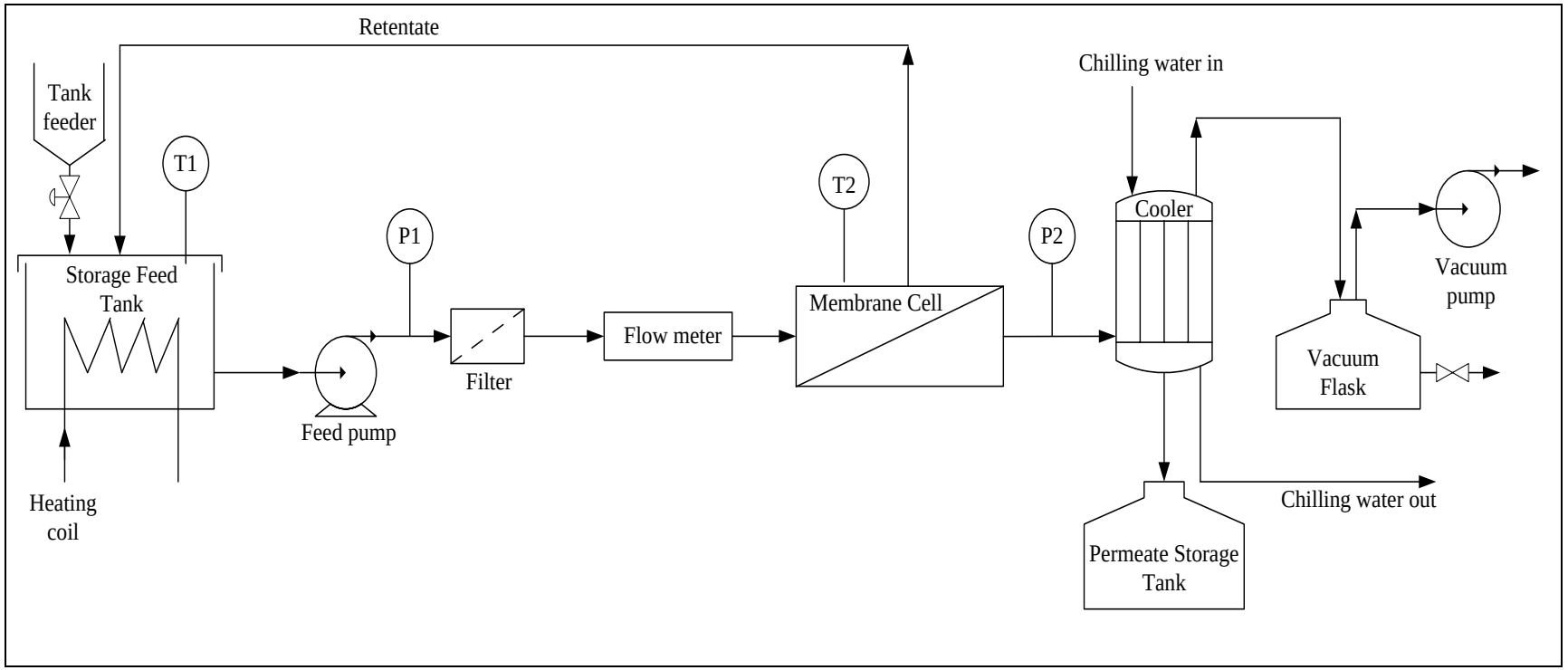

Figure 2.11: Schematic diagram of the pervaporation set-up.

P = Pressure

T = Temperature

Testing of the various parameters

The testing of the various parameters are important in determining the optimal operating conditions for pervaporation. Watson and Payne (1990) concluded in their study on the dehydration of dilute alcohol through PDMS films. Their observations include:

- As the number of carbon atoms is increased separation becomes more effective for aqueous/organic mixtures. A similar phenomenon was discovered by (Huang and Jarvis, 1970) with their study on low carbon aqueous alcohol pervaporation through cellophane and PVA. Huang and Jarvis (1970) also noted that permeation rates decreased for increasing molecular length. Lee *et al.* (1994) have showed similar tested results in tests conducted on the same systems, but also noted that sorption increased with increasing carbon content.
- The selectivity declines exponentially with increasing alcohol feed content.
- Separation is not always independent of membrane thickness (Raghunath and Huang, 1992).
- Temperature effects might be expected due to the temperature dependent terms solubility and diffusivity, however, the effect of temperature on separation is little or non-existent.
- Finally, sorption or solubility is the salient feature in the separation performance of pervaporation, often dominating the diffusion process completely. Yuzhong *et al*. (1993), conclude that diffusion is as important as sorption in affecting the flux but agrees that sorption is the dominating mechanism when it comes to selectivity. Lee *et al.* (1994) found that smaller alcohols were diffusivity dominant while larger alcohols were preferentially sorbed.

Effect of parameters

Temperature:

Flux

With increases in temperature there is a corresponding increase in the permeate rate. Most researchers have found that this relationship follows an Arrhenius pattern, confirming the predictions obtained from the conceptual model (Lund, 1995).

Selectivity

The research has been conflicting. Most investigators found that there was either no effect or the selectivity decreased slightly with increased temperature. Increased temperature causes the membrane to become more plasticized, thus its ability to distinguish between molecules of similar size and shape is diminished. However, McCandless (1973) has reported a contradictory increase in selectivity with increasing temperature and attributed it to increases in sorption with temperature increases. Therefore, it is clear that the selectivity is not an intrinsic property, but rather one which depends on the interaction between the components themselves and the interaction between the components in the feed and the membrane.

Concentration:

Flux

Most articles found that flux increase with increase concentrations of the permeant in the feed, yet there are a few reports which have shown the opposite relationship (McCandless *et al.*, 1974 and Wessling *et al.*, 1991).

Selectivity

From the literature it is apparent that selectivity decreases with increased permeant feed concentration. Wesslein *et al.* (1990) however, showed that this is

not a “hard and fast rule” as it depends on the feed mixture and component/membrane interactions.

Permeate pressure:

Flux

Flux was found to decrease with increased permeate pressure although if the permeate pressure is maintained far below that of the saturation pressure, no effect was found (Dutta and Sikdar, 1991 and Binning *et al.*, 1961).

Selectivity

Most researchers found decreases in selectivity with increased permeate pressure. Dutta and Sikdar (1991) found no effectof such behaviour in their investigations.

CHAPTER 3

THERMODYNAMIC FUNDAMENTALS

3.1 Introduction

The thermodynamic fundamentals are described and a discussion on extractive distillation and pervaporation processes are presented. Chou and Tanioka (1999) modified the Wilson model (1964) for data reduction schemes to predict the effect of salt on the behavior of alcohol/water system. The VLE data reduction using the liquid phase activity coefficient models such as Margules, Wilson, NRTL, Van Laar, UNIQUAC are also presented. Many references such as (Wilson, 1964); (Renon and Prausnitz, 1968); (Abrams and Prausnitz, 1975); (Smith and Van Ness, 1987); (Prausnitz *et al*., 1986); (Malanowski and Anderko, 1992); (Walas, 1985); (Raal and Mühlbauer, 1998) gives excellent and detailed coverage of thermodynamic fundamentals, and it is not the purpose of this report to provide details coverage of the above thermodynamic fundamentals. The pervaporation equations developed by Baker (2004) was presented in order to understand the pervaporation principles.

3.2 Vapour Liquid Equilibrium System

The application of fundamental thermodynamic concepts to the problem of describing and interpreting multicomponent phase equilibria is particularly impressive (Smith *et al*., 2001). The vapour-liquid equilibrium (VLE) relations as well as other interphase equilibrium relationships are needed in the solution of many engineering problems. The required data can be found by experiment but such measurements are seldom easy, even for binary systems and they become rapidly more difficult as the number of constituent species increase. This is the incentitive for application of thermodynamics to the calculation of phase equilibrium relationships (Smith *et al*., 2001)The general VLE problem involves a multicomponent system of N constituent species for which the independent variable are temperature, pressure and N – 1 liquid phase mole fractions and N – 1 vapour phase mole fraction. (Note that $\sum_i x_i = 1$and $\sum_i y_i = 1$, where x_i and y_i represent liquid and vapour mole fractions respectively). There are 2N independent variable, and applications of the phase rule shows exactly N of these variable must be fixed to establish the intensive state of the system. The fundamental equation of phase equilibrium based on the chemical potentials (μ_i) for phases α and β**:**

$$\mu_i^{\alpha} = \mu_i^{\beta} \qquad (i = 1,2,3.....N) \tag{3.1}$$

One can write the general expression for VLE by applying the defining relations. At equilibrium the fugacity of the species *i* in the vapour and liquid phase are equal:

$$\hat{f}_i^{\alpha} = \hat{f}_i^{\beta} \tag{3.2}$$

or

$$\hat{f}_i^{v} = \hat{f}_i^{l} \tag{3.3}$$

where**:** *v* is vapour phase and *l* is liquid phase

The definition of fugacity is completed by setting the ideal gas state fugacity of pure species *i* equal to its pressure. Consider the liquid and vapour phases and their fugacity can be expressed as follows:

$$\hat{f}_i^{\,v} = \hat{\varphi}_i y_i P \tag{3.4}$$

$$\hat{f}_i^{\,l} = \gamma_i x_i \varphi_i^{sat} p_i^{sat} \exp\left(\frac{1}{RT}\int v_j^l dP\right) \tag{3.5}$$

at equilibrium leads to

$$\hat{\varphi}_i y_i P = \gamma_i x_i \varphi_i^{sat} p_i^{sat} \exp\left(\frac{1}{RT}\int v_j^l dP\right) \tag{3.6}$$

3.3 Fugacity Coefficient

The fugacity coefficient may be evaluated from the compressibility factor (*Z*) and can be evaluated in two ways either from PVT data or obtained analytically from equations of state (EoS).

The two term virial equation of state is given by

$$Z = 1 + \frac{BP}{RT} \tag{3.7}$$

where *B* is the second virial coefficient.

The generalised correlation of the compressibility factor given by Pitzer *et al*., (1955) is applicable to all gases and is given below

$$Z = Z^0 + \omega Z^1 \tag{3.8}$$

Where Z^0 and Z^1 are both function of T_r and P_r and ω is the acentric factor.

The virial equation of state was used in the determination of the fugacity coefficients for isobaric data presented in this investigation. The details and derivation of this equation of state are presented in Smith *et al*. (2001). Presented below are the final equations and the Pitzer correlation. The fugacity coefficient for a binary mixture is given by

$$\phi_i = \exp\left(\frac{\left(B_{ii} - V_i^l\right)\left(P - P_i^{sat}\right) + Py_j^2\delta_{ij}}{RT}\right) \quad \textbf{(}3.9\textbf{)}$$

where

$$\delta i_j = 2B_{ij} - B_{ii} - B_{jj} \quad (3.10)$$

The fugacity coefficient can also be evaluated for a multi-component mixture. The two term virial equation of state is applicable to pressures up to 5 bar. There are various methods to calculate the second virial coefficients in Equation (3.7) including the Pitzer and Curl (1957) correlation, correlation of Tsonopolous (1974); Hayden and O'Connell method (1975). The method described in this section is the Pitzer-type correlation as it was employed in the calculations of second virial coefficients for isobaric data. The virial coefficients for the Pitzer-Curl correlation can be obtained from Equation (3.7) and Equation (3.8)

$$B_{ij} = \frac{RT_{c,ij}}{P_{c,ij}}\left(B^0 + \omega_{ij}B^1\right) \quad (3.11)$$

The values of B^0 and B^1 are obtain from

$$B^0 = 0.083 - \left(\frac{0.422}{T_r^{1.6}}\right) \quad (3.12)$$

and

$$B^1 = 0.139 - \left(\frac{0.172}{T_r^{4.2}}\right) \quad (3.13)$$

The cross coefficient parameters $T_{c,ij}$, $P_{c,ij}$ P and ω_{ij} can be calculated from the empirical mixing rules suggested by Prausnitz *et al.* (1999):

$$T_{c,ij} = \sqrt{T_{c,i} + T_{c,j}}\,(1 - k_{ij}) \tag{3.14}$$

$$P_{c,ij} = \frac{Z_{c,ij} R T_{c,ij}}{V_{c,ij}} \tag{3.15}$$

and

$$\omega_{ij} = \frac{\omega_i + \omega_j}{2} \tag{3.16}$$

where

$$Z_{c,ij} = \frac{Z_{c,i} + Z_{c,j}}{2} \tag{3.17}$$

and

$$V_{c,ij} = \left(\frac{(Vc)_i^{1/3} + (Vc)_j^{1/3}}{2} \right)^3 \tag{3.18}$$

The parameter k_{ij} in Equation (3.14) is an empirical binary interaction parameter. When species *i* and *j* are very similar in size and chemical nature, k_{ij} is set to a value of zero. Tarakad and Danner (1977) provide guidelines for the estimation of k_{ij} when species *i* and *j* are not similar in size or chemical nature.

3.4 Activity Coefficient

The definition was given by the relation between the activity coefficient and the liquid phase fugacity which is:

$$\gamma_i = \frac{\hat{f}_i^{\,l}}{x_i f_i} \tag{3.19}$$

According to Gess *et al*. (1991), in order to obtain some physical sense of the activity coefficient, the concept of the properties which describe the behavior of the liquid phase, must be introduced. Excess properties express the differences between actual property values of a solution and the values that would be exhibited by an ideal solution at the same temperature, pressure and composition. The significance of these excess thermodynamic properties was summarized by Wisniak and Tamir (1978) as the excess properties

- Provide key values for calculation of multicomponent mixture properties from pure component data.
- Used to define the various kinds of solutions.
- Used in testing solution theories.
- Provide data for evaluation of parameters characterizing interactions between unlike species in a mixture.
- The excess Gibbs energy, G^E, is one of the most useful thermodynamic concepts for expressing non-ideality of liquid mixture.
- G^E is the most useful quantity for determining phase stability and phase separation.
- The excess enthalpy or heat of mixing, H^E, is a very useful quantity in predicting isothermal VLE and testing the thermodynamic consistency of isobaric VLE data.

The equation inter-relating these properties is known as the fundamental excess property relation, which was derived by Van Ness (1959):

$$d\left[n\left(\frac{G^E}{RT} \right) \right] = \frac{nV^E}{RT} dP - \frac{nH^E}{RT^2} dT + \sum \ln \gamma_j dn_j \qquad (3.20)$$

G^E is the molar excess Gibbs energy, V^E is the molar excess volume and H^E is the molar excess enthalpy or the heat of mixing. The implicit in equation (3.20) is the relation:

$$\ln \gamma_i = \left[\frac{\partial \left[\left(GE / RT \right) \right]}{\partial n_i} \right]_{T,P,n_{j \neq i}} \qquad (3.21)$$

The relationship between the excess Gibbs energy and the activity coefficient can also be expressed as:

$$\frac{G^E}{RT} = \sum x_i \ln \gamma_i \tag{3.22}$$

Based on equations (3.22) and (3.20) the following equations can be obtained for the activity coefficients in binary system:

$$\gamma_1 = \exp\left[\left(\frac{G^E}{RT}\right)\right] + x_2 \frac{d\left(G^E/RT\right)}{dx_1} \tag{3.23}$$

$$\gamma_2 = \exp\left[\left(\frac{G^E}{RT}\right)\right] - x_1 \frac{d\left(G^E/RT\right)}{dx_1} \tag{3.24}$$

The molar excess Gibbs energy is function of the measurable quantities temperature, pressure and composition. Thus, it is through this excess property that the activity coefficient can be related to these experimental quantities. According to Prausnitz *et al*. (1986), at low to moderate pressures, activity coefficients are weakly dependent on pressure and therefore their dependence is primary on temperature and composition. Another thermodynamically important relation, which clearly shows the dependence of the activity coefficient on the excess properties is the Gibbs-Duhem equation is:

$$\sum x_i d \ln \gamma_i = \frac{V^E}{RT} dP - \frac{H^E}{RT^2} dT \tag{3.25}$$

Equation 3.25 also forms the basis of thermodynamic consistency tests. It is interesting to note that at constant temperature and constant pressure, equation (3.25) reduces to:

$$\sum x_i d \ln \gamma_i = 0 \tag{3.26}$$

The Gibbs-Duhem equation finds an important application in thermodynamic consistency testing of VLE data, (refer to section 3.10).

3.5 Activity Coefficient at Infinite Dilution

In the dilute regions some of the greatest departures from ideality are frequently observed and consequently activity coefficients at infinite dilution are significant importance. This can be summed up in a statement by Raal and Mühlbauer (1998) that infinite dilution activity coefficients almost always represent the most accurate characterization of system behavior in the dilute regions. Additional uses of activity coefficients at infinite dilution include:

- Screening for potential azeotropes (Palmer, 2000)
- Screening of solvents for solvent extraction (Palmer, 2000) and extractive distillation (Perry and Green, 2004)
- Prediction of binary VLE data, which in turn are used to predict multi-component VLE data (Howell *et al*., 1989)

These activity coefficients at infinite dilution can be determined experimentally by various techniques, each having their own benefits and drawbacks. Raal and Muhlbauer (1998), list following principal techniques:

- Different ebulliometry
- Use of a different dynamic or static apparatus
- Gas chromatographic methods
- Inert gas stripping

The prediction of activity coefficient at infinite dilution are usually performed with group contribution models such as UNIFAC and ASOG and some correlation such as the Margules model, Van Laar model, Wilson model, T-K-Wilson model or modified Wilson model, NRTL model, UNIQUAC model (Walas, 1985).

3.6 Activity Coefficient Models

According to Walas (1985), many equations have been proposed for correlating activity coefficients with either the composition, which is usually expressed in mole fractions or the volume or molecular surface fractions. The volume and molecular surface fractions are preferable when the molecules differ substantially in size or chemical nature. There are nine well known correlations of activity coefficients: the Margules, Van Laar, Wilson, T-K-Wilson or modified Wilson, NRTL, UNIQUAC, ASOG, the regular solution method of Sctchard-Hildebrand and the group contribution methods UNIFAC. These models offer useful means of summarizing large amounts of VLE data and allow for interpolation of data and extensions beyond regions in which measurements have been made. According to Walas (1985) the collection of binary VLE data by Gmehling and Onken, (1977-1982) (DECHEMA Chemistry Data series) present the most comprehensive comparison of five methods. These comparisons are detailed below and on these comparisons the T-K-Wilson, Scatchard-Hildebrand, UNIFAC and ASOG models are not considered. All of the models, except the Scatchard-Hildebrand model and the group contribution methods were employed in this project. The Scatchard-Hildebrand and group contribution (ASOG and UNIFAC) methods are used for the prediction of low pressure VLE.

These mathematical models are based on the molar excess Gibbs energy, as a function of the liquid mole fraction and from this relationship the activity coefficient are calculated for each component of the VLE system. Differentially the excess Gibbs free energy equation in the following manner allows for the calculation of the activity coefficient:

$$\ln \gamma_i = \left[\frac{\partial \left[\left(GE / RT \right) \right]}{\partial n_i} \right]_{T,P,n_{j \neq i}} \tag{3.27}$$

Once the activity coefficient has been determined from experimental data, the thermodynamic properties can be calculated by use of equation

$$x_i \gamma_i P_i^{sat} = y_i P \tag{3.28}$$

Margules model

The Margules equations were originally proposed in 1895 and they are the oldest of all the activity coefficient models. Despite this, they are still very useful in their ability to correlate VLE data. It has also, frequently, been found to be superior to other equations (Walas, 1985). The Margules equations for binary system are:

$$\ln \gamma_1 = \left[A_{12} + 2\left(A_{21} - A_{12}\right)x_1\right]x_2^2 \tag{3.29}$$

$$\ln \gamma_2 = \left[A_{21} + 2\left(A_{12} - A_{21}\right)x_2\right]x_1^2 \tag{3.30}$$

The molar excess Gibbs energy corresponding to these equations is:

$$\frac{G^E}{RT} = x_1 x_2 \left[A_{12}x_2 + A_{21}x_1\right] \tag{3.31}$$

The constants A_{12} and A_{21} are both nominally independent of temperature but in practice are usually found to be temperature dependent. These activity coefficients are commonly known as the 3-suffix Margules equations. By including another constant, C in the (3.31) the molar popular form of the Margules equation, the four suffix Margules equation is obtained.

$$\frac{G^E}{RT} = x_1 x_2 \left[A_{12}x_2 + A_{21}x_1 - Cx_1x_2\right] \tag{3.32}$$

Applying equation (3.27) the following relationships are obtained:

$$\ln \gamma_1 = \left[A_{12} + 2\left(A_{21} - A_{12} - C\right)x_1 + 3Cx_1^2\right]x_2^2 \tag{3.33}$$

$$\ln \gamma_2 = \left[A_{21} + 2\left(A_{12} - A_{21} - C\right)x_2 + 3Cx_2^2\right]x_1^2 \tag{3.34}$$

Van Laar model: (Prausnitz *et al*., 1986)

This model is suitable for constituents in a binary system that are similar chemically and have differing molar volumes. All interaction parameters except a_{12} are ignored. This model has been found to represent some complex systems despite its derivation which suggests that it is suitable for simple, non-polar liquids. The advantage of this model is that it is mathematically simple, yet flexible. The Gibbs excess expression is as follows:

$$\frac{G^E}{RT} = \frac{A_{12}A_{21}x_1x_2}{x_1A_{12} + x_2A_{21}} \tag{3.35}$$

$$\ln\gamma_1 = A_{12}\left[\frac{A_{21}x_2}{x_1A_{12} + x_2A_{21}}\right]^2 \tag{3.36}$$

$$\ln\gamma_2 = A_{21}\left[\frac{A_{12}x_1}{x_1A_{12} + x_2A_{21}}\right]^2 \tag{3.37}$$

The above equations take into account the size difference between molecules. However, according to Gess *et al*. (1991), the Van Laar equations do not represent highly non-ideal system well. This indicates that the interactions between molecules are not properly characterized by this activity coefficient model. Prausnitz *et al*. (1986) recommend the use of the Van Laar equations for relatively simple non-polar solutions. However, these equations have been found to be capable of represent the activity coefficient of some complex mixtures (Walas, 1985). According to Smith and Van Ness (1987) the Margules and Van Laar equations are special cases of a very general treatment based on rational functions, i.e on equation for G^E given by ratios of polynomials. They have the merit of mathematical simplicity and they provide great flexibility in the of VLE data for binary systems. However, they have no sound theoretical foundation and there is no rational basis for extension to multicomponent systems.

Wilson model

Wilson (1964) developed a model which was based on the concept of local composition. Local compositions which occur within a liquid solution are different from the overall mixture composition and are presumed to account for the short range order and non-

random molecular orientations that result from differences in molecular size and intermolecular forces Smith and Van Ness (1987). In the Wilson (1964) equation, these local compositions are expressed in terms of volume fractions Walas (1985). The Wilson expression for the excess Gibbs energy is:

$$\frac{G^E}{RT} = -x_1 \ln\left[x_1 + x_2\Lambda_{12}\right] - x_2 \ln\left[x_2 + x_1\Lambda_{21}\right] \tag{3.38}$$

The activity coefficients derived from this equation are:

$$\ln\gamma_1 = -\ln\left[x_1 + x_2\Lambda_{12}\right] + x_2\left[\frac{\Lambda_{12}}{x_1 + x_2\Lambda_{12}} - \frac{\Lambda_{21}}{x_2 + x_1\Lambda_{21}}\right] \tag{3.39}$$

$$\ln\gamma_2 = -\ln\left[x_2 + x_1\Lambda_{21}\right] - x_1\left[\frac{\Lambda_{12}}{x_1 + x_2\Lambda_{12}} - \frac{\Lambda_{21}}{x_2 + x_1\Lambda_{21}}\right] \tag{3.40}$$

The Wilson equation has two adjustable parameters, Λ_{12} and Λ_{21}, which are related to the pure component liquid molar volumes (V_i) in the following way:

$$\Lambda_{12} = \frac{V_2}{V_1}\exp\left[-\frac{\lambda_{12} - \lambda_{11}}{RT}\right] \tag{3.41}$$

$$\Lambda_{21} = \frac{V_1}{V_2}\exp\left[-\frac{\lambda_{21} - \lambda_{22}}{RT}\right] \tag{3.42}$$

Where $\left(\lambda_{12} - \lambda_{11}\right)$ and $\left(\lambda_{21} - \lambda_{22}\right)$ are parameters which characterize the molecular interactions between the components. The temperature dependence of the adjustable parameter can be clearly seen in the above equations. The infinite dilution value of the activity coefficients are given by the equations:

$$\ln\gamma_1^{\infty} = -\ln\Lambda_{12} + 1 - \Lambda_{21} \tag{3.43}$$

$$\ln\gamma_2^{\infty} = -\ln\Lambda_{21} + 1 - \Lambda_{12} \tag{3.44}$$

According to Raal and Mühlbauer (1998) the Wilson equation is considered to be good as three suffix Margules and Van Laar equations and it is frequently appreciably superior, particular for polar/non-polar mixtures. This was confirmed by Orye and Prausnitz (1965) who showed that the activity coefficients of approximately one hundred miscible mixtures of various chemical types were best correlated by the Wilson equation as compared to the three suffix Margules and the Van Laar equations. The superiority of the Wilson equation over all the other liquid phase activity coefficient models is also suggested by Gmehling and Onken (1977-1982). Another advantage of the Wilson equation is that it can be readily generalized to multicomponent systems without introducing parameter other than for the constituent binaries. According to Hirata *et al*. (1975), this equation has two disadvantages, which are not serious for most applications. Firstly, the equation can not be used be used for systems in which the logarithms of the activity coefficient, when plotted against the liquid mole fraction, exhibit a maximum or minimum. Very few systems exhibit this phenomenon. The second disadvantage is that the Wilson equation cannot predict liquid immiscibility.

Modified Wilson or T-K-Wilson model

Tsuboka and Katayama (1975) proposed a modification to the Wilson (1964) equation in 1975. The Gibbs energy function of the T-K-Wilson equation is:

$$\frac{G^E}{RT} = x_1 \ln\left[\frac{x_1 + V_{12}x_2}{x_1 + \Lambda_{12}x_2}\right] + x_2 \ln\left[\frac{x_2 + V_{21}x_1}{x_2 + \Lambda_{21}x_1}\right] \tag{3.45}$$

The corresponding activity coefficients are

$$\ln\gamma_1 = \ln\left[\frac{x_1 + V_{12}x_2}{x_1 + \Lambda_{12}x_2}\right] + \left[\beta - \beta_v\right]x_2 \tag{3.46}$$

$$\ln\gamma_2 = \ln\left[\frac{x_2 + V_{21}x_1}{x_2 + \Lambda_{21}x_1}\right] - \left[\beta - \beta_v\right]x_1 \tag{3.47}$$

Where $\beta = \frac{\Lambda_{12}}{x_1 + \Lambda_{12}x_2} - \frac{\Lambda_{21}}{x_2 + \Lambda_{21}x_1}$, $\beta_v = \frac{V_{12}}{x_1 + V_{12}x_2} - \frac{V_{21}}{x_2 + V_{21}x_1}$ (3.48)

$V_{12} = \frac{V_2}{V_1}$; $V_{21} = \frac{V_1}{V_2}$ (3.49)

An advantage of the T-K-Wilson over the Wilson, (1964) model is that this equation can predict limited miscibility regions for a system, it can be used for liquid-liquid equilibria or vapour-liquid-liquid equilibria.

NRTL *(Non-Random Two Liquid)* model

The concept of local was also incorporated in the model published by Renon and Prausnitz (1968). However this equation, unlike that of Wilson (1964), is applicable to both partial miscible and completely miscible system. The NRTL equation for the excess Gibbs energy is:

$$\frac{G^E}{RT} = x_1 x_2 \left[\frac{\tau_{21} G_{21}}{x_1 + x_2 G_{21}} + \frac{\tau_{12} G_{12}}{x_2 + x_1 G_{12}} \right] \quad (3.50)$$

The equations for the activity coefficients are

$$\ln \gamma_1 = x_2^2 \left[\tau_{21} \left(\frac{G_{21}}{x_1 + x_2 G_{21}} \right)^2 + \frac{\tau_{12} G_{12}}{\left(x_2 + x_1 G_{12} \right)^2} \right] \quad (3.51)$$

$$\ln \gamma_2 = x_1^2 \left[\tau_{12} \left(\frac{G_{12}}{x_2 + x_1 G_{12}} \right)^2 + \frac{\tau_{21} G_{21}}{\left(x_1 + x_2 G_{21} \right)^2} \right] \quad (3.52)$$

where

$$\tau_{ij} = \frac{g_{ij} - g_{ij}}{RT} \quad (3.53)$$

$$G_{ij} = \exp\left[-\alpha_{ij} \tau_{ij} \right] \quad (3.54)$$

The infinite dilution value of the activity coefficients are given by the equations:

$$\ln \gamma_i^{\infty} = \tau_{ji} + \tau_{ij} \exp(-\alpha_{ij}\tau_{ij}) \tag{3.55}$$

$$\ln \gamma_j^{\infty} = \tau_j + \tau_{ji} \exp(-\alpha_{ij}\tau_{ij}) \tag{3.56}$$

From the above equations, it is evident that the NRTL equation has three adjustable parameter i.e. ($g_{ij} - g_{jj}$), ($g_{ji} - g_{ii}$) and α_{ij} which is equal to α_{ji}. The parameter G_{ij} is an energy parameter which is characteristic of the interaction between component *i* and *j*. The parameter α_{ij} is related to the non-randomness of the mixture. For totally random mixtures, α_{ij} is zero. According to Walas (1985), the value of 0.3 for non-aqueous mixture and 0.4 aqueous mixtures should be used for α_{ij}. However, Gmehling and Onken, (1977-1982) have found that by fitting all three of the NRTL parameters, values greater than unity may be obtained. According to Raal and Mühlbauer (1998), it is best to determine α_{ij} rather then to use fixed parameters. The NRTL equation can also be generalized for multicomponent system.

UNIQUAC (UNIversal QUasi-Chemical) model

The original UNIQUAC equation was developed by Abrams and Prausnitz (1975) who incorporated the two-liquid model and the theory of local composition. The UNIQUAC equation consists of two parts: a combinatorial part that takes into account the differences in sizes and shapes of the molecules and the residual part that is due to the intermolecular forces between the molecules. In the form of an equation, this is represented as:

$$\frac{G^E}{RT} = \left(\frac{G^E}{RT}\right)_{combinatorial} + \left(\frac{G^E}{RT}\right)_{residual} \tag{3.57}$$

Anderson and Prausnitz (1978) modified the UNIQUAC equation to obtain better agreement for systems containing water or lower alcohols. Similar to the NRTL equation, the modified UNIQUAC equation may also be readily extended to represent multi-component mixtures. For a system consisting of *m* components, the two parts of the

Gibbs excess energy of the modified UNIQUAC equation, as given by Prausnitz et al. (1999), are:

$$\left(\frac{G^E}{RT}\right)_{combinatorial} = x_i \ln\frac{\Phi_i}{x_i} + x_j \ln\frac{\Phi_j}{x_j} + \frac{z}{2}\left[q_i x_i \ln\frac{\theta_i}{\phi_i} + q_j x_j \ln\frac{\theta_j}{\phi_j}\right] \tag{3.58}$$

$$\left(\frac{G^E}{RT}\right)_{residual} = -q_i x_i \ln\left[\theta_i + \theta_j \tau_{ji}\right] - q_j x_j \ln\left[\theta_j + \theta i \tau_{ij}\right] \tag{3.59}$$

where the co-ordination number, z set equal to ten, and the segment fraction, Φ_i and area fraction, θ_i are given by:

$$\Phi_i = \frac{x_i r_i}{x_i r_i - x_j r_j} \tag{3.60}$$

$$\theta_i = \frac{x_i q_i}{x_i q_i - x_j q_j} \tag{3.61}$$

The parameters, r and q are the pure component molecular structure constants. The former is the size parameter and the latter is the parameter. The parameters are evaluated from molecular structure is outlined in Raal and Mühlbauer (1998) and Fredenslund *et al*. (1977). The UNIQUAC equation has two adjustable parameters, τ_{ij} and τ_{ji}. These in turn are given terms of the characteristic energies ($u_{ij} - u_{jj}$) and ($u_{ji} - u_{ii}$) by:

$$\tau_{ij} = \exp\left[-\frac{(u_{ij} - u_{jj})}{RT}\right] \tag{3.62}$$

$$\tau_{ji} = \exp\left[-\frac{(u_{ji} - u_{ii})}{RT}\right] \tag{3.63}$$

The activity coefficients for a binary mixture are given by:

$$\ln\gamma_j^C = \ln\frac{\Phi_j}{x_j} + \frac{z}{2} q_j \ln\frac{\theta_j}{\Phi_j} + \Phi_i\left[l_j - \frac{r_j}{r_i} l_i\right] \tag{3.64}$$

$$\ln \gamma_j^R = -q_j \ln\left[\theta j + \theta_i \tau_{ij}\right] + \theta_i q_j \left[\frac{\tau_{ji}}{\theta_i + \theta_j \tau_{ji}} - \frac{\tau_{ij}}{\theta j + \theta_i \tau_{ij}}\right] \tag{3.65}$$

where

$$l_i = \frac{z}{2}\left[r_i - q_i\right] - \left[r_i - 1\right] \tag{3.66}$$

Abrams and Prausnitz (1975) defined the size and area parameters as the following:

$$r_i = \frac{V_{wi}}{0.01517} \tag{3.67}$$

$$q_i = \frac{A_{wi}}{2.5 * 10^8} \tag{3.68}$$

where V_{wi} (m^3/kmol) and A_{wi} (m^3/kmol) are the Van der Waals volumes and areas, respectively. A much simpler approach for the evaluation of the r_i and the surface q_i parameters is achieved by obtain the parameter as the sum of the molecular structure contributions (r and q, respectively) of the various functional groups that are present in the molecule i.e the group contribution method (Sandler, 1999). In this method, the r and q values of a relatively small number of functional groups or subgroups can be used to obtain the molecular structural parameters of a huge collection of different molecular structures involved in phase equilibrium studies.

The UNIQUAC equation is applicable to a various of liquid mixtures containing polar or non-polar fluids. It can also be applied to multicomponent and partially miscible mixtures. The UNIQUAC equation was slightly modified by Anderson and Prausnitz, (1978). The aim of their modification was to improve the performance of the UNIQUAC equation with systems containing lower alcohols or water. Anderson and Prausnitz (1978) recommended the use of empirically adjusted values of q_1 for water and lower alcohols in the calculation of the residual term.

3.7 Comparison of Models Equations

According to Walas (1985) the merits of the individual activity coefficient correlation methods have been cited locally. The comparisons of equation are summarized;

- The Margules, Van Laar equations and related algebraic forms have the merit of mathematical simplicity, ease of evaluation of the parameter from activity coefficient data and often adequate representation of even fairly nonideal binary mixture, including partially miscible liquid system. They are not applicable to multicomponent system without ternary or higher interaction parameter.
- The Wilson equation represents vapour liquid equilibria (VLE) of binary and multicomponent mixtures very well with only binary parameters, because of its greater simplicity it may be preferable to the NRTL and UNIQUAC equations for this purpose. Although it is not directly applicable to liquid-liquid equilibria (LLE), the equally simple T-K-Wilson equation probably is satisfactory, though it has not been tested as thoroughly as some others. The Wilson equation is the basis of the ASOG group contribution method for the activity coefficients.
- The NRTL equation represents vapour-liquid equilibria and liquid-liquid equilibria of the binary and multicomponent system quite well and its often superior of binary others for aqueous systems. It is simpler in the form than the UNIQUAC method but has the disadvantage of involving three parameters for each pair of constituents.
- The UNIQUAC equation is algebraically the most complex one, although it employs only two parameters per pairs of components. It utilizes knowledge of molecular surfaces and volume the pure components, which can be estimated from structural contributions and for this reason the method may be particular applicable to mixture of widely different molecular sizes. It is applicable to vapour-liquid equilibria and liquid-liquid equilibria of multicomponent data only. UNIQUAC is the basis of the UNIFAC group contribution methods for activity coefficients from structure and receives much support in the literature.

3.8 VLE PREDICTION OF THE ALCOHOL-WATER-SALT SYSTEM

The proposed model based on solvation between pure solvent and salt, for the prediction of salt effect on vapour-liquid equilibria was presented by using only the vapour pressure data of pure solvent and salt systems that compose the mixed solvent with salt system (Ohe, 1998). The proposed models predicts thermodynamically the salt effect by solvation number between each pure solvent and salt determined from vapour pressure data (Ohe, 1976). In this study, the modified Wilson model was used to predict interaction parameters for the ternary system of ethanol-water-salt (calcium chloride salt).

Modified Wilson model

According to Chou and Tanioka (1999) at low pressure, it can be assumed that the vapour phase is ideal ($\phi_i = 1$) and the activity coefficient of solvent n, γ_n in the mixed solvent-salt system can be expressed by

$$\gamma_n = \frac{y_n P}{x_n' P_n^{sat}} \tag{3.69}$$

Where y_n is the mole fraction of solvent n in the vapour phase, P is the total pressure, x_n' is the salt-free mole fraction of solvent n the liquid phase, and P_n^{sat} is the saturation vapour pressure of pure solvent n at the given system temperature.

For the binary mixture containing a dissolved salt system, the activity coefficients of the solvents can be calculated using the modified Wilson model

$$\ln \gamma_1 = -\ln\left(\Lambda_{1s} x_1' + \Lambda_{12} x_2'\right) + x_2' \Phi \tag{3.70}$$

$$\ln \gamma_2 = -\ln\left(\Lambda_{2s} x_2' + \Lambda_{21} x_1'\right) + x_1' \Phi \tag{3.71}$$

Where

$$\Phi = \frac{\Lambda_{12}}{\Lambda_{1s} x_1' + \Lambda_{12} x_2'} - \frac{\Lambda_{21}}{\Lambda_{2s} x_2' + \Lambda_{21} x_1'} \tag{3.72}$$

Λ_{12} and Λ_{21} are the solvent-solvent interaction parameters which are the same as those for the original Wilson model, and Λ_{1s} and Λ_{2s} are the solvent-salt interaction parameter which can be estimated by considering the ion-ion and solvent-ion interactions describe the salting effect on the VLE (Chou and Tanioka, 1999).

For binary system of solvent-salt solution, $x_1' = 1$ and $x_2' = 0$

Therefore equations (3.69) and (3.70) reduces to

$$\ln \gamma_1 = -\ln \Lambda_{1s} \tag{3.73}$$

$$\ln \gamma_2 = -\ln \Lambda_{2s} \tag{3.74}$$

It can also shown that at the system temperature, T, the equation (3.70) becomes

$$\gamma_1 = \frac{P}{P_1^{sat}} \tag{3.75}$$

Similarly for the solvent-salt solution, P_1^s

$$\gamma_1 = \frac{P_1^s}{P_1^{sat}} \tag{3.76}$$

Substituting equation (3.73) into (3.76), the solvent-salt interaction parameter is derived as

$$\Lambda_{1s} = \frac{P_1^{sat}(T)}{P_1^s(T, m_1)} \tag{3.79}$$

where m_1 is the salt motility distributed in the solvent. The distribution of salt in the mixed solvent is estimated by a simple mixing rule based on the solubility of the salt (Chou and Tanioka, 1999).

$$m_1 = \frac{s_1 x_1'}{\sum_n s_n x_n'} m \tag{3.80}$$

where s_n is the solubility of salt in solvent n, and m is the total salt molality in the ternary system. Similarly, Λ_{2s} could be obtained by the same method. At low pressures, the vapour pressure of the alcohol-salt and water-salt solutions, P_1^s and P_2^s is determined from

$$P_n^s = x_n \gamma_n^{bi} P_n^{sat} \tag{3.81}$$

where n = 1 or 2 and γ_n^{bi} is the activity coefficient of solvent n in the binary mixture.

3.9 Low pressure VLE data reduction

There are different methods available for the regression of isothermal and isobaric VLE data. However, only the two well-known methods were used to study the VLE data measured for this project. The first method is known as the gamma/phi (γ-Φ) formulation of VLE or more commonly known as the combined method, while the second method is known as the phi/phi (Φ-Φ) method or the direct method. The combined method was used in this work to regress the VLE data. The combined method uses an equation of state to calculate the fugacity coefficients that describe the vapour phase nonidealities, while an activity coefficient model is used to calculate the activity coefficients that describe the liquid phase non-idealities. In the direct method, the fugacity coefficients are used to describe the non-idealities in both the vapour and liquid phases and are calculated using an equation of state.

There are different calculation procedures for each method which depend on the nature of the VLE data. For isothermal VLE data, the pressure and vapour composition are calculated (bubble point pressure computation), whereas for isobaric VLE data, the temperature and vapour composition are calculated (bubble point temperature computation) for each experimental point. Therefore, a set of data points comprising of *P-x* values at a specified temperature or *T-x* values at a specified pressure are sufficient to allow determination of the activity coefficient model parameters. However, (Smith *et al*., 2001) encourages the measurement of the vapour phase mole fractions to allow

thermodynamic consistency testing, which is discussed in section 3.10. It should be noted that the activity coefficient model parameters are temperature dependent (Walas, 1985). The data reduction for isothermal VLE data is simple as the temperature dependence of the model parameters can be considered insignificant and thus the model parameters can be treated as constants. However, the temperature dependence of the model parameters is significant for the reduction of isobaric VLE data and must therefore be taken into account. The direct method was not used for the data regression and it is not describe in this study, (refer to Smith *et al*. 2001 for the details).

The Combined (gamma/phi) method

The gamma/phi method relies upon liquid phase activity coefficient models to represent VLE data. The model has been proposed to correlate the activity coefficients from a relationship of the molar excess Gibbs energy, the liquid composition and temperature, with the liquid composition expressed as a mole fraction (x_i). Usually, more than one model is used for VLE data regression, as one can determine which model provides a better fit of the experimental data for a particular system. In this study, two well-known models were used: the Wilson and NRTL models. In order to obtain the model parameters, a suitable algorithm must be used for VLE regression.

The following steps were used for the regression of an isothermal set of experimental binary VLE data using the gamma/phi method follows from Smith *et al.* (2001)

1. The temperature, liquid phase compositions and the pure component properties are used as inputs for the regression. A suitable expression for the excess Gibbs energy, as a function of composition, is then selected.

2. The parameters corresponding to the G^E expression from step 1 are assigned with reasonable estimates. The activity coefficients that correspond to the G^E expression from step 1 are then determined from Equation (3.21). The vapour phase is initially assumed ideal and therefore the fugacity coefficients (Φi) are initially set to unity to allow an initial calculation of the overall system pressure. The saturated pressures (P_i^{sat}) are then evaluated from a suitable vapour pressure correlation (such as the Antoine equation).

3. According to the law of mass conservation, $\Sigma x_i = \Sigma y_i = 1$, the overall system pressure is therefore obtained from the equations

$$y_i \phi_i P = x_i \gamma_i P_i^{sat} \tag{3.82}$$

$$P = \frac{x_1 \gamma_1 P_1^{sat}}{\phi_1} + \frac{x_2 \gamma_2 P_2^{sat}}{\phi_2} \tag{3.83}$$

4. The vapour mole fractions are then found from:

$$y_i = \frac{x_i \gamma_i P_i^{sat}}{\phi_i P} \tag{3.84}$$

5. Once the vapour mole fractions have been calculated, the fugacity coefficients are then evaluated using a suitable equation of state for the second virial coefficients from equation (3.85)

$$\phi_i = \exp\left(\frac{\left(B_{ii} - V_i^l\right)\left(P - P_i^{sat}\right) + P y_j^2 \delta_{ij}}{RT} \right) \tag{3.85}$$

6. The system pressure is then recalculated using Equation (3.83). The model parameters are then optimised by employing a regression technique with a suitable objective function that yields the best fit to the experimental *P-x* data for the entire composition range.

The regression procedure outlined above is the same for isobaric data with the exception that the temperature is constant. The following equations were used:

$$S = \sum \left(\delta P\right)^2 \tag{3.86}$$

where the difference between the model and experimental values is commonly termed a residual and symbolised as δ. Other objective functions may also be used such as δy_1, $\delta \gamma_1$, $\delta \gamma_2$ and $\delta(G^E/RT)$. However, according to Van Ness *et al.* (1978), equation (3.86) is at least as good as any other and is the most simplest and direct objective function. Furthermore, Van Ness and Abbott (1982) state that the objective function of equation (3.86) is successful in reducing isothermal VLE data and may even be superior to any other maximum likelihood method. Van Ness and Abbott (1982) also mention that replacing the pressure with temperature in equation (3.86), provides the best objective

function for regressing isobaric VLE data. Therefore, equation (3.86) was chosen as the objective function for regressing isothermal VLE data measured in this project. According to Narasigadu (2006) the following researchers Marquardt (1963) and Gess *et al*. (1991) have developed methods that use the objective function of equation (3.86) in the above mentioned algorithm. However, computer software programmes such as MATLAB (employed in this project) have built in functions that allow such calculations to be performed with much ease. The regression procedure for isobaric and isothermal data are summarised in Figures 3.1 and 3.2 respectively.

The vapour pressure of component j gives:

$$P_j^{sat} = \frac{P}{\sum_i \left[\left(\frac{x_i \gamma_i}{\phi_i} \right) \left(\frac{P_i^{sat}}{P_j^{sat}} \right) \right]} \tag{3.87}$$

The summations are over all species including j, which is an arbitrarily selected species. Once P_i^{sat} is known, the corresponding value of T is obtained from the following equation:

$$T = \frac{B_j}{A_j - \ln P_j^{sat}} - C \qquad \text{or} \qquad T_i^{sat} = \frac{B_i}{A_i - \ln P} - C_i \tag{3.88}$$

where A_i, B_i, and C_i are Antoine constants.

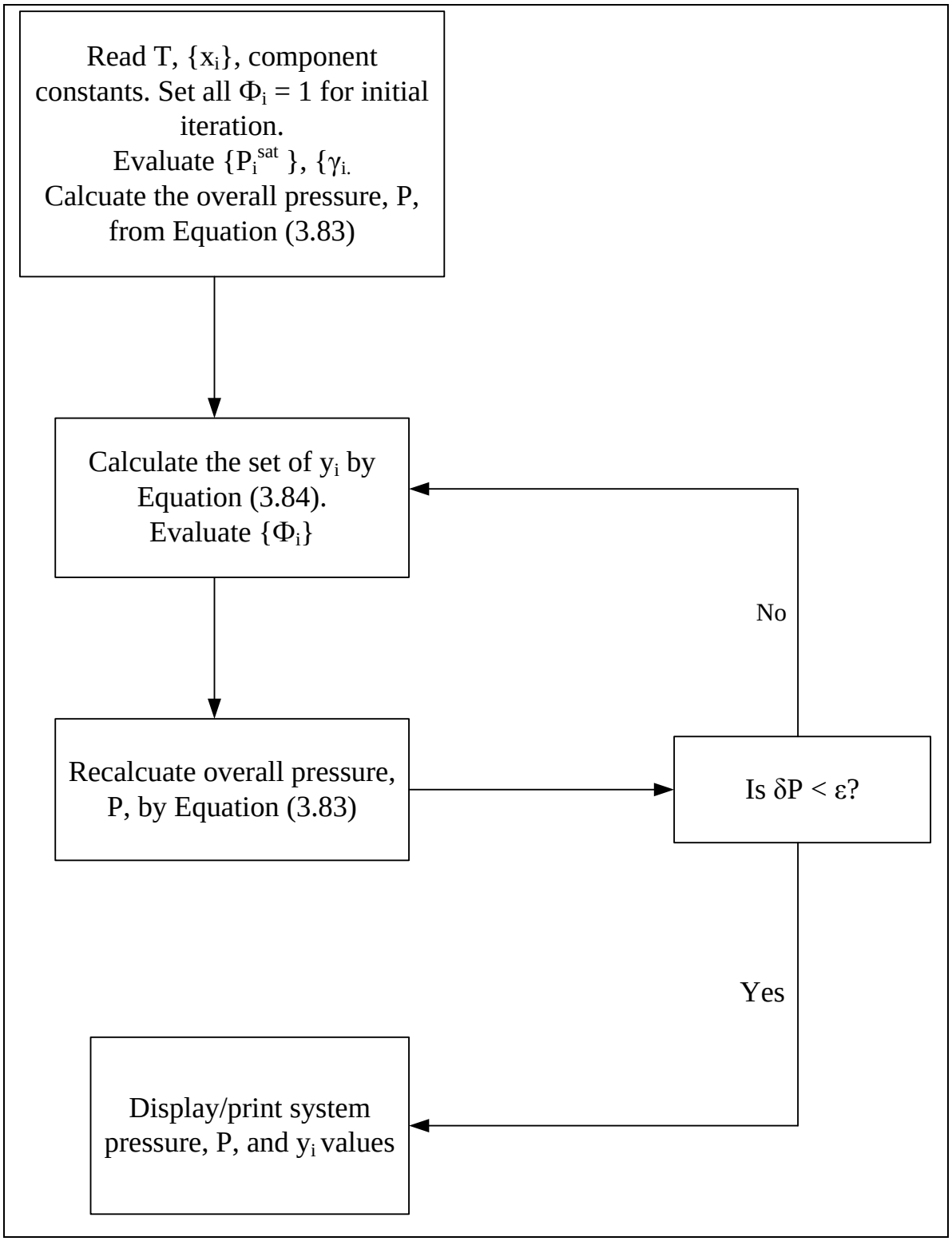

Figure 3.1: Block diagram for the bubble point pressure iteration for the combined method (Smith *et al.*, 2001).

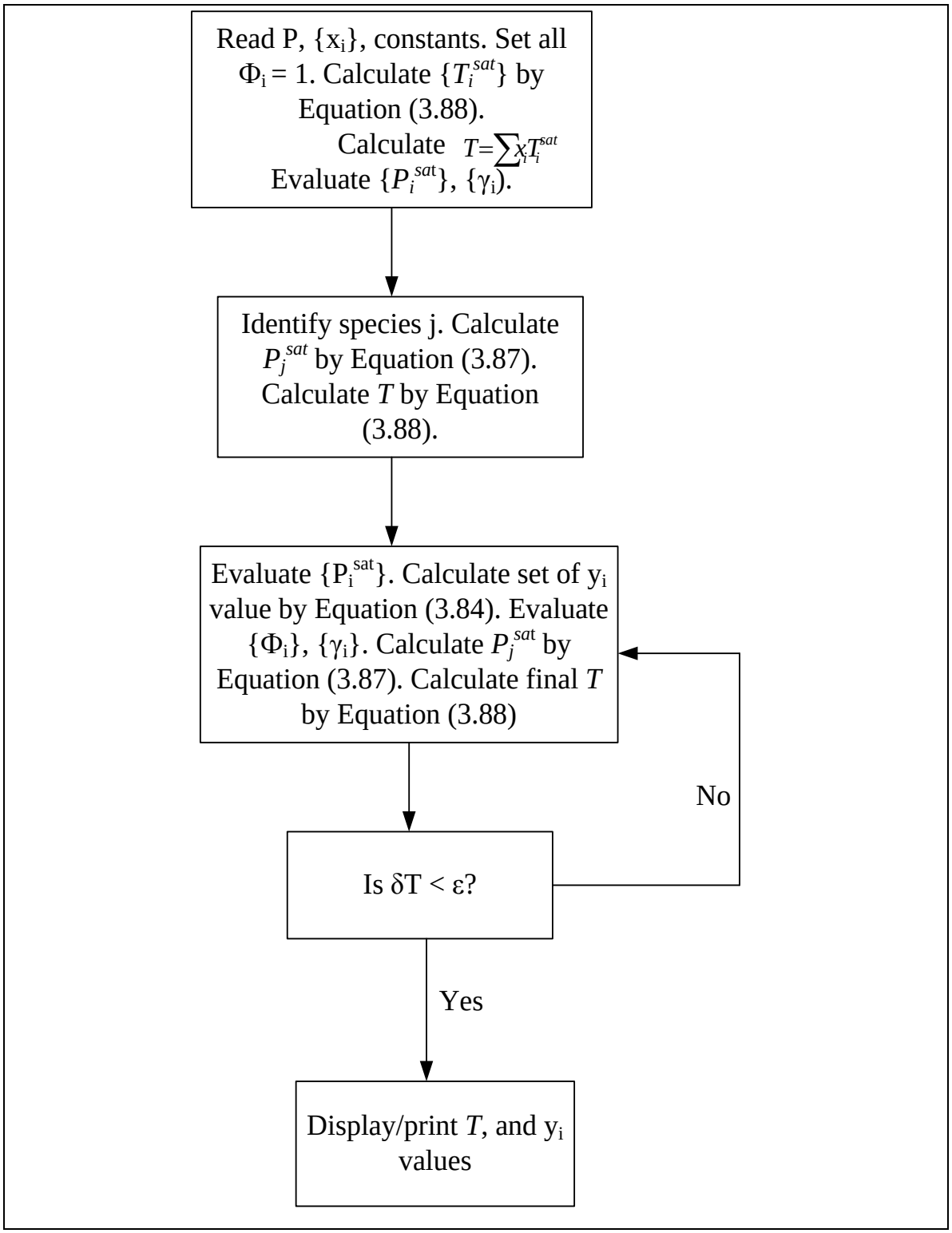

Figure 3.2: Block diagram for the bubble point temperature iteration for the combined method (Smith *et al.*, 2001).

3.10 Thermodynamic Consistency Test

The measurement of temperature, pressure and both liquid and vapour compositions for a binary VLE system, results in an "over-specification" of the system. Nevertheless, this allows one of the four measured variables to be used to test for thermodynamic consistency. According to Smith *et al*. (2001), the vapour compositions usually display the greatest error and thus the thermodynamic consistency tests usually focus on the vapour compositions (y-data) to determine the thermodynamic consistency of the VLE data. The Gibbs-Duhem equation forms the basis of all thermodynamic consistency tests.

$$\sum x_i d \ln \gamma_i = \frac{V^E}{RT} dP - \frac{H^E}{RT^2} dT \tag{3.89}$$

At constant temperature and pressure equation (3.89) becomes

$$\sum x_i d \ln \gamma_i = 0 \tag{3.90}$$

VLE data is said to be thermodynamically consistent if it conforms to the Gibbs-Duhem equation. Over the years, the evaluation of thermodynamic consistency of VLE data has received a great deal of attention in the literature with many adaptations of the Gibbs-Duhem equation being introduced. The *slope test*, which compared slopes of curves drawn to fit $\ln\gamma_1$ and $\ln\gamma_2$ vs x_1 graphs, was one of the earliest tests used but according to Van Ness (1995), this test proved to be tedious and led to uncertainty. However, Walas (1985) mentions that the *area test* is a necessary but insufficient condition as individual data may be off in ways that compensate each other. For instance, the pressure is cancelled off and hence one of the most accurately measured system properties is lost. This means that the test would sometimes pass data sets that were inconsistent while failing data sets that actually were consistent. Therefore, the *area test* was not considered for this project but two thermodynamic consistency tests were employed: the *point test* of Van Ness *et al*. (1973) and the *direct test* of Van Ness (1995). The direct test is not discussed in this work because it was not used to test the thermodynamic consistent of this work. A more detailed description of the direct test is provided in Van Ness (1995).

The Area test

The area test was proposed by Herington (1947); Redlich and Kister (1948) and Van Ness (1995). The test is relatively simple and provides a necessary but not sufficient condition for the evaluation of thermodynamic consistency, as discussed above.

Rewrite the following for experimental data

$$\left(\frac{G^E}{RT}\right)\exp = x_1 \ln \gamma_1^{\exp} + x_2 \ln \gamma_2^{\exp} \tag{3.91}$$

Differentiating the above equation and integrating over the entire composition range, and considering that

$$\left(\frac{G^E}{RT}\right)^{\exp} = 0 \tag{3.92}$$

At $x_1 = 0$ and $x_1 = 1$

One obtains the following intergral expressions

$$\int_0^1 \left(\ln \frac{\gamma_1^{\exp}}{\lambda_2^{\exp}} + \varepsilon \right) dx_1 = 0 \tag{3.93}$$

The bracketed term is plotted against the mole fraction of the component such that a graph creating an area both above and below the x_1-axis exists. The area test requires that the area above the x_1- axis be similar to area below the x_1-axis (net area = 0).

Van Ness (1995) imposed the criterion for using the test that stated that the difference of areas divided by the sum of the absolute areas should be less than or equal to 0.1 or 10%.

$$\frac{a_1 - a_2}{a_1 + a_2} \leq 10\% \tag{3.94}$$

This is a necessary but not sufficient condition because the most important and accurately measured variable pressure is ignored in the test due to the ratio of activity coefficients, given below. Van Ness, 1995 also states that while the pressure can be ignored it does however enter into the calculation of the minor factor Φ_i

$$\frac{\gamma_1}{\gamma_2} = \frac{y_1\phi_1 P \Big/ x_1 P_1^{sat}}{y_2\phi_2 P \Big/ x_2 P_2^{sat}} = \frac{y_1\phi_1 x_2 P_2^{sat}}{y_2\phi_2 x_1 P_1^{sat}} \tag{3.95}$$

According to Van Ness (1995), the area test only checks the appropriateness of the vapour pressure ratio, $\left(\frac{P_2^{sat}}{P_1^{sat}}\right)$ to the x-y data of an isothermal system.

The Point Test

Van Ness *et al*. (1973) introduced the *point test* as an improvement to the *area test*. Four variables are measured for a complete binary VLE data set such as T, P, x and y. Any three experimentally determined variables can be used to obtain the fourth variable by employing a suitable correlation. As mentioned above, the vapour compositions introduce the most error and are thus used to test for thermodynamic consistency. The *point test* compares the measured vapour compositions (y_{exp}) to the calculated values (y_{calc}), the calculated values are found from data regression using the combined method. This comparison generates residuals, Δy, which provides a good indication of the consistency of the VLE data. Danner and Gess (1990) provide a quantitative criterion for the consistency of VLE data by proposing that the absolute average deviation, Δy_{ad}, should be less than 0.03 for the data to be thermodynamically consistent:

$$\Delta y(AAD) = \frac{1}{N}\left(\left|y_{\exp} - y_{calc}\right|\right) \tag{3.96}$$

where N refers to the number of experimental data points. This criterion was also used for the data measured in this work.

3.11 PERVAPORATION MEMBRANE

The flux (J_i) of a component *i* through a pervaporation membrane can be expressed in terms of partial vapour pressures on either side of the membrane, p_{io} and p_{il}, by the equation:

$$J_i = \frac{P_i^G}{l}(p_{i_o} - p_{i_l}) \tag{3.97}$$

where J_i is the flux, *l* is the membrane thickness and P_i^G is the gas separation permeability coefficient. A similar equation can be written for component *j*. The separation achieved by a pervaporation membrane is proportional to the fluxes J*i* and J*j* through the membrane. The bulk of the pervaporation literature continues to report membrane performance in terms of total flux through the membrane and a separation factor, β_{pervap}, defined for a two component fluid as the ratio of the two components on the permeate side of the membrane divided by the ratio of the two components on the ***membrane*** divided by the ratio of the two components on the ***feed side***. The β_{pervap} can be written in several ways;

$$\beta_{pervap} = \frac{c_{i_l} / c_{j_l}}{c_{i_o} / c_{j_o}} = \frac{n_{i_l} / n_{j_l}}{n_{i_o} / n_{j_o}} = \frac{p_{i_l} / p_{j_l}}{p_{i_o} / p_{j_o}} \tag{3.98}$$

where c_i and c_j are the concentration, n_i and n_j are the mole fraction and p_i and p_j are vapour pressure of the two component of two component *i* and *j*.

The separation factor, β_{pervap} contains contributions from the intrinsic permeation properties of the membrane, the composition and temperature of the feed liquid and the permeate pressure of the membrane. These separation factors provides better understanding of the peravaporation process that is divided into two steps as shown in figure 3.3. The first step is evaporation of the feed liquid to form a saturated vapour in

contact with the membrane and the second step is diffusion of the vapour through the membrane to the low pressure permeate side.

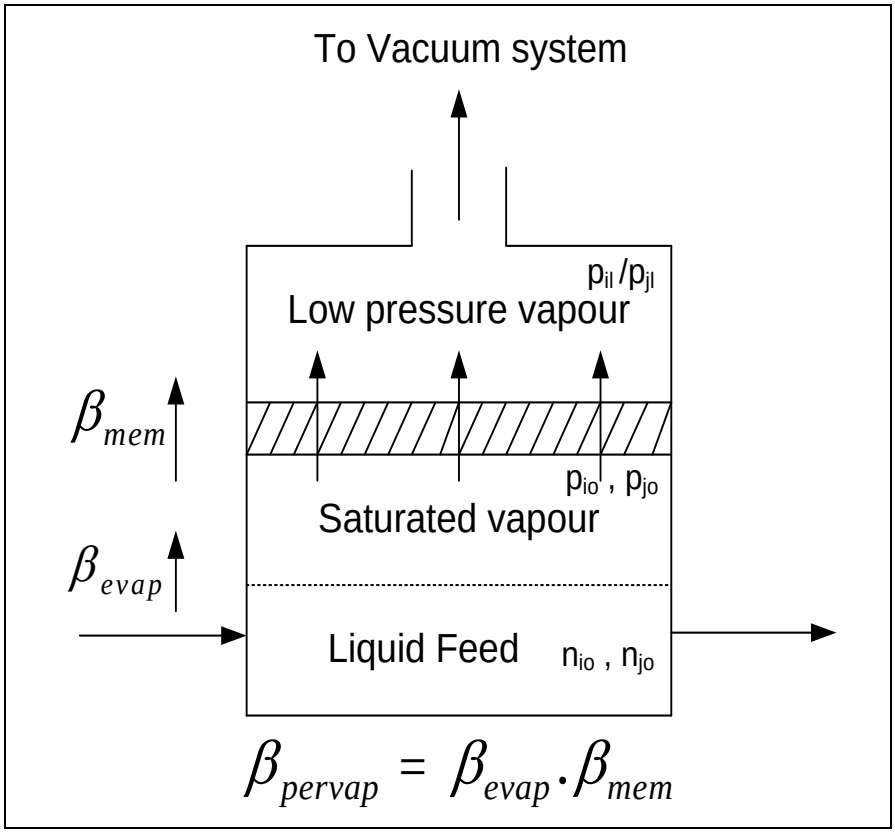

Figure 3.3: Pervaporation Process (Baker, 2004).

This evaporation step produces a separation because of the different volatilities of the components of the feed liquid. The separation can defined as β_{evap}, the ratio of the component concentration in the feed vapour to their concentrations in the feed liquid:

$$\beta_{evap} = \frac{p_{i_o} / p_{j_o}}{n_{i_o} / n_{j_o}} \tag{3.99}$$

The second step in the process is permeation of components i and j through the membrane, this step is equivalent to conventional gas separation. The driving force for permeation is the difference in vapour pressure of the components in the feed and

permeates vapours (Baker, 2004). The separation factor defined as β_{mem}, is the ratio of the components in the permeate vapour to the ratio of the components in the feed vapour:

$$\beta_{mem} = \frac{p_{i_l} / p_{j_l}}{p_{i_o} / p_{j_o}} \tag{3.100}$$

Therefore, the separation factor achieved in pervaporation is equal to the product of the separation achieved by evaporation of the liquid and the separation achieved by selective permeation through the membrane:

$$\beta_{pervap} = (\beta_{evap})(\beta_{mem}) \tag{3.101}$$

The evaporation separation factor, β_{evap} for the azeotropic mixture is 1 because, at the azeotropic concentration of the vapour and liquid phases have the same composition and is equal 1 again in the closely boiling point mixture, but a substantial separation is achieved due to the greater permeability of the membrane for the aromatic components. The membrane fluxes can be written as

$$J_i = \frac{P_i^G (p_{i_o} - p_{i_l})}{l} \tag{3.102}$$

$$J_j = \frac{P_j^G (p_{j_o} - p_{j_l})}{l} \tag{3.103}$$

Dividing equation 3.102 by equation 3.103

$$\frac{J_i}{J_j} = \frac{P_i^G (p_{i_o} - p_{i_l})}{P_j^G (p_{j_o} - p_{j_l})} \tag{3.104}$$

The fluxes J_i and J_j in equation 3.102 and 3.103 are weight fluxes (g/cm^2.s), similarly the permabilities P_i^G and P_j^G are weight based (g.cm/cm^2.s.cmHg). The equation 3.97 is more conveniently written in molar terms as

$$\frac{j_i}{j_j} = \frac{P_i^G (p_{i_o} - p_{i_l})}{P_j^G (p_{j_o} - p_{j_l})} \quad , \tag{3.105}$$

In these case j_i and j_j are molar fluxes with unit (mol/cm^2) or cm^3 (STP)/cm^2.s , P_i^G and P_j^G and molar permeabilities with units mol.cm/cm^2.s unit pressure or cm^3(STP).cm/cm^2.s.cmHg). The ratio of the molar membrane permeability coefficient P_i^G / P_j^G is the conventional gas membrane selectivity, α_{mem} .

The ratio of the molar fluxes is also similar as the ratio of the permeate partial pressures

$$\frac{j_i}{j_j} = \frac{p_{i_l}}{p_{j_l}} \tag{3.106}$$

Combining Equations 3.99, 3.100, 3.105 and 3.106

$$\beta_{pervap} = \frac{\beta_{evap}\alpha_{mem}(p_{i_o} - p_{i_l})}{(p_{j_o} - p_{j_l})(p_{i_o} / p_{j_o})} \tag{3.107}$$

Equation 3.107 identifies the three factors that determine the performance of a pervaporation system. The first factor, β_{evap}, is the vapour-liquid equilibrium, determined mainly by the feed liquid composition and temperature. The second in the membrane selectivity, α_{mem}, an intrinsic permeability property of the membrane material and the third includes the feed and permeate vapour pressure, reflecting the effect of operating parameters on membrane performance, α_{mem}.

According to Teng *et al.* (2000) the separation factor of ethanol/water is given by Equation (3.108)

$$\alpha = \frac{Y_{water} / Y_{ethanol}}{X_{water} / X_{ethanol}} \tag{3.108}$$

Where $Y_{ethanol}$ and Y_{water} are represents the weight fractions of ethanol and water in the permeate. $X_{ethanol}$ and X_{water} are representing the weight fractions of ethanol and water in the feed.

In this study, pervaporation membrane flux was calculated using the following equations

$$J = \left(\frac{Volumetric\ \ flowrate}{surface\ area} \right) * density = \left[\frac{kg}{m^2.s} \right] \quad (3.109)$$

Or $$J = \frac{Q}{A * T} \quad (3.110)$$

Where Q is the total mass of permeate collected through the effective area of membrane (A) during time, T is the temperature after the steady state has been reached.

CHAPTER 4

EXPERIMENTAL PROCEDURE

PART I: VAPOUR-LIQUID EQUILIBRUIM

4.1 Introduction

In this chapter, the experimental equipment and procedures are presented. The equipment used for the assessment of salt as an extractive agent was a low pressure VLE still of Joseph (2001) and associated chemicals analysis equipment. The equipment used for the pervaporation studies was a unit constructed and tested specifically for this study. Details of the constructed unit and the associated analysis equipment are presented.

The criteria used for choosing the test system were:

- The system must be non-ideal (the classification of Danner and Gess, 1990) for ideal and non-ideal system was used)
- The literature data for the binary system must be consistent
- The chemicals of the binary system must be available at a high purity (>99% pure)
- The chemical must be available at a reasonable cost

- The chemical must be non-toxic
- The chemicals must be stable

4.2 Description of the VLE recirculating still

The low pressure VLE still (Raal and Mühlbauer, 1998) was used for VLE experiments of this project. The VLE still is constructed from specially blown glass and is suitable for low pressure measurement. It was tested using non-ideal mixture of ethanol and water according (Raal and Mühlbauer, 1998). Refer to Figure 4.1 for a schematic of the VLE re-circulating still. The capacity of the VLE still is approximately 170 – 180 ml and this is slightly variable with regards to the pressure and temperature range (as affecting the density of the vapour phase), the thermophysical properties of the chemical components (thermal expansivities, volatilities, etc) and the circulation rate as controlled by heat input into the still. The chemical components were fed slowly into reboiler using 10 ml plastic syringe until the liquid level was just above the boiling chamber. A special feature on the still is the Cottrell pump, which is pressure, jacketed to prevent the superheated mixture from transferring heat to the packed chamber, where the separation takes place. The packed chamber is an annular space which houses 3 mm stainless steel wire mesh packing. A thermowell is embedded in the packing chamber where the temperature of the two phase mixture is measured using a Pt-100. The mixture then exits through small holes at the bottom of the packed chamber where the phases separate.

The liquid phase collects in the sampling chamber and the overflow is directed to the reboiler through a liquid return line. The vapour enters the condenser. The circulation of cooling water is used to condense the vapours and the condensate collects in a sampling chamber or condenser receiver. The temperature of the cooling water must be 268.15 K. It is important that the pressure used be higher than the vapour pressure of the components at the temperature of the still to prevent the occurrences of flashing during the introduction of the second component into still. The overflow of the vapour sample chamber is directed to the reboiler through a tube that feeds into the liquid return leg through a capillary tube to reduce flashing, the cold vapour (rich in volatile component) coming into contact with the hot liquid (rich non volatile component). Both sampling

chambers contain magnetic stirrers to reduce flashing and uniform composition. These chambers allows for sampling through septa without interrupting the boiling.

Heating supplied in the boiling chamber

There are two heaters connected in the boiling chamber or reboiler. These are internal and external heaters. The external heater of the equilibrium chamber was then turned on and initial heating was at a low voltage input (usually 20V) from the respective Chuan HSIN (model: SRV – 10) variable voltage transformers (0 – 240V). This compensates for heat loss to the surroundings. The internal heater is used to directly control boiling or smooth boiling of the mixture. Increasing the voltage the internal heater with the small increment until the plateau region is reached. The mixture was heated in the boiling chamber or the reboiler via a cartridge heater, which heats the inside of the chamber, while a nichrome wire wrapped around the chamber heats the outer surface of the chamber. The cartridge sits in a glass sheath which has the surface exposed to the liquid activated with powered glass in order to promote vapour bubble formation.

The Limitations of LPVLE dynamic still

The greatest limitations in the operation of LPVLE dynamic recirculation apparatus are:

- The attainment of a true equilibrium (Marsh, 1989).
- The partial condensation of the vapour phase in the equilibrium chamber.
- The inability to achieve smooth boiling and an equilibrium state with minimal fluctuations in pressure and temperature.
- Avoid superheating of the mixture.
- The determination of the true values of equilibrium temperature and vapour compositions (Abbott, 1986).

Experimental requirement

In order to obtain the isobaric VLE data, certain parameters need to be determined experimentally or controlled:

- Pressure in the still must be controlled and maintained steady
- Equilibrium temperature of the vapour and liquid must be measured
- The vapour and liquid sample must be taken at time intervals and must be analyzed using a gas chromatograph for mole fractions of the respective components

Chemicals

The non-ideal mixtures ethanol-water system was used in the VLE still. Distilled water, high purity acetone (99.2%), high purity ethanol (99.5%) and calcium chloride salt were used. Ethanol and acetone were purchased from Merck Chemicals Laboratories and calcium chloride was purchased from DLD Scientific. The acetone was used for cleaning purposes. The chilling water from Labcon low temperature water bath CPM 50 was used as a coolant in the shell of the condenser at the temperature of 268.15 K.

Equipment

The precision class A Pt-100 temperature probe was used to measure equilibrium temperature with a minimum error of ±0.01 K. The Pt-100 temperature probe was calibrated using bath oil WIKA CTB 9100 and WIKA temperature probe which was connected to WIKA CTH 6500 multi-meter. The uncertainty in the temperature reading was ± 0.03 K. Measured equilibrium temperature was interpreted and display in ohms by the Agilent digital multi-meter.

The pressure was controlled below atmospheric using a KNF vacuum pump controller (type NC800). The system pressure was monitored with the aid of a Sensotec Super TJE pressure transducer. The pressure was set using BÜCHI vacuum controller B-721 and the signal from the transducer was interpreted and displayed in ‘kPa’ by a Sensotec Model

HM display. The pressure display was calibrated with WIKA CPH 6000 unit. The uncertainty in the pressure reading was ± 0.05 kPa.

The thermodynamic equilibrium was estimated to be reached when the pressure measured remained constant for at least 45 minutes. Thereafter, vapour and liquid samples were withdrawn for composition analysis. The analytical tool used was a gas chromatograph Shimadzu, type HP 5890 series II. Each vapour and liquid was analysed three times in the GC to determine vapour and liquid composition, with the average of the three being taken as the final value. The separation was performed using a LANGET column, 3 m length, 2.2 mm i.d., o.d 3.2 mm, column material S/S and support was carbosieve S-11 using the helium as the carrier gas at a pressure of 150 kPa. The maximum column temperature was 523.15 K. The analysis was realized using a thermal conductivity detector (TCD) kept at column temperature of 453.15 K with a current set at 70 mA. The procedure for calibrating the GC was the area ratio method, as discussed by Raal and Mühlbauer (1998).

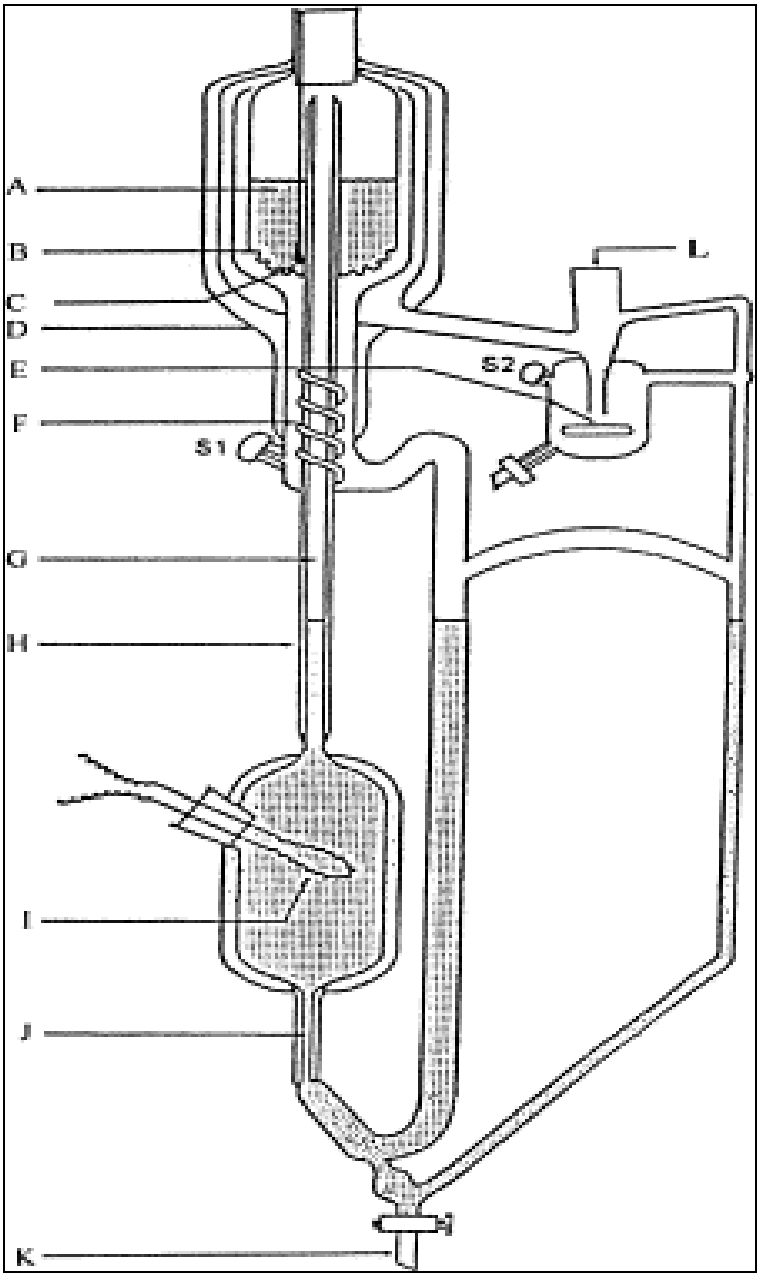

Figure 4.1: Schematic diagram of vapour liquid equilibrium still (Raal and Mühlbauer, 1998) A: SS wire mesh packing; B: drain holes; C: Pt-100 bulb; D: pressure jacket; E: magnetic stirrer; F: SS mixing spiral; G: insulated Cottrell pump; H: pressure jacket; I: internal heater; J: capillary; K: drain valve; S1: liquid sampling point; S2: vapour sampling point; L: condenser is attached here.

4.3 Experimental procedure for the VLE still

Air Leaks

An air leak test was performed by drawing a vacuum in the dry still, using a vacuum pump at low pressure of 20 kPa. When pressure was reached 20 kPa, the pressure pump was switch off. Air leak in the system can be identified by the increase in pressure or the controller is not reached the set point. Then check all drain valves that are fully closed and joins, fittings and septa in the VLE still. A very small air leak in the system causes one of the components in the VLE still to evaporate.

Start-Up Procedure

- Check that all the drain valves that are closed
- Add approximately 80ml of component one through the liquid sampling septum into the reboiler. Allow for the capillary tube to raise at least 3 – 4 cm above reboiler.
- Close both liquid and vapour sampling septum points
- Switch on Pt-100 temperature sensor
- Set pressure at 40 kPa and switch on pressure pump
- Set chilling water temperature at 268.15 K and allow chilling water to circulate in the condenser
- Wait for chilling water temperature and the pressure to reached the set points
- Switch on internal and external heaters
- Set external heater at 40 Volts
- Switch on both magnetic stirrers
- Find the plateau* region by increasing the voltage of the internal heater with a small increment (5 Volts).
- Record temperature and pressure
- Switch off internal and external heaters
- Add component two in 3ml increments into the liquid sampling port; switch on internal and external heaters and find the plateau region for each mixture composition

- Take 1µL liquid and vapour samples, at regular intervals, through their respective sampling septa for analysis in the GC
- Normally the equilibrium is attained in 60 minutes.

Shut down Procedure

- Turn off heaters, magnetic stirrer and vacuum pump
- Set atmospheric pressure by opening both liquid and vapour sampling septum (slowly)
- Stop cooling water circulation in the condenser
- Open drain valve to empty the VLE still

Cleaning the VLE Still

This is done by circulating acetone in the VLE still under atmospheric pressure

- Add 80ml of acetone into the still via the liquid sampling septum
- Set atmospheric pressure
- Find plateau*region. Allow the acetone to boil for 45 minutes and collect liquid and vapour samples for GC analysis. If the samples showing more than one peak on a gas chromatograph then repeat acetone wash until the gas chromatograph reveals one acetone peak.
- Drain out acetone by opening drain valves.
- Set the pressure at 20 kPa and switch on the vacuum pump for 10 minutes to dry the acetone residue from still.

4.4 VLE Still Setup

The condenser of the VLE still is connected to the ballast flask, which serves to reduce pressure fluctuations and to trap condensable chemicals if the condenser fails. A vacuum pump controller unit was used to evacuate the still and to maintain a constant pressure. The vacuum pump draws incondensable gases from the VLE still. Once the set point pressure has been achieved the controller shuts off the vacuum pump. If and when this set

point pressure is exceeded then the vacuum pump is switched on. A needle valve installed between the vacuum pump and the VLE still was used to throttle the flow through the pump, which ensures that a pressure fluctuation was minimized.

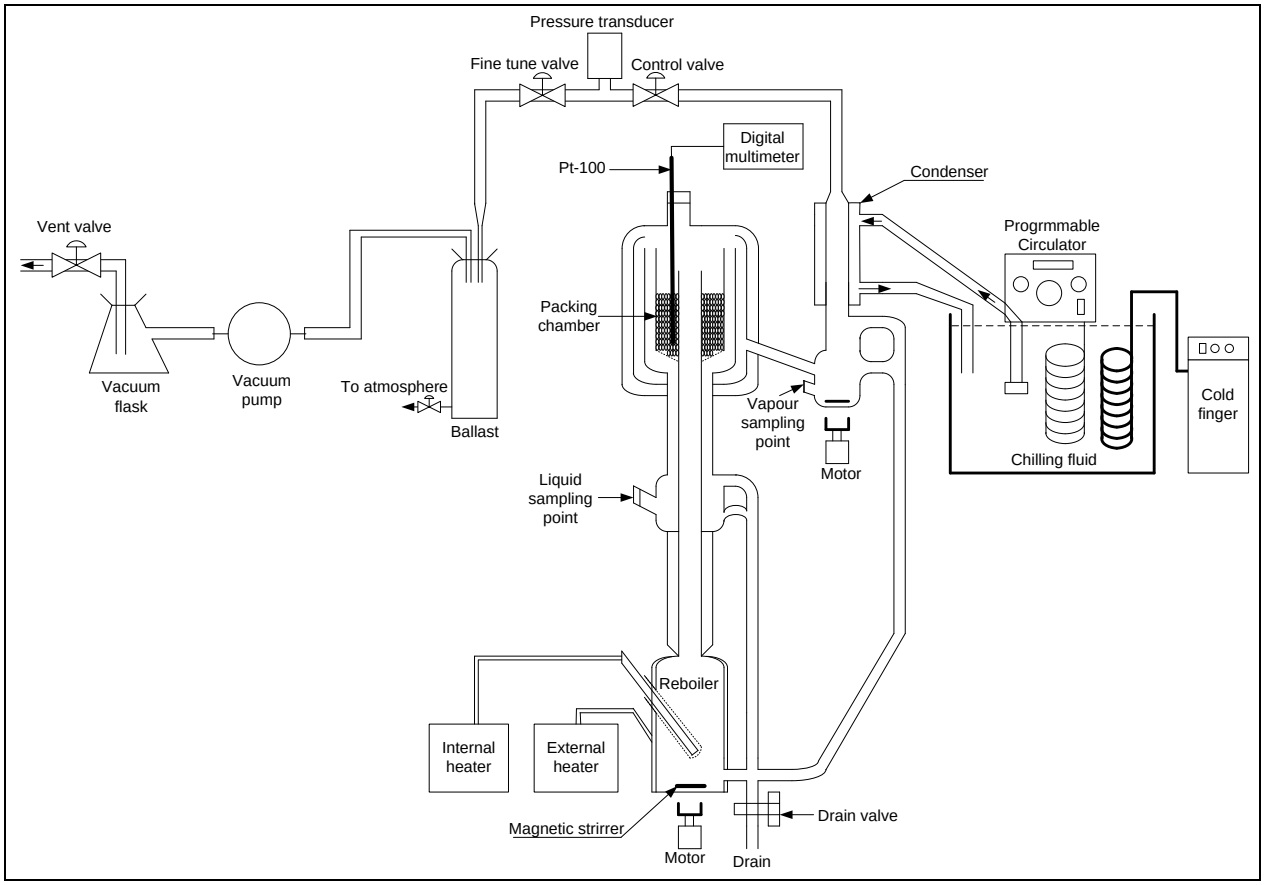

Figure 4.2: Schematic of the equipment layout.

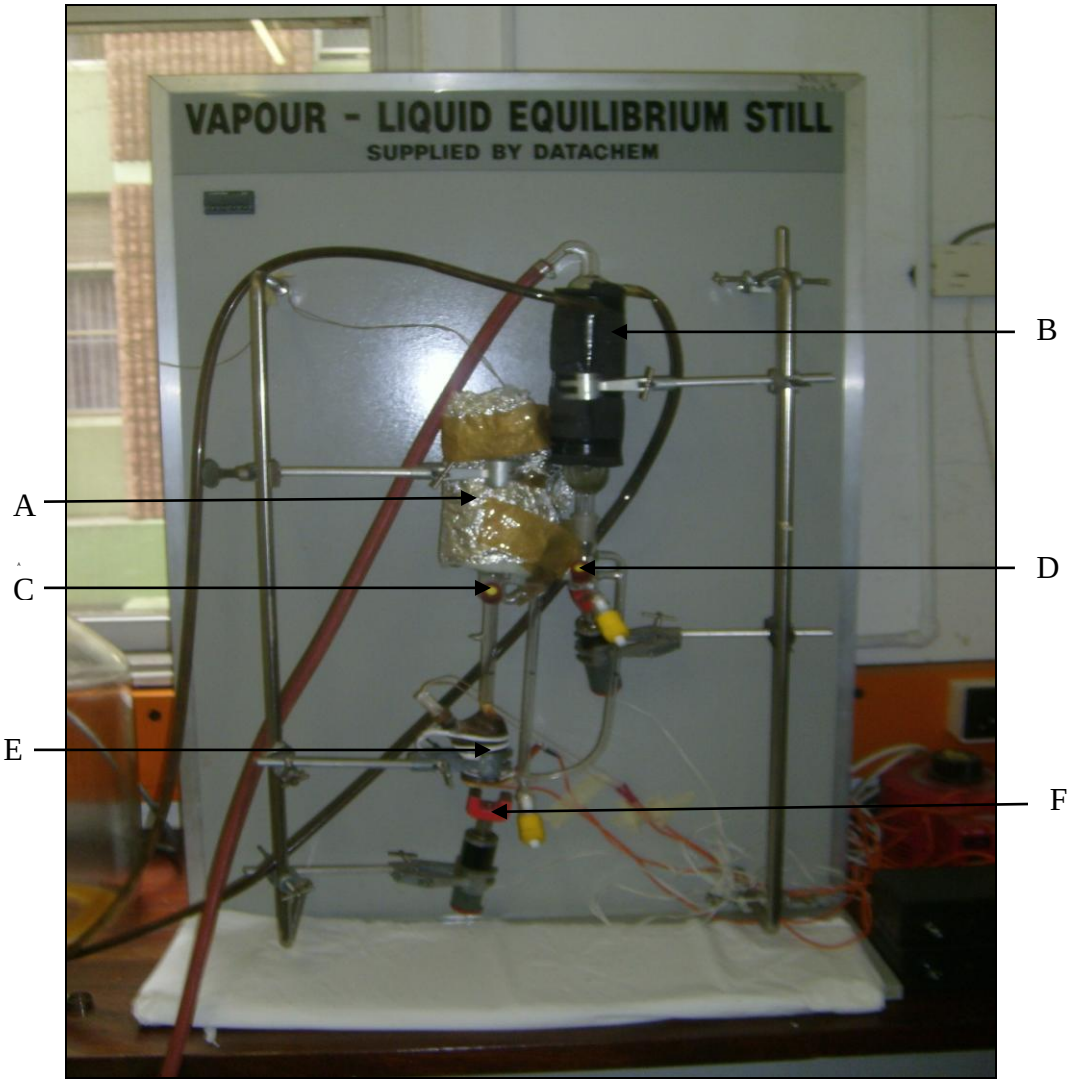

Photograph 4.1: Vapour-liquid equilibrium still set-up (A: Equilibrium chamber, B: Condenser, C: Liquid sample point, D: Vapour sample point, E: Reboiler and F: Magnetic stirrer).

4.5 VLE Still Parameters Calibrations

Pressure Calibration

The atmospheric pressure was measured using the calibrated electronic pressure transducer or barometer. The PTB101B series barometer was connect to the multimeter and the reading of resistance was taken; the multimeter was set VDC. The barometric pressure or atmospheric pressure can be calculated from the measured output voltage (U) using a simple equation:

$$P_{atm} = 600hPa + \frac{460hPa}{2.5V} * U[V] \qquad (4.1)$$

Where the unit of hPa is hectapascals

The mercury (Hg) manometer was connected parallel to the pressure transducer display of the pressure controller for the calibration. The pressure was set from 100 kPa to 10 kPa.

The values of mercury manometer were compared with the values of the pressure transducer display. The linear relationship between the actual pressure and VLE still pressure display shows the accuracy of the pressure transducer. A vacuum pump was used to control the set point pressure below atmosphere. The uncertainty in the pressure reading is ± 0.05 kPa. The pressure calibration curves are presented in Appendix C in Figure C3.

Temperature Calibration

A Pt-100 thermowell sensor was embedded in the packing chamber and it is used to measure the temperature of the two phase mixture traveling down the packing where equilibrium is reached. The sensor was calibrated by running the VLE still at atmospheric pressure with highly pure components (in this case were acetone and ethanol) and the boiling point temperature was noted and compared with the actual boiling point temperature from the literature. According to Raal and Mühlbauer (1998) the recirculation VLE still was charged with 80 ml of pure component and at various set

point vapour pressure, the boiling temperatures were recorded. The linear relationship between the actual boiling point temperature of ethanol and the saturation temperatures of ethanol calculated using the Antoine equation shows the accuracy of the sensor reading. The purity of the ethanol was 99.5%. The uncertainty in the temperature reading is ± 0.01 K. The temperature calibration curve is included in Appendix C in Figure C2.

The plateau region

The boiling point temperature where remains unchanged when the power input increased by small increments is called a plateau region. The still was charged with a pure component namely (ethanol) and operating at the pressure of 40 kPa. The attainment of a plateau region for the system temperature on the isobaric mode, as a function of small voltage increment (~ 5V or 10V) from the variac into the internal heater in the reboiler. The external heater must be kept constant at 20V. With each voltage increment, the system was allowed a response time of 20 – 30 minutes before the next voltage increment. When a stable temperature reading was recorded as a function of energy input for a satisfactory time or voltage increment period, the first of the two principal for the determination of the equilibrium condition was satisfied. The drop rate in the condenser ranged between 60 – 100 drops per minute in the still.

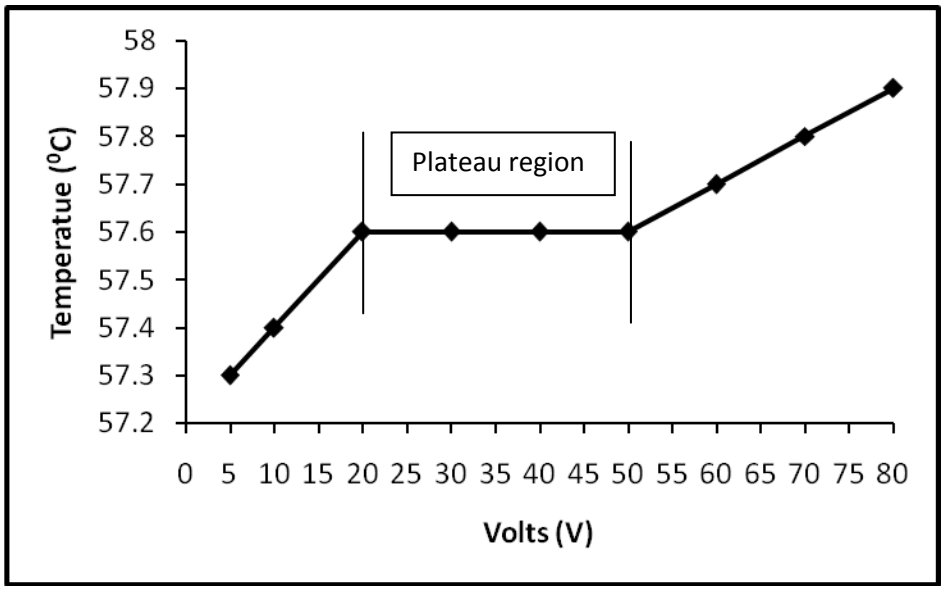

Figure 4.3: Plateau region for pure ethanol at 40 kPa.

Gas chromatography (GC) Calibration

It is important to calibrate the GC detector (Raal and Mühlbauer, 1998) as the percentage composition given by the integrator may not be a true representation of component mole fraction. Binary systems exhibit the following relationship in the dilute regions.

$$\frac{x_1}{x_2} = \frac{1}{G}\frac{A_1}{A_2} = \frac{n_1}{n_2} \qquad (4.2)$$

where: x = mole fraction in the sample

A = is the produced by the GC integrator or GC peak area

G = is the response factor

The determination of vapour and liquid sample composition of the binary mixture are gravimetrically produced and analysed by the GC. As ternary measurements were all on a solvent-free basis binary calibrations were sufficient. The prepared samples covered the composition range of mole ratios equal to 0 up to 1.2.. Six or more samples are usually necessary for calibration. Two plots are produced from the calibration data. The first is a plot of x_1/x_2 vs A_1/A_2 and the x_1/x_2 values range from 0 to 1.5. The second plot is x_2/x_1 vs A_2/A_1 with the range values of 0 to 1.2. Both plots are linear and the gradient of plot 1 is compared to the inverse of the gradient of plot 2. The gradient is equated to the response factor (Raal and Mühlbauer, 1998). The uncertainty in the GC detector for the composition analysis for the systems investigated is ± 0.005.

To solve for the individual mole fractions or compositiona, using the GC Areas obtained from the chromatograph, if x_2/x_1 = a and for ternary measurements x_3/x_1 = b, x_4/x_1 = c, etc, then:

for a binary system

$$\frac{1}{x_1} = 1 + \frac{x_2}{x_1} = 1 + a \qquad (4.3)$$

for ternary measurements

$$\frac{1}{x_1} = 1 + \frac{x_2}{x_1} + \frac{x_3}{x_1} + \frac{x_4}{x_1} = 1 + a + b + c \tag{4.4}$$

for binary system

$$x_1 = \frac{1}{1 + a} \tag{4.5}$$

In general or for ternary measurements

$$x_1 = \frac{1}{1 + \sum_{i=2}^{n} \left(\frac{x_i}{x_1} \right)} \tag{4.6}$$

Photograph 4.2: The HP 5890 series II (TCD) gas chromatography.

PART II: PERVAPORATION

4.6 Description of the cylindrical pervaporation cell membrane

The cylindrical pervaporation cell membrane was constructed using PVC, bolts, lock nuts, rubber gasket, PVC flanges, Pt-100 and flexible hose for pressure line, feed line and retentate line. Figure 4.4 and 4.5 shows a diagram of the pervaporation cell or unit. The cell has the top part and the bottom part. Both parts have equal dimensions. The height of the top part including the flange was 100 mm and outside diameter 80 mm. Similar to the bottom part. The feed line was located 10 mm from top of the cell and retentate line was 70 mm from top of the cell. The diameter of the cell was 80 mm. The flanges were square with a length of 140 mm. The bolts holes were 10 mm from the edge of the flange. The rubber gasket has the outside diameter of 96 mm and inner diameter of 80 mm. The flat membrane was cut with the diameter of 96 mm. The support stainless steel wire gauze was 98 mm in diameter.

A flexible 10 mm hose was used for the connections of feed line, retentate line and pressure line. The pressure line was connected in the bottom part of the cell from 20 mm bottom edge of the cell. The wire gauze was sitting between gasket of the top part and the bottom part to support the flat sheet membrane. The flat sheet membrane was placed on top of the wire gauze between the top gasket and bottom gasket as shown in Figure 4.4. The gasket was used to prevent leaking between the flanges and the flat sheet membrane. The flanges have 8 holes for bolts as shown in Figure 4.5. Close the top part and bottom part using 8 bolts and nuts as shown in Figure 4.6. The Pt-100 was installed in the top part of the cell to measure the temperature of the mixture inside the cylindrical cell. The pressure indicator was connected on top of the cell to read the pressure inside the cell. The cell was operating below atmospheric pressure. The operating pressure was controlled using the vacuum pump as shown in Figure 4.7.

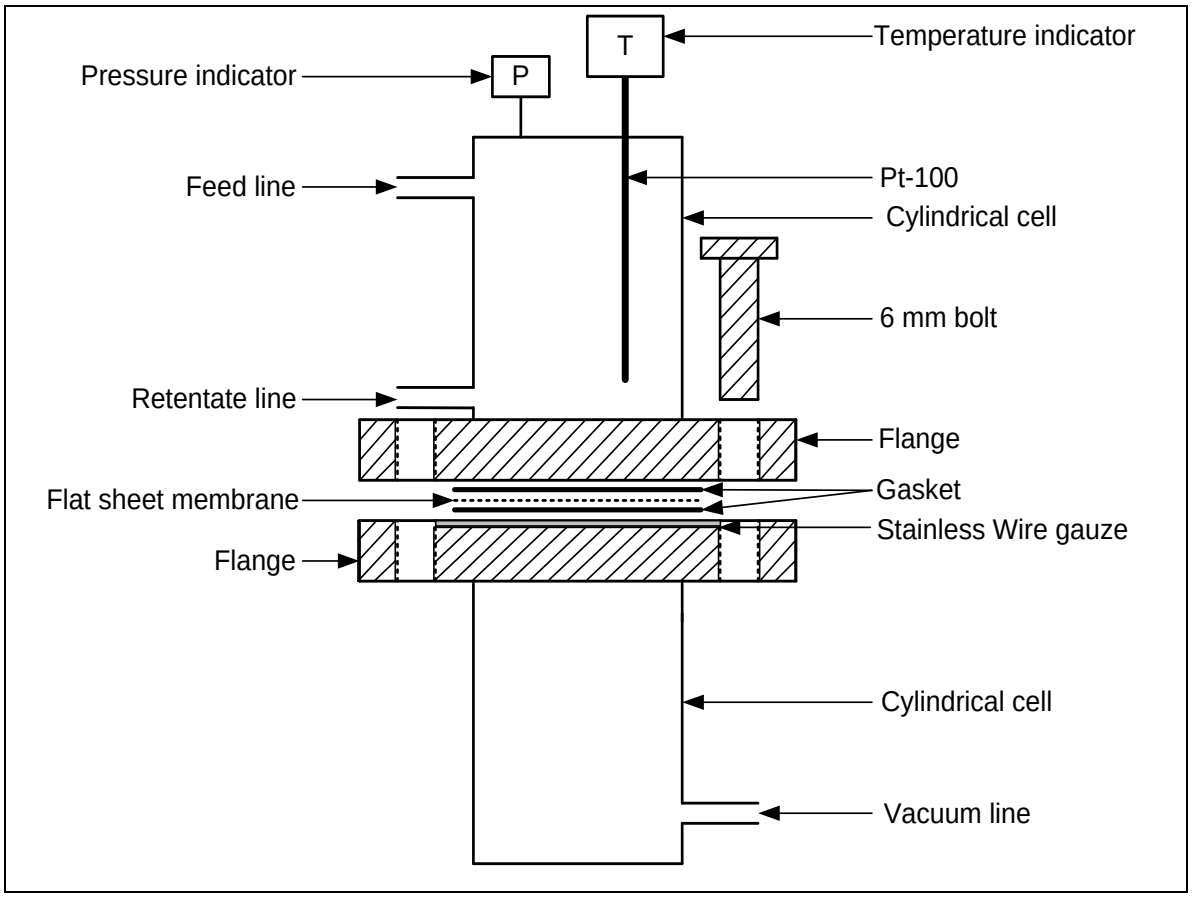

Figure 4.4: Cross-sectional of the cylindrical pervaporation cell.

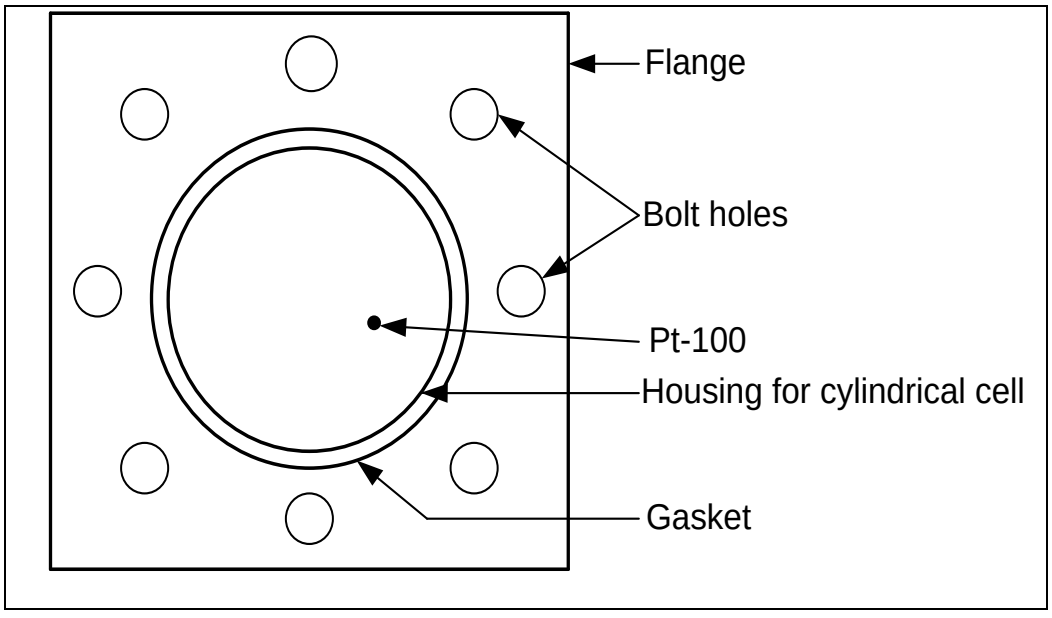

Figure 4.5: Top view of the cylindrical pervaporation cell.

Check air leak

In order to check for air leaks, the cylindrical cell was closed tightly and connected to a vacuum pump. The feed and retentate valves were closed. The vacuum pump was switched on and set at a low pressure of 20 kPa. Once a pressure of 20 kPa was reached, Snoop® was used to check for leaks in the pipe connections, flanges and lock nuts. Before switching on the system, the pressure was set at 20 kPa and one had to wait for 15 minutes. If the set pressure was not reached or there were fluctuates, then there was a possibility of leaks somewhere in the system. The air leaks could cause the ethanol to evaporate or water vapour to escape.

Description of the pervaporation process

The heated mixture of ethanol and water in the storage feed tank was pumped using an adjustable centrifugal pump to the filter. The mixture from the filter was passed through the flow meter and entered at the top of the cylindrical membrane cell. The pump was run at the different speeds to change the flow rates. The separation of the ethanol/water mixture took place inside the cylindrical membrane cell. The vacuum pump was connected to the top of the condenser using vacuum tubing. The vacuum in the cell was drawn through the vacuum line attached to the bottom part of the cell via the condenser. The condenser was connected at the top of the permeate tank. The chilling water was circulated in the shell of the condenser at the temperature of 268.15 K. As the vacuum pump drew the water vapour from the membrane from the cell, the water vapour condensed. The liquid was collected in the permeate tank. The vacuum flask was used to collect excess gas and it was connected in line with the vacuum pump as shown in Figure 4.7. The samples were taken from the collected volume in the permeate tank and in the feed tank for analysis. The refractometer and Karl-Firscher apparatus were used for analyses.

Ethanol of 99.5% purity was diluted with distill water to the concentration of 90 wt% ethanol and 10 wt% water. The acetone was used for cleaning. The separation of ethanol-water system at concentrations of 90% ethanol and 10% water to 99% ethanol to 1% water was studied using pervaporation at different operating pressure from 20 kPa to 80

kPa and temperatures from 313.15 K to 343.15 K. The pressure on the pervaporation system was controlled using the vacuum pump which was connected in the pressure flask via the condenser or cooler to the permeate side of pervaporation unit. The chilled water was circulated in the condenser at the temperature of 268.15 K. The temperature of the pervaporation system was controlled using the heating coil inside the feed tank. The ethanol-water mixture was heated and recirculated for 2 hours before the samples were taken for analysis. The water was collected in the permeate tank.

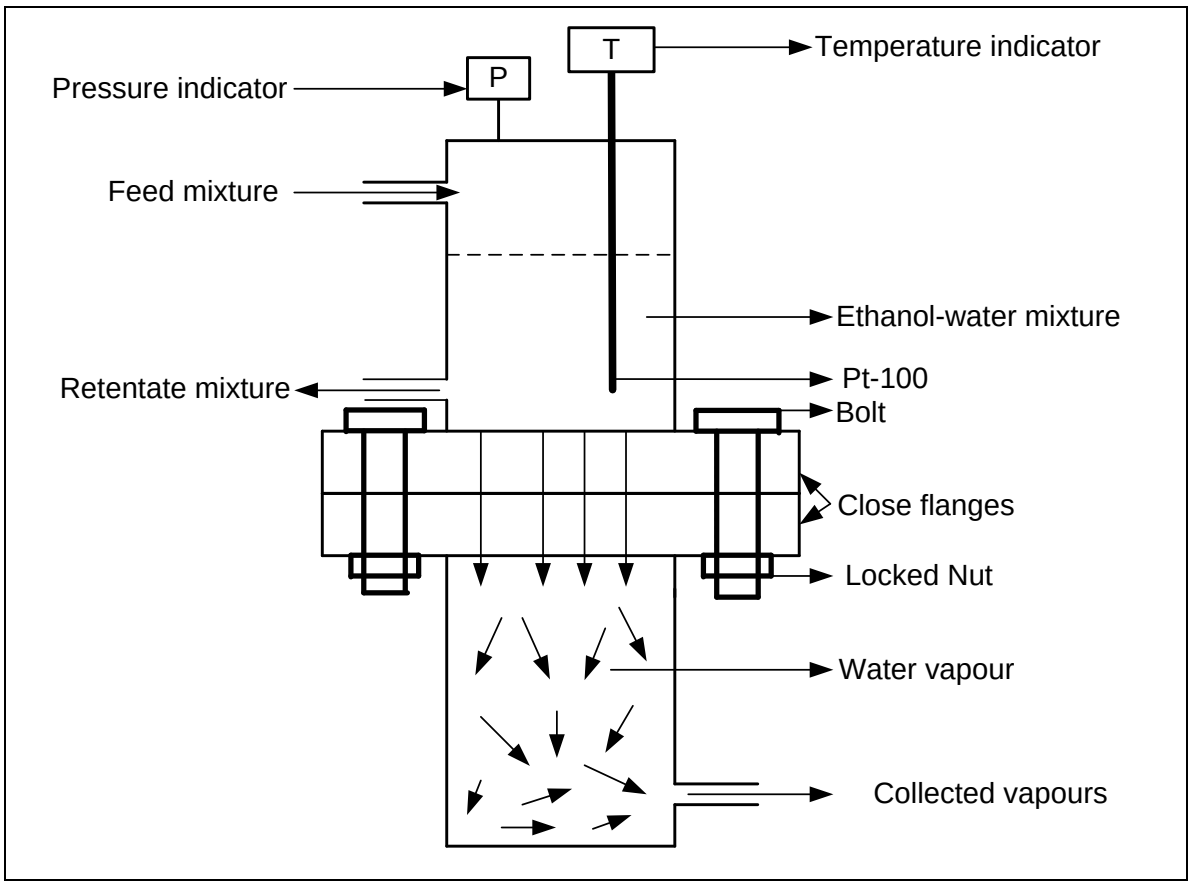

Figure 4.6: Cylindrical pervaporation cell.

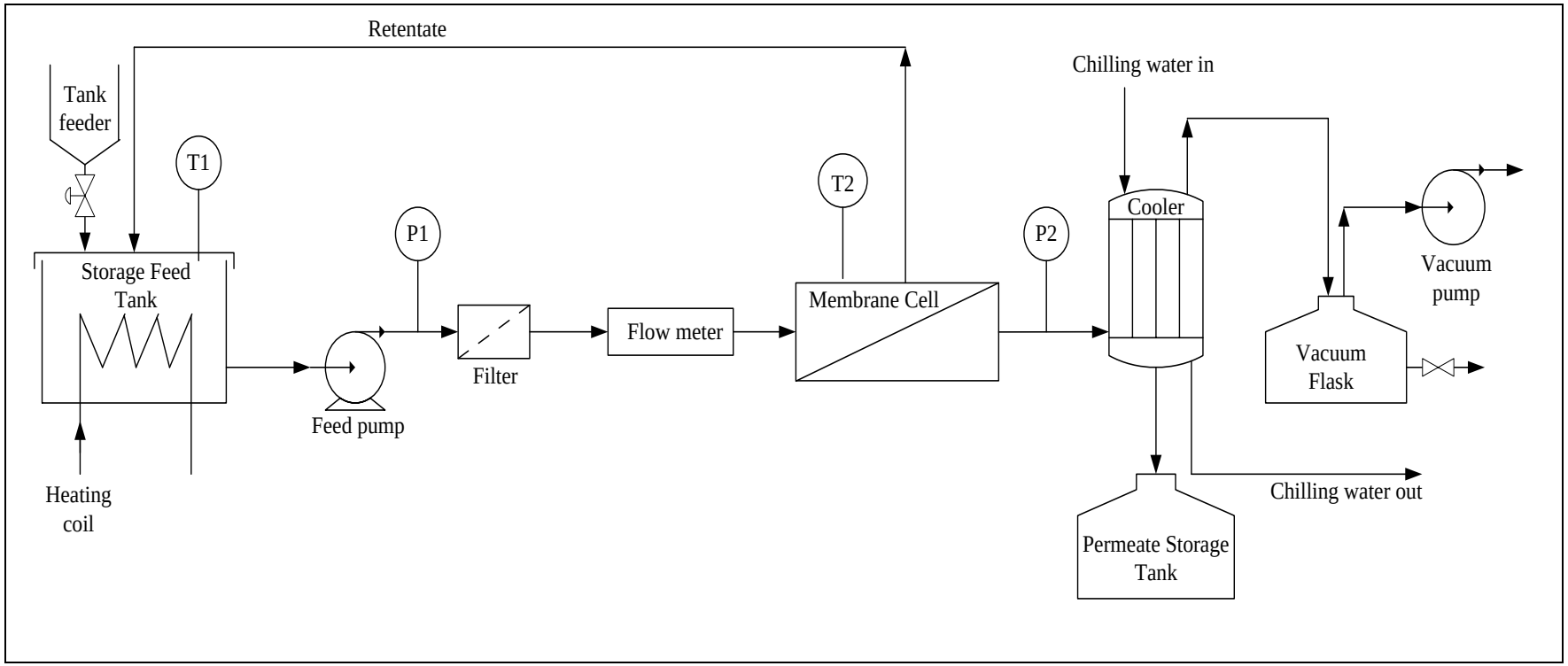

Figure 4.7: Schematic diagram for the pervapoartion process set-up.

Chemicals and materials

Distilled water, high purity acetone (99.2%) and high purity ethanol (99.5%) were used. Ethanol and acetone were purchased from Merck Chemical Laboratories. The low pressure pervaporation membrane cell was design and constructed at the School of Chemical Engineering, Durban University of Technology. The pervaporation polymer dehydration membrane was purchased from Sulzer Chemtech in Germany and this membrane was a composite membrane consisting of a very thin separation layer on top of a porous support, coated on a polymer fleece. The type of the pervaporation membrane used in this study was composite flat sheet membrane 1210 and the specification is listed in Table 4.2. The active area of the pervaporation membrane used in the cell was 0.0055 m^2 and the membrane was supported by wire gauze. In this study, the pervaporation membrane used was a hydrophilic membrane; which is a membrane that removes water. The chilling water from the Labcon low temperature water bath CPM 50 was used as a coolant in the shell of the condenser at the temperature of 268.15K.

Equipment

A precision class A Pt-100 temperature probe was used to measure the temperature inside the pervaporation cell with a minimum error of 0.01K. The Pt-100 temperature probe was calibrated using bath oil WIKA CTB 9100 and WIKA temperature probe which was connected to WIKA CTH 6500 multi-meter. The measured equilibrium temperature was interpreted and display by a Sensotec Model HM display.

The pressure was controlled below atmospheric using a KNF vacuum pump controller (Model NSE 800). The system pressure was monitored with the aid of a WIKA pressure transducer (Model D – 10 – P) and it range from 0 – 1.6 bar absolute. The pressure was set using BÜCHI vacuum controller V–800 and the signal from the transducer was interpreted and displayed in 'kPa' by a Sensotec Model HM display. The pressure transducer was calibrated using WIKA instrument CPH 6000 unit. A Watson Marlow (peristaltic pump 323 or centrifugal pump) was used to pump the ethanol/water mixture from the storage feed tank to the pervaporation cell. Polyscience circulator temperature controller was used to heat the water in the water bath in order to heat the mixture to the

set point temperature. The storage feed tank was immersed in the water bath. The magnetic stirrer was used inside the storage feed tank in order to keep the compositions constant.

After 2 hours the volume collected in the permeate tank was recorded as well as pressure and temperature. Thereafter, the sample from the permeate tank and from the retentate stream were taken for analysis. The analytical tools used were the Metrohm Karl – Fischer (Model 702 SM Titrino) with a 20 ml burette and ATAGO RX-7000α refractometer was used to measured the refractive indices of the retentate and permeate.

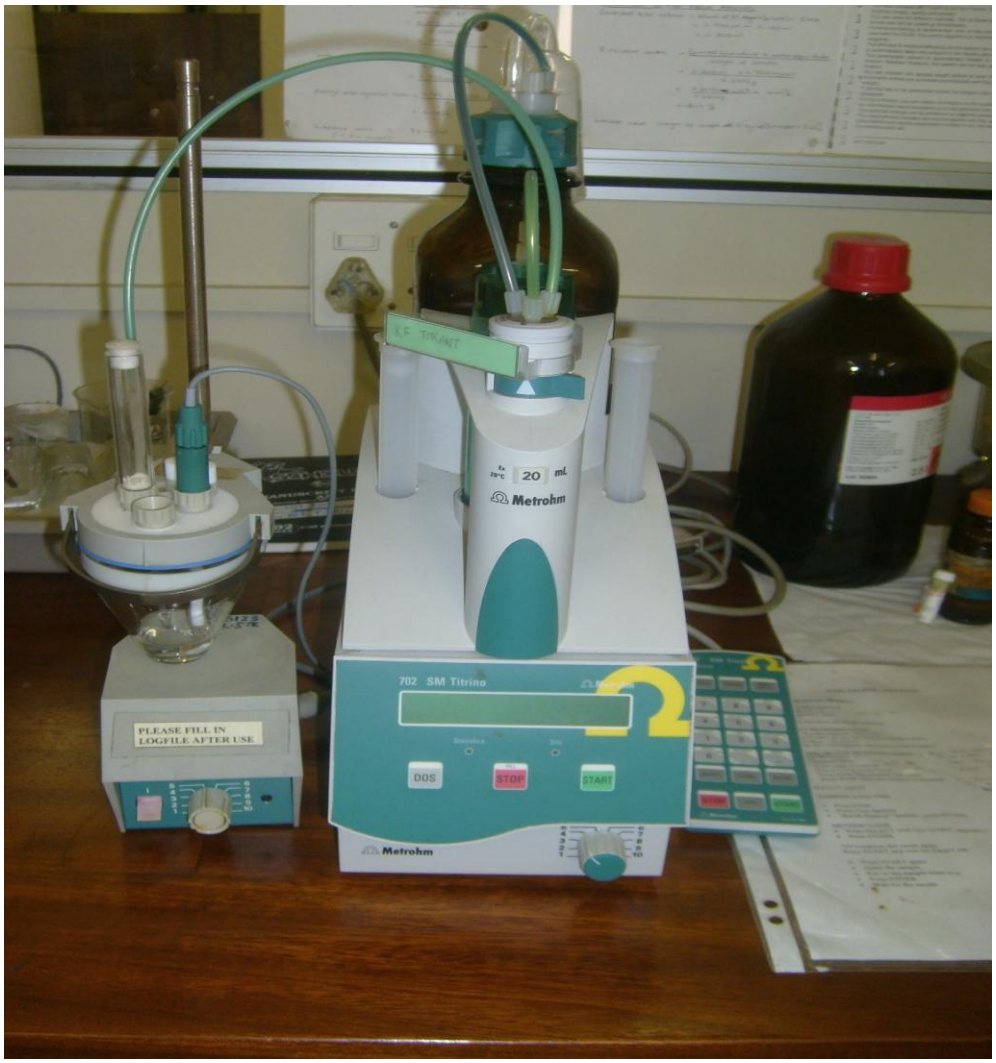

Photograph 4.3: Karl-Firscher instrument.

In this study, the Sulzer Chemtech polymer pervaporation membranes used was composite membrane consisting of a very thin separation layer on top (polyvinylalcohol) of a porous support (polyacrylonitrile) coated on a polymer fleece (polyester) as shown in Figure 4.8.

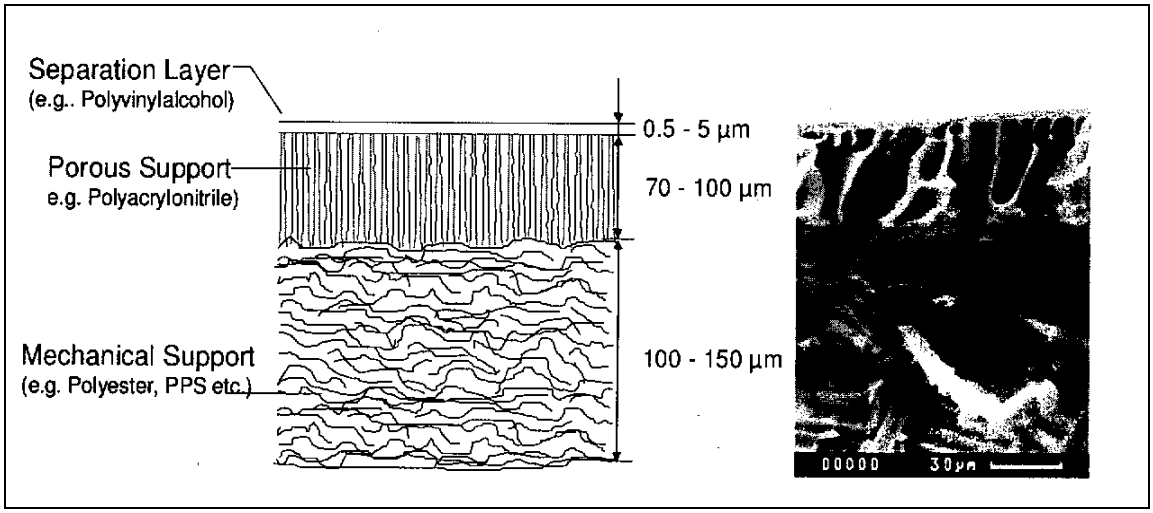

Figure 4.8: Polymer pervaporation membrane (Published with permission from Sulzer Chemtech).

4.7 Experimental procedure for the pervaporation process

Start-up procedure

- Prepare a solution of ethanol/water mixture in the beaker and fill into the storage tank vessel.
- Switch on the chilling water until the temperature is 5^0C and allow the cold water to circulate in the condenser.
- Place the polymeric pervaporation membrane in the membrane cell; place the membrane onto the wire gauze support. Place the top rubber gasket and close the cell tight and evenly using eight bolts provided.
- The known mixture of ethanol and water was immersed in the water bath.
- The water bath was heated up to the set temperature (313.15, 323.15, 333.15 and 343.15) K.
- Check that all valves and all pipes are fitted properly.

- Set the operating pressure and start the pressure pump..
- Wait for the system to stabilize.
- Circulate the mixture in the feed tank until set temperature is reached.
- Switch on the feed pump, then the mixture enters the pervaporation membrane cell unit and re-circulate back into the feed tank.
- Start the stop watch.
- Wait for 2 hours to collect the volume of permeate (water).
- Take a sample from the permeate tank and the retentate line for analysis
- The sample must be taken every 2 hours.

Experimental run

This consisted of letting the run continue with sampling of the retentate and permeate taken every two hours to verify that the composition was reproducible. When this was satisfied then the composition of the feed was changed accordingly (after the refractive index and hence the composition was known).

Shutdown procedure

- Stop the pressure pump
- Stop the feed pump
- Switch off heaters in water bath
- Wait for 5 minutes in order to collect all the condensed vapours
- Open membrane cell unit
- Remove the pervaporation membrane from the cell unit
- Place the membrane on the clean flat surface.
- Drain the feed tank

.

Cleaning procedure

- Clean top and bottom the cylindrical cell with soft brush using acetone.
- Clean the gasket, wire gauze support and bolts.

- Close the cell and dry it under vacuum.
- Open the cell to check that there is no black stain or black spot in the pervaporation cell.
- Rinse the feed tank with acetone and dry it.

Pervaporation test cell or calibration

The pervaporation method was tested at the high temperature and low pressure in order to make sure that the pervaporation unit provides consistent results. The ethanol-water mixture was prepared and run at the temperature of 343.15 K and pressure of 80 kPa. The mixture was run at constant temperature and pressure for 10 hours, during the first 1-2 hours the water flux was increasing and from two hours to ten hours the water flux obtained was constant and it showed that the volume collect every two hours was constant. The volume collected during this period showed that the pervaporation cell provides accurate results. This calibration was repeated twice for consistency. Figure 4.9 confirms that cell can be used to perform the ethanol-water system.

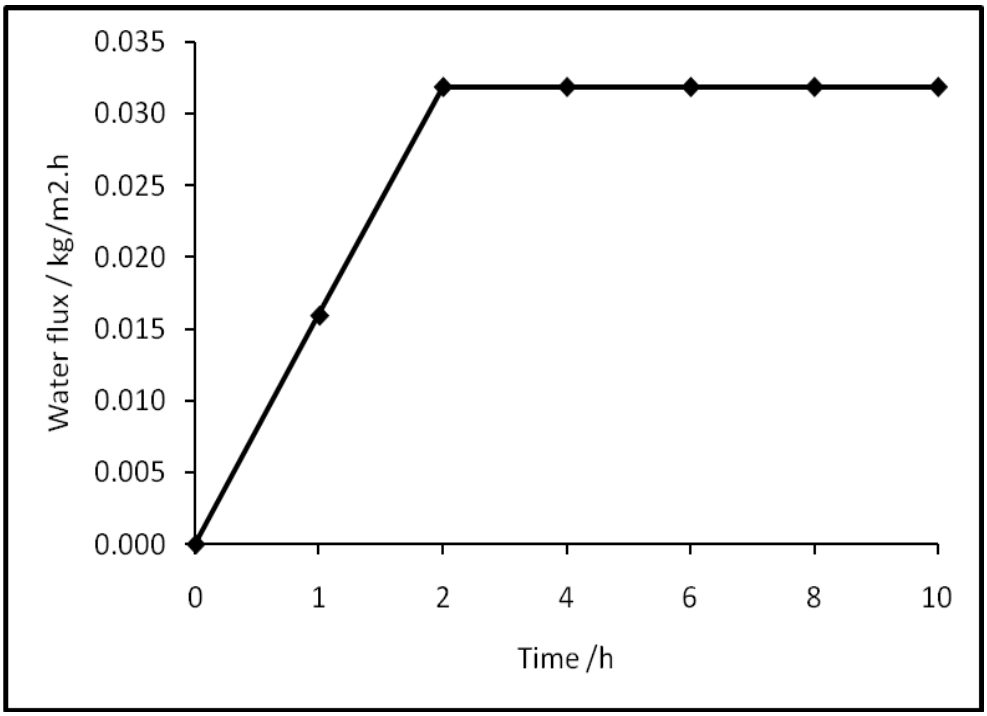

Figure 4.9: The pervaporation test of ethanol/water system at temperature of 343.15 K and pressure of 80 kPa.

Table 4.1: Specification of pervaporation composite flat sheet membrane.

Membrane type	**Pervaporation 1210**	**Pervaporation 1211**	**Pervaporation 4101**
Equivalent to	*Pervaporation 2210*	*Pervaporation 2211*	---
Main Application	For volatile organics and their mixtures	For volatile organics and their mixtures	For volatile organics and their mixtures
Max. Temperature long term, K	100	100 (105 for EtOH)	100 (103 for EtOH)
Max. Temperature short term, K	107	107	105
Max. water content in feed, % b.w	$\leq$ 30	$\leq$ 40	$\leq$ 30
Major limitation			
Aprotic solvent (e.g. DMF, DMSO)	$\leq$ 0.1%	$\leq$ 0.1%	$\leq$ 0.1%
Aldehydes and derivates (as acet aldehydes	$\leq$ 10 ppm	$\leq$ 100 ppm	$\leq$ 100 ppm
Organic Acid (e.g. acetic acid)	$\leq$ 0.1%	$\leq$ 10%	$\leq$ 0.1%
Formic acid	Excluded	$\leq$ 0.1%	$\leq$ 0.05%
Aromatic Amines (e.g Pyridine)	Excluded	$\leq$ 50%	$\leq$ 0.01%
Aromatic HCs, ketones, Kester, Cyclic Ethers, halogenated HCs	No limitations	No limitations	No limitations
pH (indicative)	5 - 7	5 - 7	5 - 7

CHAPTER 5

RESULTS AND DISCUSSIONS

5.1 Introduction

The experimental and computational results for the salt assessment study and pervaporation investigation are presented in this chapter. The ethanol-water system at 100 kPa was used as a test system and the baseline to see the effect of salt in the system at different pressures and salt concentrations. The relative volatility has the value of unity at the azeotropic point, and hence an increase in relative volatility value from unity will mean an elimination of the azeotrope in the ethanol-water system. The experimental vapour pressure data for ethanol and water were measured. The Wilson and NRTL models were used for the data reduction of the salt experimental VLE data. Salt was not used in the pervaporation because pervaporation has the advantage of direct separation.

The objectives of this study was met and are discussed in this Chapter (i) the effect of operating pressure and operating temperature on the pervaporation process in order to produce high purity ethanol and (ii) the effect of separating agent (calcium chloride salt)

and operating pressure in extractive distillation (VLE still) in order to produce high purity ethanol.

5.2 Pure component properties

Ethanol and water purity were checked before use for this study to ensure that they were not contaminated. The refractive index and conductivity of pure ethanol and distilled water were measured and compared with the literature as shown in Table 5.1. The deviation between literature and experimental values within uncetainties, and hence the chemicals were not contaminated. Table 5.2 shows the physical properties of ethanol, water and calcium chloride salt. The critical properties of ethanol and water play an important role in the data reduction and data analysis.

Table 5.1: Refractive Index n_D and conductivity.

Component	Refractive Index at 293.15 K		Conductivity	
	n_D		μS	
	Experimental	Literature[a]	Experimental	Literature[b]
Ethanol	1.3605	1.3612	1.41	1.5
Water	1.334	1.336	4.98	2 - 5

a and b were literature values (Weast, 1983-1984)

Table 5.2: Physical properties of ethanol and water.

Component	Boiling point	Molecular weight	Density	Liquid molar volume	Purity
	K	g/mol	kg/m^3	$cm^3/g.mol$	wt%
Ethanol	351.15	46	760.02	58.68	99.5
Water	373.15	18.02	1000.00	18.07	98.5
$CaCl_2$	1873.15	110.98	2150.12	-	98

All these data were taken from Weast (1983-1984)

5.3 Vapour pressure data

Vapour pressures of ethanol and water were measured using the VLE still. The experimental vapour pressure data are presented in Tables 5.3 and 5.4. Figure 5.1 and 5.2 shows the graphical representation of the measured data. The experimental vapour pressure data were compared with literature values and it shows good agreement. The difference in temperature (ΔT) was determined using equation 5.1.

$$\Delta T = \left| T_{\exp} - T_{lit} \right| \tag{5.1}$$

$$\log P(kPa) = A - \frac{B}{C + T(^{0}C)} \tag{5.2}$$

The vapour pressure of ethanol and water was measured separately for the following reasons: (i) to ensure that the VLE equipment is functioning properly, (ii) to ensure the chemicals are not contaminated, (iii) the chemicals have not changed phase or oxidized at certain temperature and pressure and (iv) to calibrate experimental technique or procedure. Antoine constants from Poling et al. (2001) were used to develop literature values of ethanol and water. Equation 5.2 was used to determine the temperature values at different pressures. It was found that the difference in temperature was less than 0.1 K, meaning that the equipment produces reliable results.

Table 5.3: Experimental vapour pressure data for ethanol.

Pressure (kPa)	Temperature (K)		ΔT
	Experimental	Literature[a]	
10	302.351	302.428	0.077
20	315.309	315.391	0.082
30	323.518	323.592	0.074
40	329.729	329.717	0.012
50	334.677	334.655	0.022
60	338.771	338.817	0.046
70	342.385	342.430	0.045
80	345.662	345.632	0.030
90	348.543	348.514	0.029
100	351.041	351.138	0.097

[a]Literature values (Poling *et al.*, 2001)

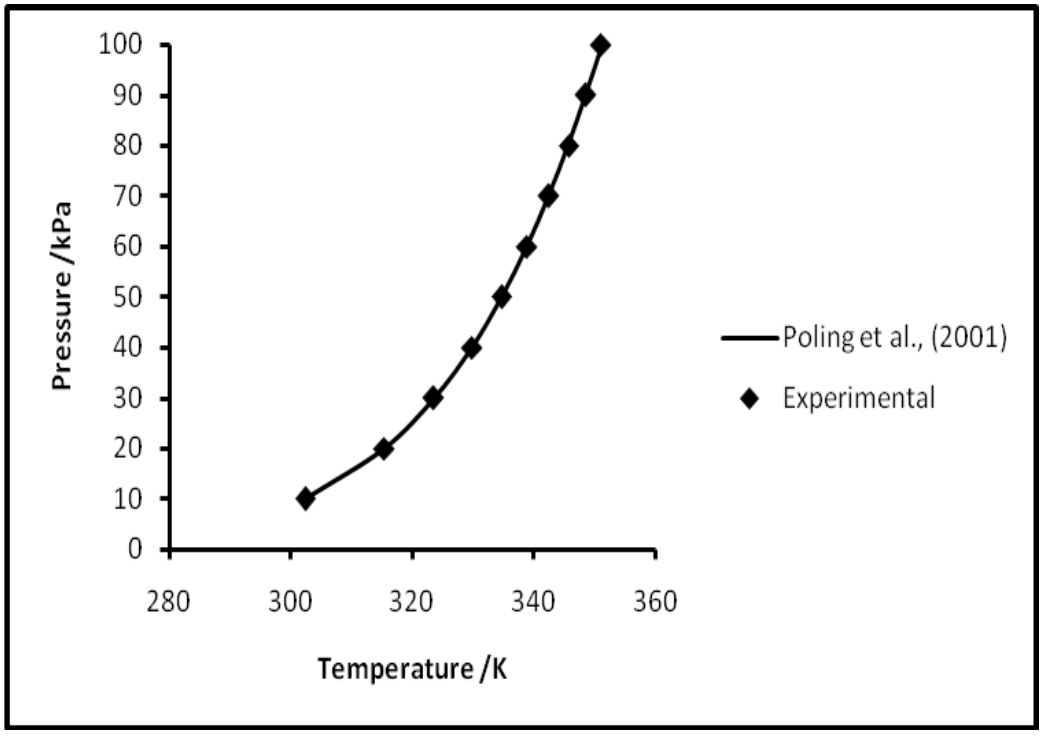

Figure 5.1: Vapour pressure data for ethanol.

Table 5.4: Experimental vapour pressure data for water.

Pressure (kPa)	Temperature (K)		ΔT
	Experimental	Literature[a]	
10	318.130	318.195	0.065
20	332.482	332.589	0.107
30	341.733	341.718	0.015
40	348.445	348.546	0.101
50	354.006	354.059	0.053
60	358.771	358.711	0.060
70	362.785	362.753	0.032
80	366.275	366.338	0.063
90	369.543	369.566	0.023
100	372.848	372.909	0.061

[a]Literature values (Poling *et al.*, 2001)

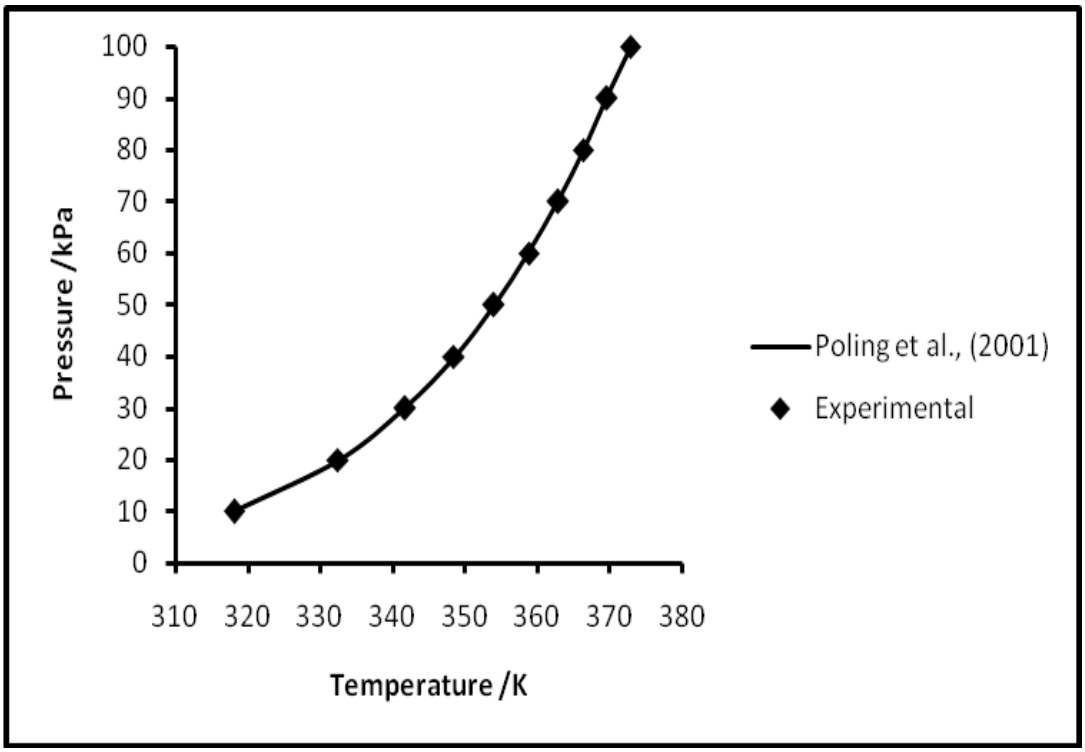

Figure 5.2: Vapour pressure data for water.

5.4 Results of calibration of VLE still

Experimental VLE data for the ethanol-water system in the absence of salt at 100 kPa was used to verify and test experimental technique and procedure of the dynamic VLE still. The objectives for studying the VLE for this system in the absence of salt were: (i) to check the practical feasibility of using the VLE still, (ii) to study the effect of having active packing material on the VLE of binary mixtures, and (iii) to establish the baseline for the ethanol-water system in order to see the effect of calcium chloride salt in the system. This was done by comparing the results obtained using this still with published results for the given system under same the conditions. Comparison of the measured results was done with those published in literature (Ohe, 1991; Perry and Green, 1997). If the data correspond with the literature values, a high degree of confidence can be placed in the correct functioning of the equipment. Table 5.5 shows the experimental VLE data for ethanol and water system without salt addition. Figure 5.3 indicates the ethanol-water system without salt and Figure 5.4 represents the temperature vapour-liquid diagram.

Table 5.5: Experimental VLE data for the ethanol (1) – water (2) system at 100 kPa (with no salt).

T/K	x_1	y_1	T/K	x_1	y_1
372.97	0.000	0.000	355.13	0.337	0.590
368.64	0.024	0.241	354.88	0.374	0.606
367.09	0.051	0.339	354.08	0.417	0.624
364.32	0.071	0.386	353.95	0.489	0.624
363.35	0.088	0.413	353.10	0.564	0.645
361.57	0.109	0.457	352.67	0.605	0.666
359.89	0.126	0.478	352.17	0.649	0.709
358.98	0.152	0.506	351.98	0.712	0.742
358.13	0.182	0.522	351.28	0.789	0.785
357.47	0.209	0.530	351.18	0.832	0.831
357.07	0.232	0.536	351.12	0.870	0.872
356.66	0.256	0.545	351.12	1.000	1.000
355.95	0.288	0.556			

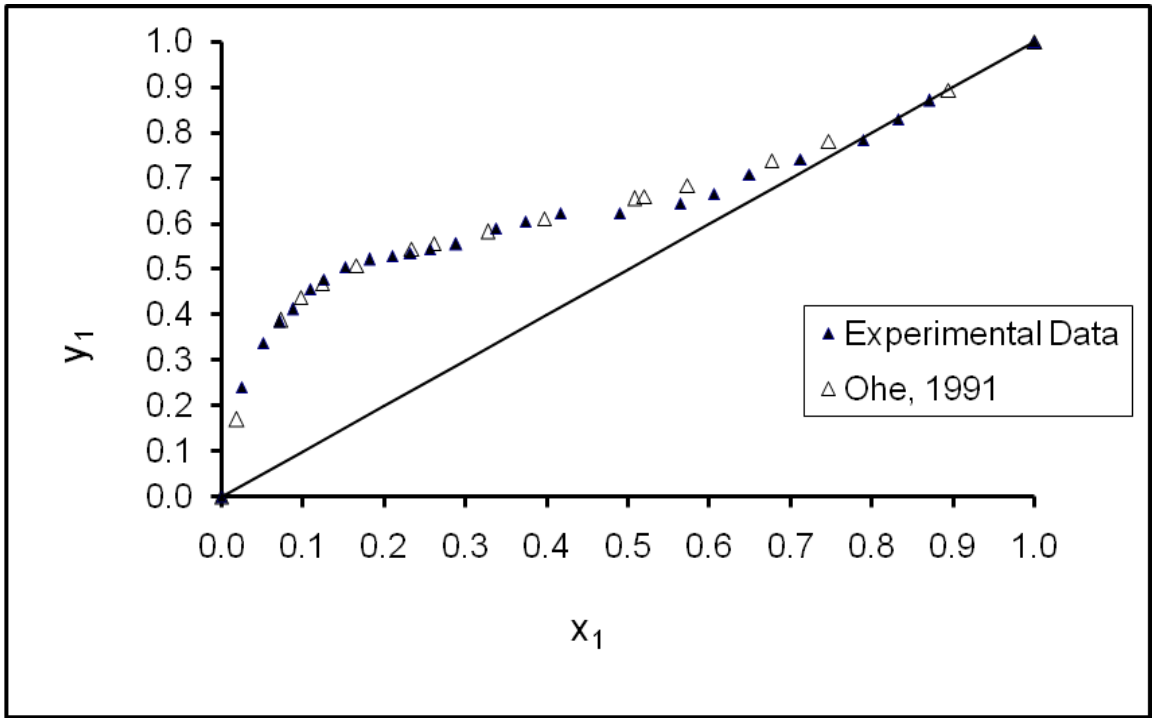

Figure 5.3: Experimental data for the ethanol (1) – water (2) system at 100 kPa with no salt.

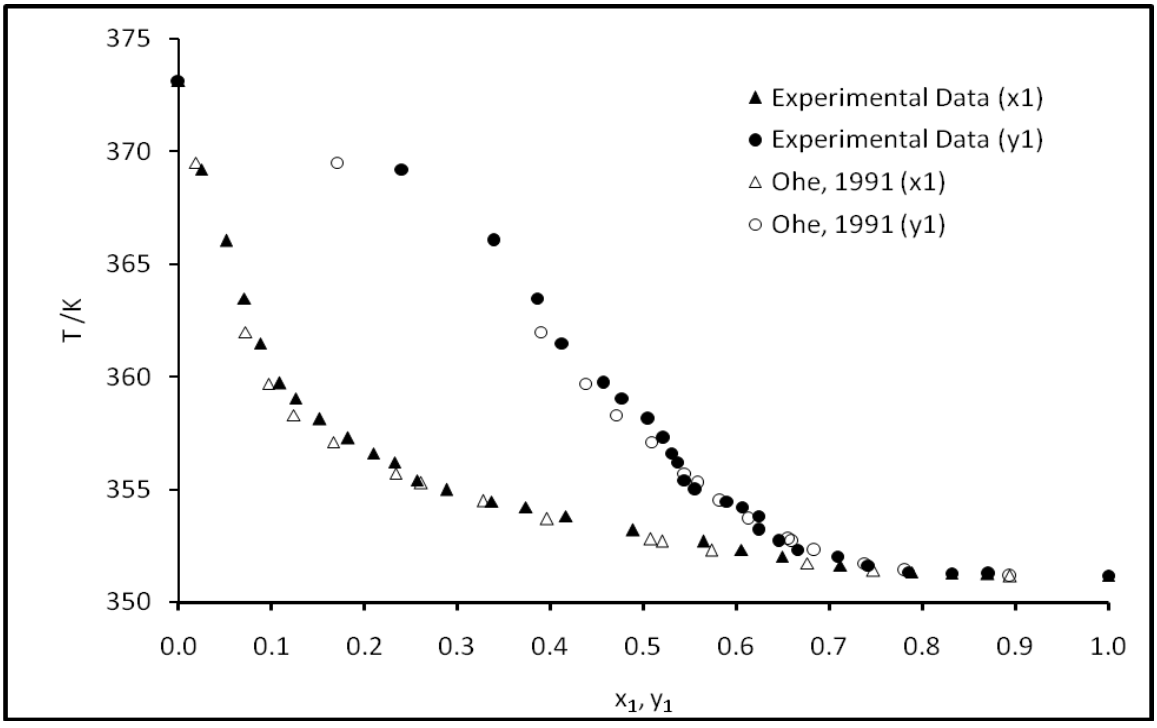

Figure 5.4: T-x-y diagram for ethanol (1) – water (2) system at 100 kPa with no salt.

5.5 Relative volatility of ethanol and water in the presence of $CaCl_2$

In this study, distilled water was used in the preparation of the ethanol-water mixture from 90% ethanol and 10% water (vol/vol) to 10% ethanol and 90% ethanol (vol/vol) mixtures, and calcium chloride was dissolve in the mixture at concentrations of 0.1 g/ml to 0.3 g/ml. At 0.4 g/ml calcium chloride became saturated at 90% ethanol and 10% water (vol/vol) because calcium chloride is less soluble in ethanol than water. Tables 5.6 – 5.10 show an increase in relative volatility at pressures of 20 kPa to 100 kPa as the calcium chloride concentration changes from 0.1 g/ml to 0.3 g/ml. An increase in relative volatility at the azeotropic point will mean an elimination of the azeotrope in the ethanol-water system.

Table 5.6: Relative volatility, α at pressure of 20 kPa.

Ethanol-water mixture	0.1 g/ml	0.2 g/ml	0.3 g/ml
Ethanol 90/10 water (vol/vol)	4.24	4.67	5.28
80/20	3.22	3.46	3.72
70/30	2.62	2.38	3.77
60/40	1.86	2.30	2.87
50/50	1.58	1.86	2.45
40/60	1.26	1.60	1.80
30/70	1.04	1.43	1.65
20/80	1.03	1.30	1.59
Ethanol 10/90 water (vol/vol)	0.98	1.21	1.60

Table 5.7: Relative volatility, α at pressure of 40 kPa.

Ethanol-water mixture	0.1 g/ml	0.2 g/ml	0.3 g/ml
Ethanol 90/10 water (vol/vol)	4.37	5.09	5.86
80/20	3.37	3.98	4.46
70/30	2.14	2.84	4.36
60/40	2.12	2.61	2.82
50/50	1.62	2.02	2.55
40/60	1.32	1.61	1.79
30/70	1.10	1.53	1.79
20/80	1.01	1.46	1.74
Ethanol 10/90 water	0.97	1.28	1.72

Table 5.8: Relative volatility, α at pressure of 60 kPa.

Ethanol-water mixture	0.1 g/ml	0.2 g/ml	0.3 g/ml
Ethanol 90/10 water	4.05	6.00	6.66
80/20	3.65	4.58	5.43
70/30	3.30	3.40	4.78
60/40	2.16	2.75	3.16
50/50	1.68	2.18	2.60
40/60	1.43	1.93	2.00
30/70	1.12	1.57	1.81
20/80	0.98	1.47	1.75
Ethanol 10/90 water (vol/vol)	0.93	1.42	1.68

Table 5.9: Relative volatility, α at pressure of 80 kPa.

Ethanol-water mixture	**0.1 g/ml**	**0.2 g/ml**	**0.3 g/ml**
Ethanol 90/10 water (vol/vol)	3.98	6.51	8.91
80/20	3.73	5.32	6.15
70/30	3.39	3.63	5.08
60/40	2.24	2.87	3.37
50/50	1.68	2.40	2.79
40/60	1.45	1.94	2.18
30/70	1.02	1.49	2.09
20/80	0.98	1.59	2.00
Ethanol 10/90 water (vol/vol)	0.94	1.42	1.89

Table 5.10: Relative volatility, α at pressure of 100 kPa.

Ethanol-water mixture	0.1 g/ml	0.2 g/ml	0.3 g/ml
Ethanol 90/10 water (vol/vol)	4.01	7.49	13.40
80/20	3.81	5.93	7.75
70/30	3.49	4.13	5.95
60/40	2.50	3.17	3.57
50/50	1.74	2.46	2.79
40/60	1.47	2.04	2.33
30/70	1.10	1.65	2.09
20/80	1.06	1.57	2.06
Ethanol 10/90 water (vol/vol)	1.01	1.67	2.12

5.6 VLE results for the ethanol-water system in the presence of $CaCl_2$

The study of the effect of $CaCl_2$ salt concentration was done by operating the still at different pressures range from 20 kPa to 100 kPa and changing the $CaCl_2$ concentration from 0.1 g/ml to 0.3 g/ml. This was done to produce the absolute ethanol from dilute ethanol-water solutions. The successful use of calcium chloride salt as a separating agent to eliminate or remove the ethanol-water azeotrope was done experimentally as shown in the trends below. This was achieved by comparing the results obtained in the addition of salt with those of the salt free system (baseline). A baseline is ethanol-water system with no salt at 100 kPa.

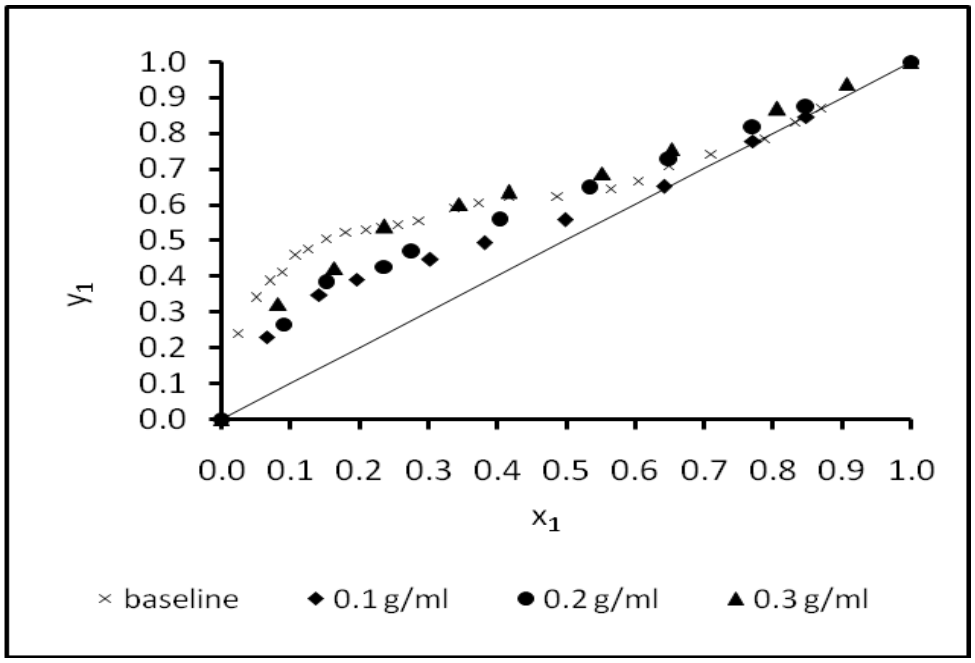

Figure 5.5: Effect of $CaCl_2$ concentration in ethanol (1) – water (2) system at pressure of 20 kPa.

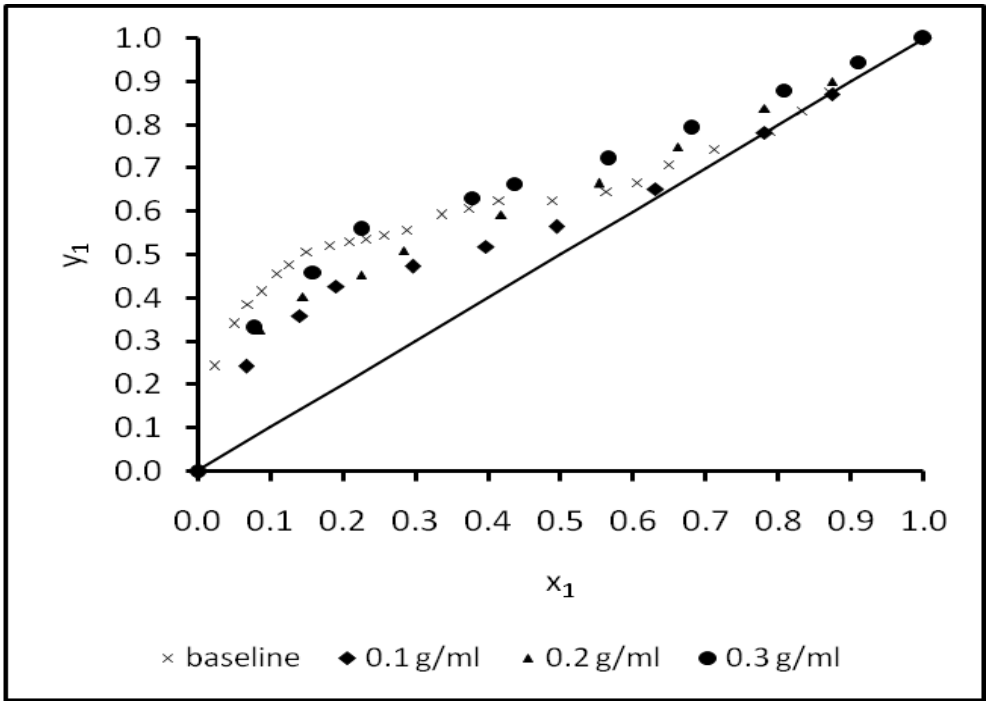

Figure 5.6: Effect of $CaCl_2$ concentration in ethanol (1) – water (2) system at pressure of 40 kPa.

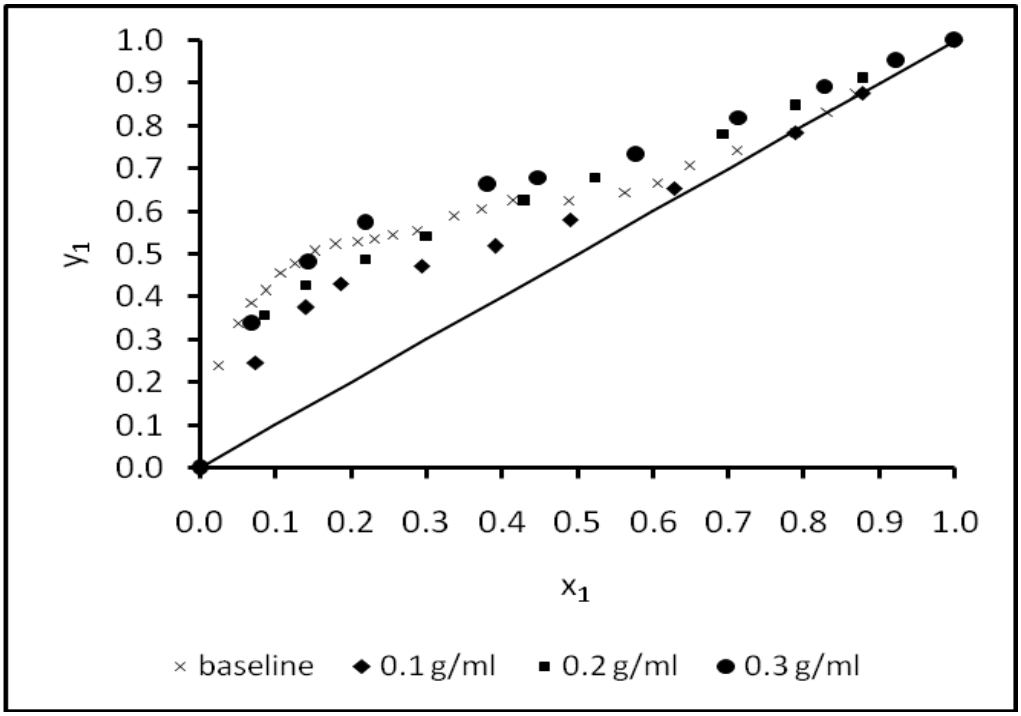

Figure 5.7: Effect of $CaCl_2$ concentration in ethanol (1) – water (2) system at pressure of 60 kPa.

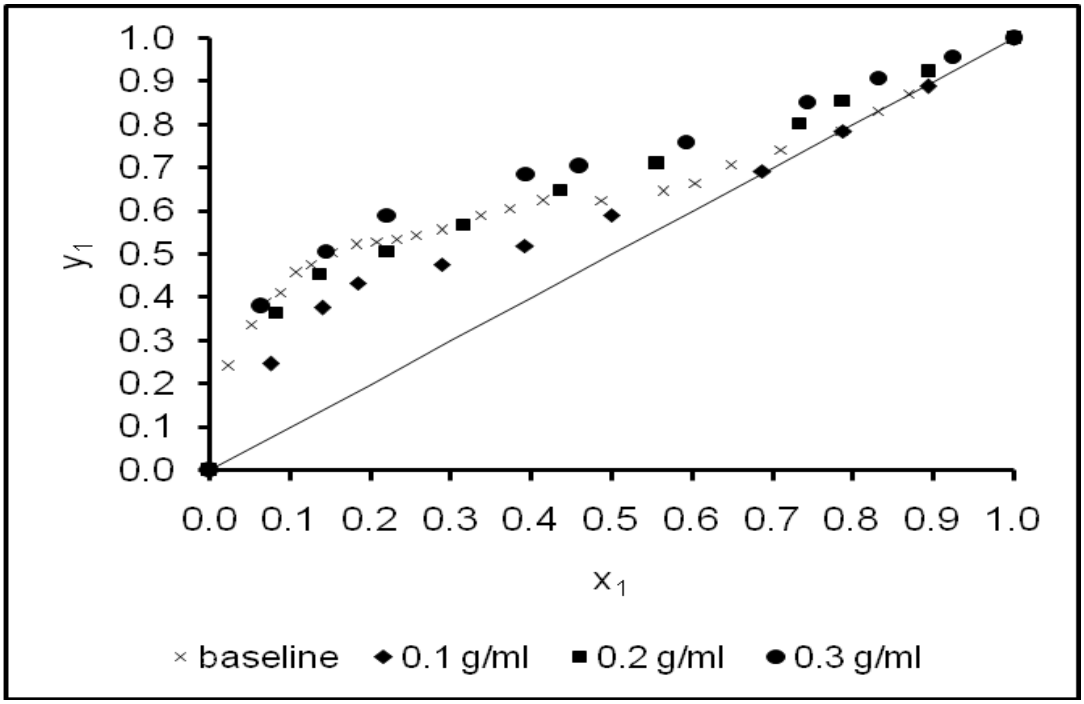

Figure 5.8: Effect of $CaCl_2$ concentration in ethanol (1) – water (2) system at pressure of 80 kPa.

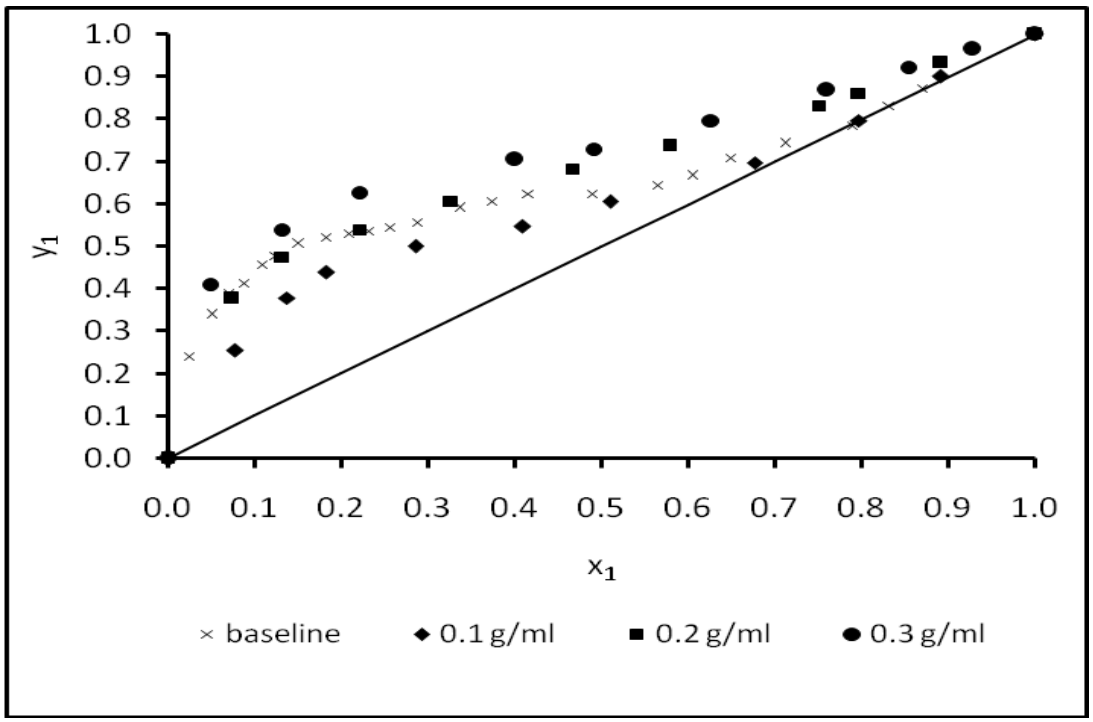

Figure 5.9: Effect of $CaCl_2$ concentration in ethanol (1) – water (2) system at 100 kPa.

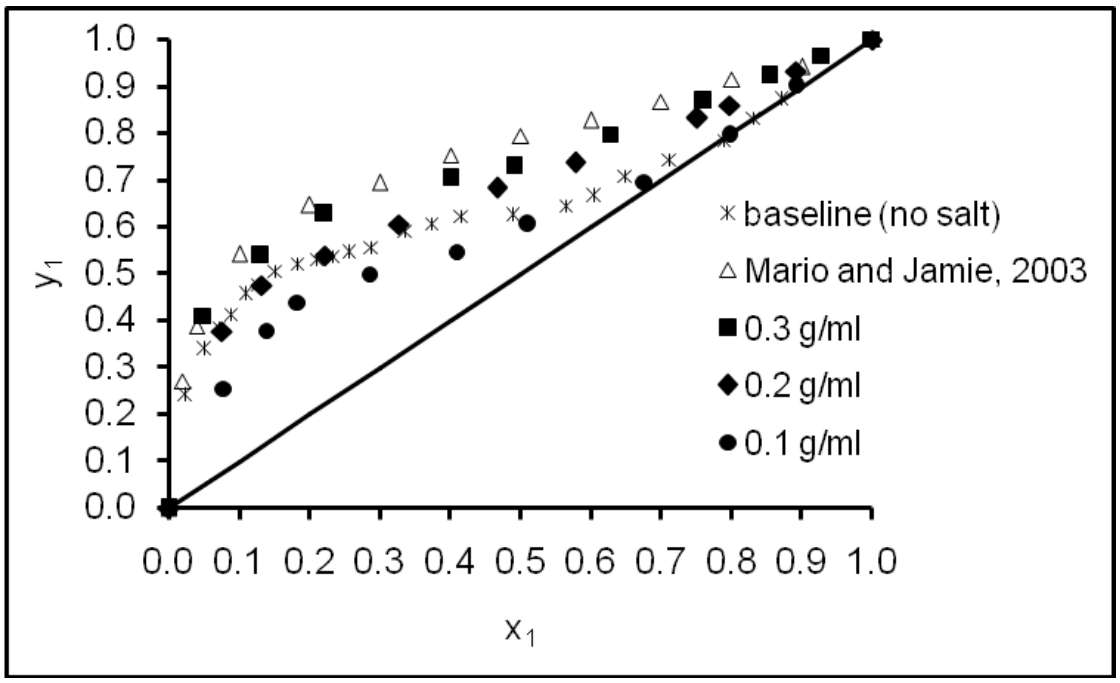

Figure 5.10: Comparison of the $CaCl_2$ concentration for the ethanol (1) – water (2) system at 100 kPa.

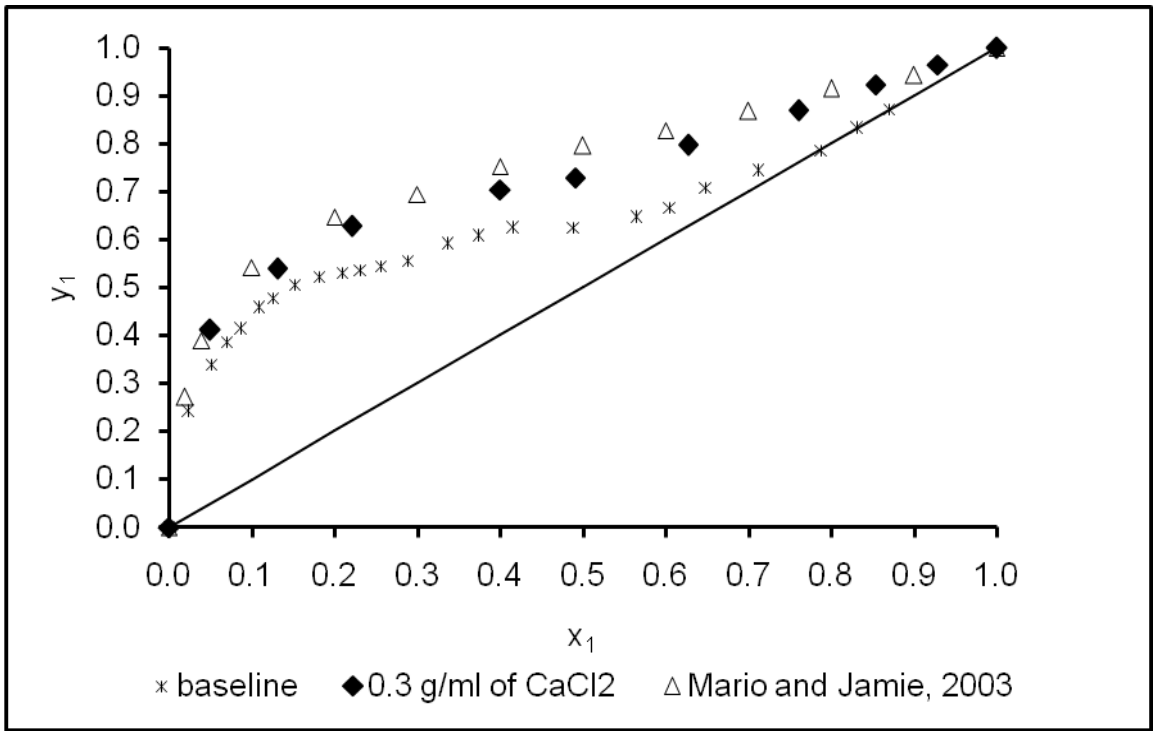

Figure 5.11: Comparison of the $CaCl_2$ concentration of 0.3 g/ml for the ethanol (1) – water (2) system at 100 kPa.

5.7 Effect of calcium chloride salt in extractive distillation

The aim of this study was to propose a steady state equilibrium stage model of saline extractive distillation in the production of high purity ethanol by operating at different pressures range from 20 kPa to 100 kPa at different concentrations of 0.1 g/ml to 0.3 g/ml of calcium chloride salt. In previous studies, Mario and Jamie (2003) measured the ethanol-water system in the addition of 16.7 wt% of the $CaCl_2$ in the production of absolute ethanol at atmospheric pressure. Mario and Jamie (2003) found that calcium chloride salt provides the large salting out effect on ethanol. In this study, the ethanol + water + $CaCl_2$ system was measured below atmospheric pressure in order to find the effect of salt over the range pressures from 20 kPa to 100 kPa at different concentration of $CaCl_2$.

The measured vapour liquid equilibrium data were compared with Mario and Jamie (2003) at 16.7 wt% of the calcium chloride at 100 kPa as shown in Figures 5.10 and 5.11. It was found that at high concentrations of salt (0.2 g/ml and 0.3 g/ml), the azeotrope in ethanol-water system could be eliminated. According to Agarwa *et al*. (2001) calcium chloride provides the largest salting out effect on ethanol at high concentration other than salt like NaCl, KI, and KCl. The separation of ethanol and water is the most important application of extractive distillation with solid salt. The influence of various salts on the relative volatility of ethanol and water was also investigated (Duan *et al*., 1980). It was found some salts could improve relative volatility and other could not improve relative volatility even at high concentrations. Zhigang *et al.*, (2005) have found and arranged the order of salt effect as follows: $AlCl_3 > CaCl_2 > NaCl_2$, $Al(NO_3)_3 > Cu(NO_3)_2 > KNO_3$.

Figures 5.5 – 5.9 provides the plots of the pressure from 20 kPa to 100 kPa at the concentration of 0.2 g/ml and 0.3 g/ml of calcium chloride. From this data, the effect of salt in the system is clearly seen that as the salt concentration increases, there would be the change in composition and relative volatility. Tables 5.6 – 5.10 shows the improvement in relative volatility even at azoetropic point as the calcium chloride concentration increases at different pressures. The increase of pressure from 20 to 100 kPa indicates the separation of the ethanol and water mixture even at the azoetropic point.

The temperature of the system was high at the pressure of 80 kPa and 100 kPa; it was because the ions molecule moves faster and the reaction occurs faster. The addition of $CaCl_2$ salt increases the boiling point of the water because calcium chloride was more soluble in water. The increase of the water boiling point causes the ethanol to become more volatility. Therefore, the elimination of the azeotrope takes place. Ethanol moves to the top of column were the pure vapours condensed to liquid. The liquid product was pure ethanol, and purity was found to be 99.8%. The volatile component is called a"salting out" from the liquid. The change in concentration from 0.2 g/ml to 0.3 g/ml, shows the significant impact on relative volatility which improves the separation.

At the concentration of 0.3 g/ml of $CaCl_2$, the existing azeotrope was eliminated easier even at low pressure of 20 kPa because the high concentration of ions of calcium chloride in the solution of ethanol and water results in high purity of the ethanol production. Therefore, calcium chloride salt could be used as the separation agent for the ethanol-water system. This could be applied in the extractive distillation industry to produce high purity of ethanol. It was found that the preferable operating conditions of the extractive distillation were at the high pressure of 80 kPa and 100 kPa as well as at high concentrations of 0.3 g/ml of $CaCl_2$ salt. The azoetrope in the ethanol-water system could be eliminated. This was achieved by comparing the results obtained with the addition of salt to those results of the salt free system (baseline).

At the concentration of 0.1 g/ml of $CaCl_2$, the system showed the negative effect of salt in the ethanol-water mixture as shown in figures 5.5 – 5.10. The VLE data at the concentration of 0.1 g/ml was below the baseline and it causes the negative effect. It was found that at this concentration it was difficult to break the azeotrope of the ethanol-water mixture even at high pressure. The increase in pressure affect the boiling of the system, but at the concentration of 0.1 g/ml, the increase in pressure has slight effect on composition. At low pressure of 20 kPa the $CaCl_2$ salt did not show significant impact on composition as compared to pressures of 40 kPa, 60 kPa, 80 kPa and 100 kPa.

5.8 Calcium chloride as an extractive agent

Calcium chloride salt is a molecular solid, in which the individual molecules are held together by relatively weak intermolecular forces. When calcium chloride dissolves in the ethanol-water mixture, the weak bonds between the individual $CaCl_2$ molecules are broken and these molecules are released into the solution. It takes energy to beak the bonds between the $CaCl_2$ molecules, as well as the hydrogen bonds in ethanol-water mixture. Hydrogen bonds in ethanol and water were disrupted by the addition of calcium chloride. As calcium chloride salt dissolves in the ethanol-water mixture, energy is given off. The slightly polar calcium chloride molecules form intermolecular bonds with polar ethanol and water molecules. The weak bonds formed between the solute and the solvent compensate for the energy needed to disrupt the structure of both the pure solute and the solvent. Calcium chloride salt completely dissolved in the ethanol-water mixture at the concentrations of 0.1 g/ml to 0.3 g/ml and it became saturated at the concentration of 0.4 g/ml.

To overcome the difficulty of eliminating existing azeotrope in the ethanol-water system, the use of solid salts instead of liquid separating agents has been gaining more attention in the past few years (Zhigang *et al.*, 2005). By using salt as an extractive agent, the extractive distillation has the advantages of producing a solvent-free extract at the top of the column and requires no additional separating column. This consumes less energy when compared to conventional methods of extractive distillation. In addition, the calcium chloride salt is a common salt, which is much cheaper than liquid solvents. Thus, it is unnecessary to recover the salt ($CaCl_2$) at the bottom of distillation column.

It is known that when a salt is dissolved in a solution, it dissociates into ions so as to exhibit preferential salvation by one of the solvents (usually less volatile) and salting-out of the other solvent (usually more volatile), as shown in experimental behavior of the ethanol-water system in the presence of calcium chloride salt. It may also happen that only a part of it dissociates leaving some un-dissociated molecules in the solution. Consequently the interaction forces between un-dissociates salt molecules, ion-molecules and ion-ion can coexist (Mario and Jamie, 2003). The strength of interaction forces depends on the configuration of ions and molecules, polarities of molecules, ionic

strength and composition of the mixture. Due to the above reasons, a sound theoretical basis of the salt effect is yet to be developed. As a result, most investigations concerned with the study of salt addition on the vapour-liquid equilibrium of the binary systems are limited to only presentation of experimental data with no attempt to develop new correlations. At the same time attempts to correlate experimental data by Van Laar (1962); (Redlich *et al*., 1979); Wilson (1964); NRTL (1962); Renon and Prausnitz (1979) have gained some success.

5.9 DATA REDUCTION RESULTS

In this study, two excess Gibbs free energy correlations were used to undertake the data reduction; these were Wilson and NRTL models. It is desirable to fit experimental data to an appropriate correlating equation for the Gibbs free energy by a data reduction (Raal and Muhlbauer, 1998). The combinations of variables P, T, x and y were known and the interaction parameters were calculated to confirm the experimental data. The procedure for the data reduction is presented in chapter 3.

Table 5.11 provides the interaction parameters for the Wilson and NRTL models for the ethanol-water-$CaCl_2$ system at different pressures with 0.1 g/ml concentration of calcium chloride. Both correlations show good fit to the experimental data as represented in Figure 5.12 – 5.16 and hence can be used in the specified range. Tables 5.12 – 5.16 are represents the difference in vapour composition (Δy) for the Wilson and NRTL models at 0.1g/ml concentration of calcium chloride. In addition, absolute average deviation (AAD) was calculated using the follow equation 5.4.

$$\Delta y = \left| \left(y_{1,\exp} - y_{1,calc} \right) \right| \tag{5.3}$$

$$AAD = \frac{100}{N} \left| \frac{y_{1,\exp} - y_{1,calc}}{y_{1,\exp}} \right| \tag{5.4}$$

Table 5.11: Interaction parameter for the Wilson and NRTL models for ethanol (1) – water (2) system at 0.1 g/ml of $CaCl_2$.

Pressure/ kPa	20	40	60	80	100
Wilson					
$(\lambda_{12}- \lambda_{11})$/J.mol^{-1}	942.20	1137.28	1498.27	1724.17	1943.65
$(\lambda_{21}- \lambda_{22})$/J.mol^{-1}	3198.26	3488.61	3811.26	3712.91	3878.13
AAD	0.473	0.37	0.33	0.284	0.422
NRTL					
$(g_{12}-g_{11})$/J.mol^{-1}	263.28	786.98	1444.32	1886.54	2118.89
$(g_{21}-g_{22})$/J.mol^{-1}	4123.32	3163.32	4466.28	4583.63	4095.86
A	0.45	0.46	0.47	0.46	0.45
AAD	0.279	0.328	0.312	0.285	0.283

Table 5.12: Experimental vapour compositions at 0.1 g/ml of $CaCl_2$ concentration in the ethanol (1) – water (2) system at pressure of 20 kPa.

Experimental		Wilson	NRTL
x_1	y_1	Δy	Δy
0.000	0.000		
0.066	0.230	0.046	0.019
0.142	0.348	0.048	0.024
0.196	0.390	0.029	0.017
0.303	0.447	0.036	0.001
0.381	0.493	0.025	0.001
0.499	0.557	0.017	0.014
0.642	0.650	0.036	0.024
0.772	0.777	0.035	0.004
0.849	0.846	0.005	0.002
1.000	1.000		

$\Delta y = \left| y_{\exp} - y_{calc} \right|$

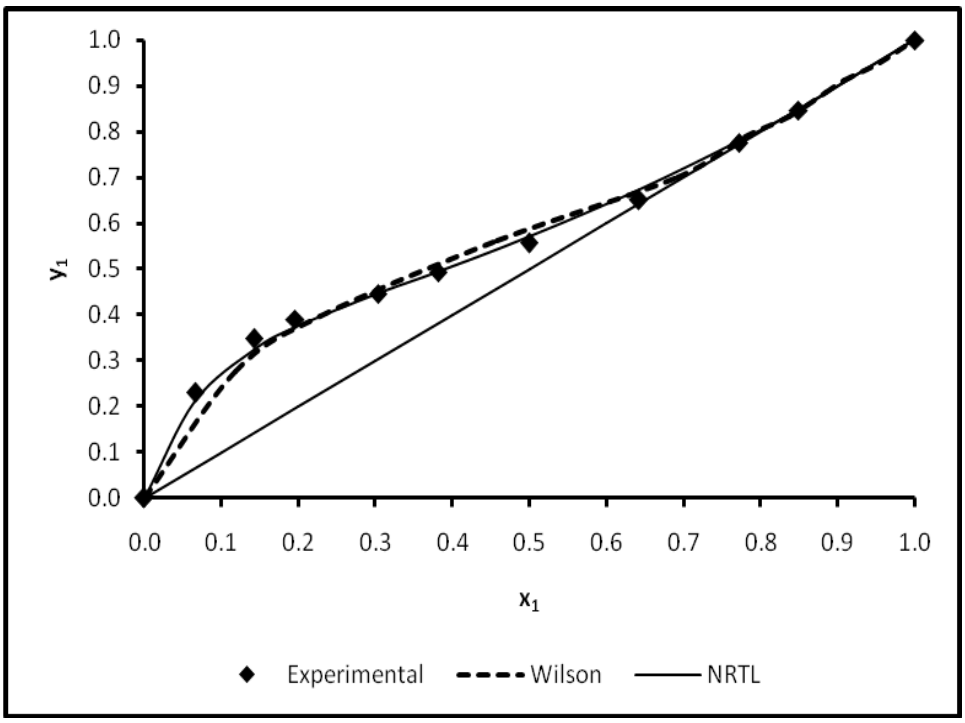

Figure 5.12: NRTL and Wilson model fit for the ethanol (1) – water (2) system at 0.1 g/ml $CaCl_2$ concentration at 20 kPa.

Table 5.13: Experimental vapour compositions at 0.1 g/ml of $CaCl_2$ concentration in the ethanol (1) – water (2) system at pressure of 40 kPa.

Experimental		Wilson	NRTL
x_1	y_1	Δy	Δy
0.000	0.000		
0.068	0.241	0.035	0.030
0.142	0.357	0.039	0.033
0.191	0.426	0.015	0.027
0.296	0.472	0.021	0.026
0.398	0.518	0.010	0.023
0.494	0.564	0.014	0.007
0.631	0.652	0.029	0.022
0.781	0.782	0.030	0.002
0.874	0.870	0.009	0.022
1.000	1.000		

$\Delta y = \left| y_{\exp} - y_{calc} \right|$

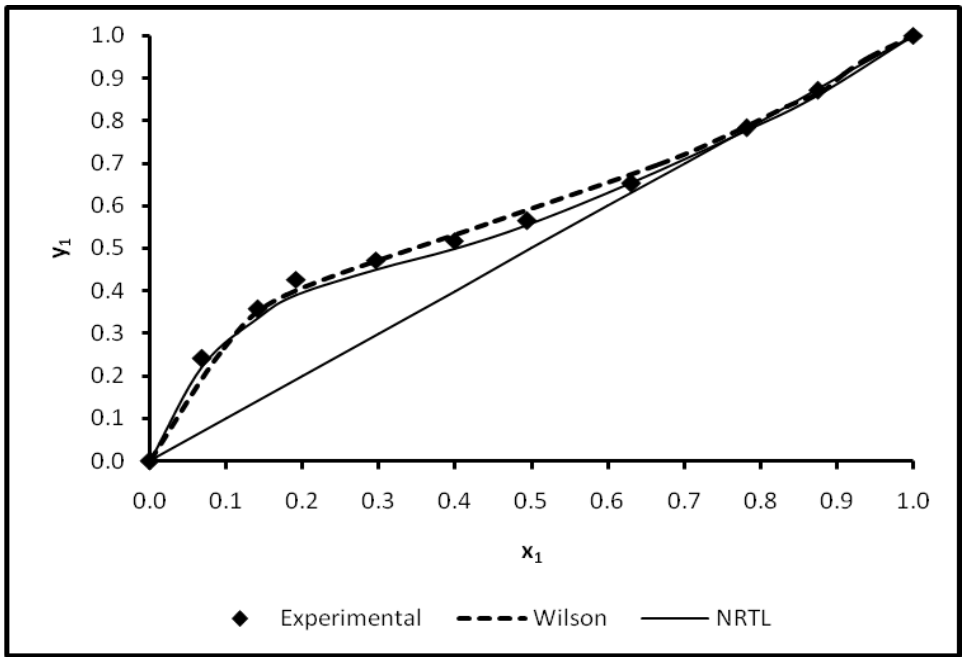

Figure 5.13: NRTL and Wilson model fit for the ethanol (1) – water (2) system at 0.1 g/ml $CaCl_2$ concentration at 40 kPa.

Table 5.14: Experimental vapour compositions at 0.1 g/ml of $CaCl_2$ concentration in the ethanol (1) – water (2) system at pressure of 60 kPa.

Experimental		Wilson	NRTL
x_1	y_1	Δy	Δy
0.000	0.000		
0.074	0.246	0.033	0.025
0.141	0.375	0.024	0.030
0.187	0.432	0.030	0.033
0.294	0.473	0.018	0.017
0.391	0.519	0.011	0.021
0.491	0.580	0.011	0.027
0.628	0.654	0.011	0.003
0.789	0.785	0.016	0.004
0.877	0.877	0.017	0.009
1.000	1.000		

$\Delta y = \left| y_{\exp} - y_{calc} \right|$

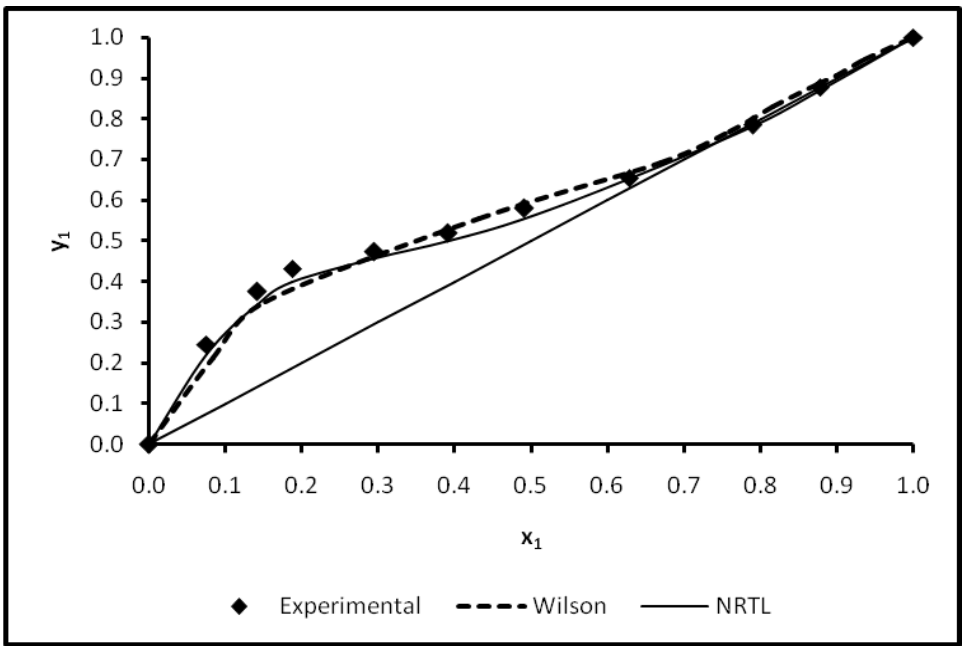

Figure 5.14 NRTL and Wilson model fit for the ethanol (1) – water (2) system at 0.1 g/ml $CaCl_2$ concentration at 60 kPa.

Table 5.15: Experimental vapour compositions at 0.1 g/ml of $CaCl_2$ concentration in the ethanol (1) – water (2) system at pressure of 80 kPa.

Experimental		Wilson	NRTL
x_1	y_1	Δy	Δy
0.000	0.000		
0.076	0.247	0.017	0.016
0.140	0.377	0.001	0.034
0.184	0.433	0.048	0.035
0.289	0.477	0.002	0.029
0.392	0.520	0.023	0.024
0.500	0.591	0.030	0.024
0.688	0.693	0.029	0.012
0.788	0.785	0.017	0.002
0.894	0.888	0.015	0.007
1.000	1.000		

$\Delta y = \left| y_{\exp} - y_{calc} \right|$

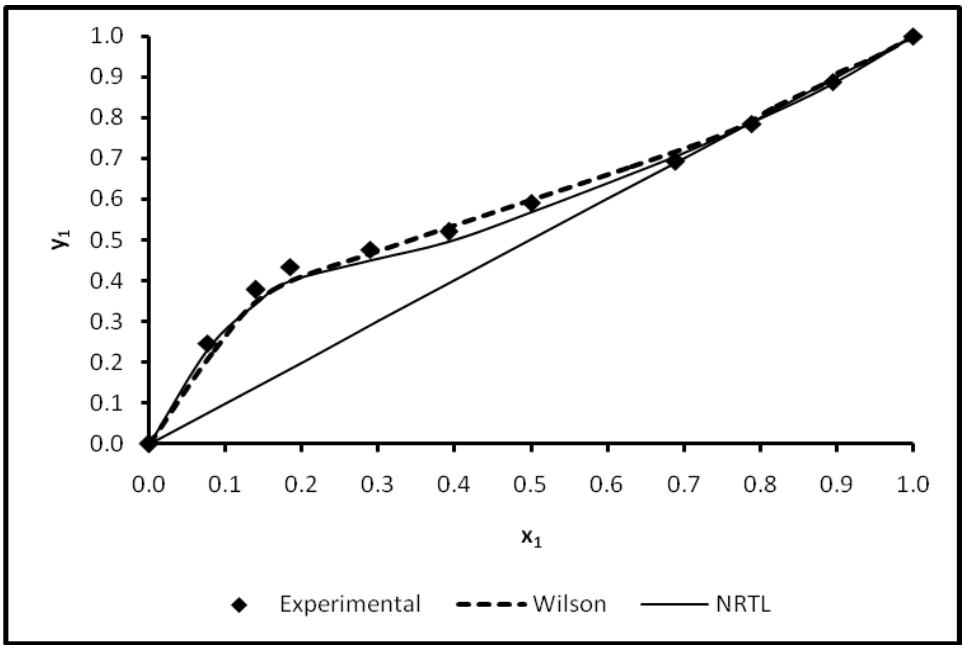

Figure 5.15: NRTL and Wilson model fit for the ethanol (1) – water (2) system at 0.1 g/ml $CaCl_2$ concentration at 80 kPa.

Table 5.16: Experimental vapour compositions at 0.1 g/ml of $CaCl_2$ concentration in the ethanol (1) – water (2) system at pressure of 100 kPa.

Experimental		Wilson	NRTL
x_1	y_1	Δy	Δy
0.000	0.000		
0.078	0.254	0.034	0.011
0.138	0.379	0.030	0.031
0.183	0.439	0.050	0.041
0.286	0.500	0.018	0.011
0.409	0.547	0.019	0.006
0.511	0.605	0.014	0.000
0.677	0.696	0.008	0.024
0.797	0.796	0.022	0.019
0.891	0.900	0.007	0.003
1.000	1.000		

$\Delta y = \left| y_{\exp} - y_{calc} \right|$

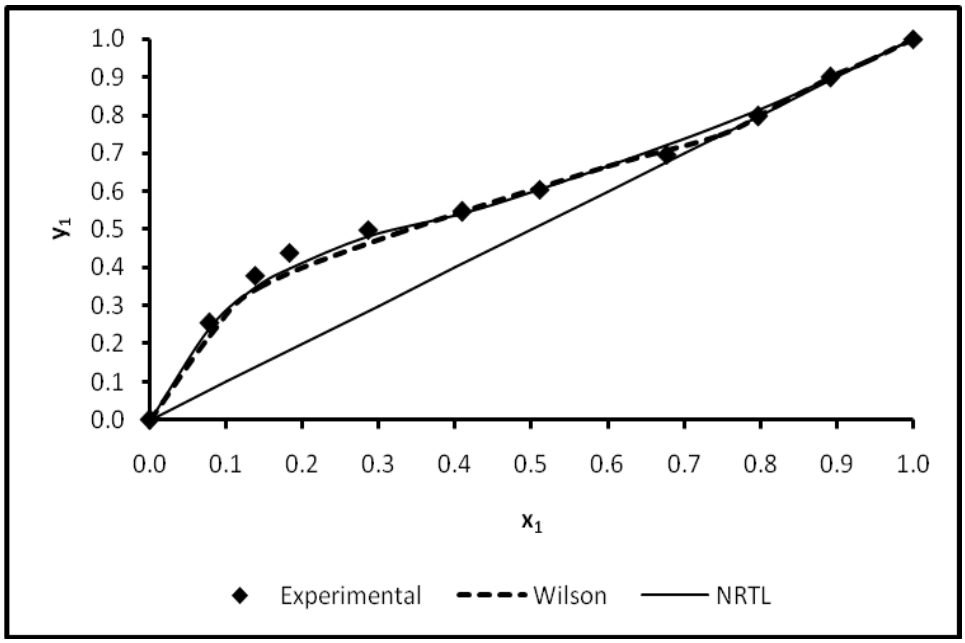

Figure 5.16: NRTL and Wilson model fit for the ethanol (1) – water (2) system at 0.1 g/ml $CaCl_2$ concentration at 100 kPa.

Table 5.17 provides the interaction parameters the Wilson and the NRTL models for the ethanol-water-$CaCl_2$ system at different pressures with 0.2 g/ml concentration of calcium chloride. Both correlations show good fit of the experimental data as represented in Figure 5.17 – 5.21 and hence can be used in the specified range. Tables 5.18 – 5.22 are represents the difference in vapour composition (Δy) for Wilson and NRTL models with 0.2g/ml concentration of calcium chloride. In addition, the absolute average deviation for vapour composition (AAD) was calculated using equation (5.3)

Table 5.17: Interaction parameter for the Wilson and NRTL models for ethanol (1) – water (2) system at 0.2 g/ml of $CaCl_2$.

Pressure/ kPa	20	40	60	80	100
Wilson					
$(\lambda_{12}- \lambda_{11})$/J.mol^{-1}	1074.38	1257.39	1525.81	1765.23	1855.41
$(\lambda_{21}- \lambda_{22})$/J.mol^{-1}	3011.14	3319.11	3579.44	3528.19	3688.65
AAD	0.081	0.273	0.321	0.037	0.249
NRTL					
$(g_{12}-g_{11})$/J.mol^{-1}	-314.25	276.98	844.32	1024.14	1380.21
$(g_{21}-g_{22})$/J.mol^{-1}	4675.86	4864.28	4554.67	4583.63	4625.37
α	0.45	0.47	0.47	0.46	0.46
AAD	0.118	0.201	0.11	0.124	0.072

Table 5.18: Experimental vapour compositions at 0.2 g/ml of $CaCl_2$ concentration in the ethanol (1) – water (2) system at pressure of 20 kPa.

Experimental		Wilson	NRTL
x_1	y_1	Δy	Δy
0.000	0.000		
0.090	0.266	0.005	0.010
0.152	0.382	0.001	0.023
0.237	0.426	0.011	0.008
0.277	0.469	0.002	0.015
0.404	0.558	0.005	0.014
0.534	0.646	0.007	0.015
0.650	0.725	0.012	0.002
0.772	0.815	0.011	0.016
0.849	0.872	0.026	0.024
1.000	1.000		

$\Delta y = \left| y_{\exp} - y_{calc} \right|$

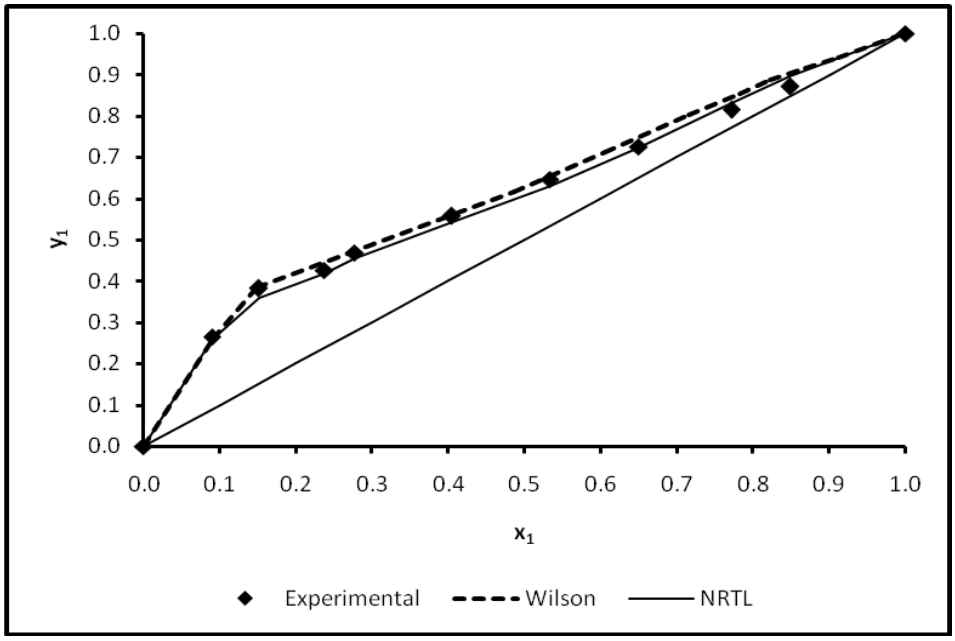

Figure 5.17: NRTL and Wilson model fit for the ethanol (1) – water (2) system at 0.2 g/ml $CaCl_2$ concentration at 20 kPa.

Table 5.19: Experimental vapour compositions at 0.2 g/ml of $CaCl_2$ concentration in the ethanol (1) – water (2) system at pressure of 40 kPa.

Experimental		Wilson	NRTL
x_1	y_1	Δy	Δy
0.000	0.000		
0.087	0.326	0.033	0.031
0.145	0.404	0.001	0.011
0.225	0.452	0.016	0.003
0.284	0.509	0.010	0.008
0.418	0.592	0.009	0.008
0.553	0.665	0.010	0.004
0.662	0.750	0.016	0.001
0.781	0.839	0.060	0.004
0.874	0.899	0.043	0.012
1.000	1.000		

$\Delta y = \left| y_{\exp} - y_{calc} \right|$

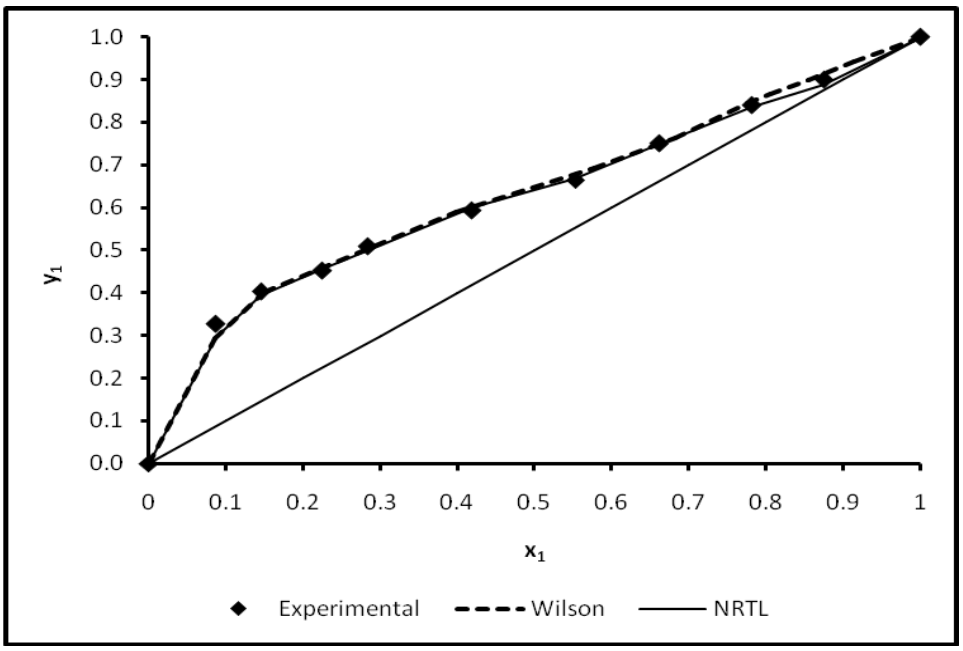

Figure 5.18: NRTL and Wilson model fit for the ethanol (1) – water (2) system at 0.2 g/ml $CaCl_2$ concentration at 40 kPa.

Table 5.20: Experimental vapour compositions at 0.2 g/ml of $CaCl_2$ concentration in the ethanol (1) – water (2) system at pressure of 60 kPa.

Experimental		Wilson	NRTL
x_1	y_1	Δy	Δy
0.000	0.000		
0.085	0.359	0.001	0.014
0.140	0.427	0.002	0.003
0.219	0.488	0.053	0.008
0.301	0.542	0.037	0.002
0.431	0.623	0.024	0.013
0.523	0.680	0.018	0.021
0.694	0.781	0.016	0.018
0.789	0.846	0.060	0.015
0.877	0.910	0.011	0.007
1.000	1.000		

$\Delta y = \left| y_{\exp} - y_{calc} \right|$

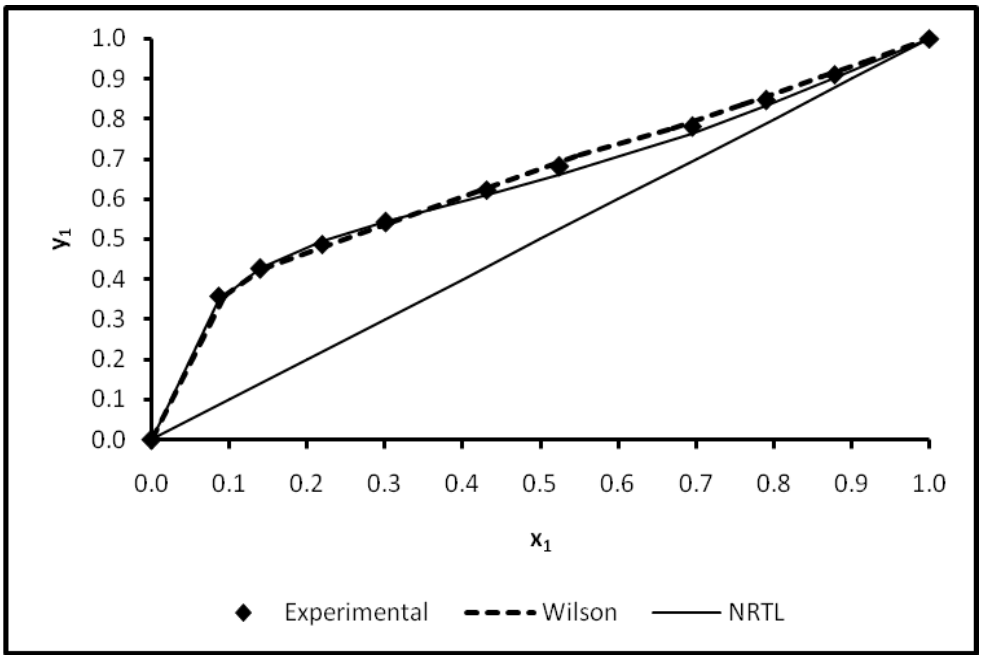

Figure 5.19: NRTL and Wilson model fit for the ethanol (1) – water (2) system at 0.2 g/ml $CaCl_2$ concentration at 60 kPa.

Table 5.21: Experimental vapour compositions at 0.2 g/ml of $CaCl_2$ concentration in the ethanol (1) – water (2) system at pressure of 80 kPa.

Experimental		Wilson	NRTL
x_1	y_1	Δy	Δy
0.000	0.000		
0.081	0.366	0.003	0.017
0.136	0.456	0.025	0.018
0.222	0.508	0.003	0.001
0.315	0.569	0.099	0.006
0.436	0.649	0.010	0.018
0.557	0.710	0.026	0.016
0.733	0.804	0.027	0.012
0.788	0.855	0.037	0.025
0.894	0.903	0.039	0.013
1.000	1.000		

$\Delta y = \left| y_{\exp} - y_{calc} \right|$

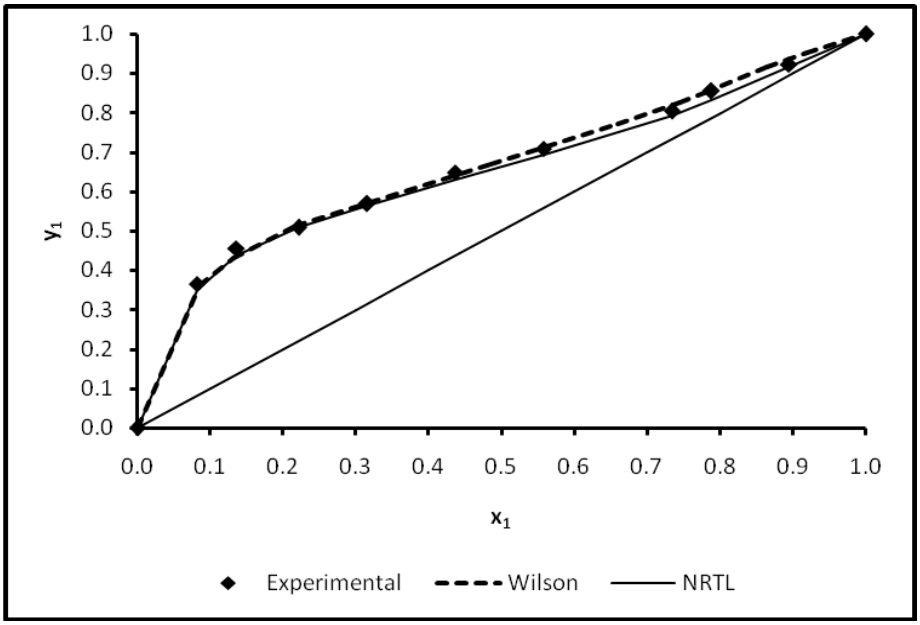

Figure 5.20: NRTL and Wilson model fit for the ethanol (1) – water (2) system at 0.2 g/ml $CaCl_2$ concentration at 80 kPa.

Table 5.22: Experimental vapour compositions at 0.2 g/ml of $CaCl_2$ concentration in the ethanol (1) – water (2) system at pressure of 100 kPa.

Experimental		Wilson	NRTL
x_1	y_1	Δy	Δy
0.000	0.000		
0.075	0.377	0.045	0.012
0.132	0.475	0.027	0.005
0.221	0.540	0.009	0.010
0.327	0.606	0.038	0.004
0.467	0.683	0.029	0.009
0.578	0.737	0.027	0.008
0.750	0.832	0.030	0.001
0.797	0.860	0.028	0.004
0.891	0.932	0.010	0.007
1.000	1.000		

$\Delta y = \left| y_{\exp} - y_{calc} \right|$

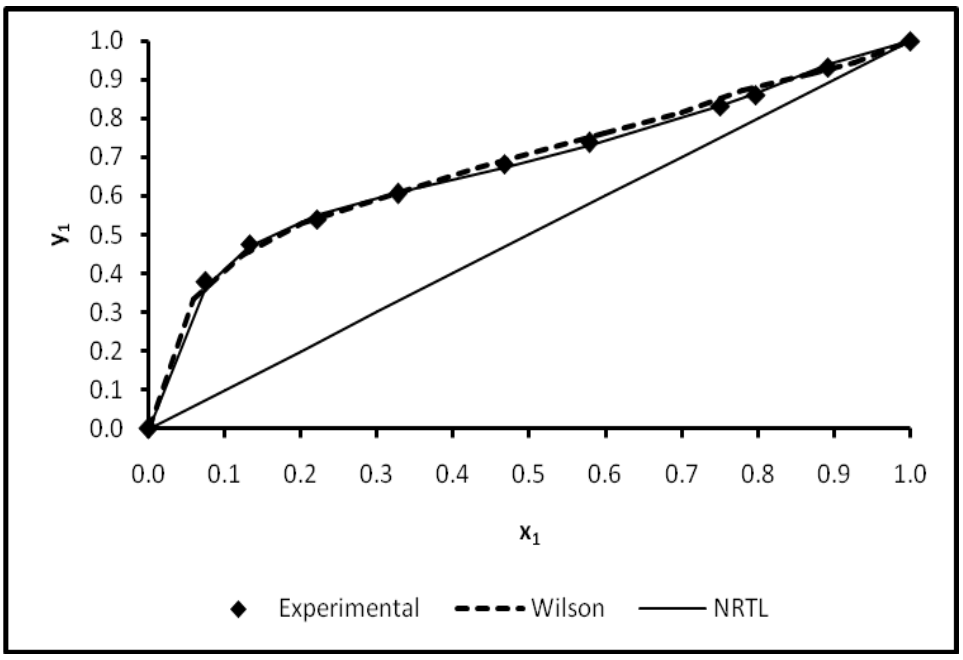

Figure 5.21: NRTL and Wilson model fit for the ethanol (1) – water (2) system at 0.2 g/ml $CaCl_2$ concentration at 100 kPa.

Table 5.23 provides the interaction parameters of the Wilson and the NRTL models for the ethanol-water-$CaCl_2$ system at different pressures with 0.3 g/ml concentration of calcium chloride. Both correlations show good fit to the experimental data as represented in Figures 5.22 – 5.26 and hence can be used in the specified range. Tables 5.24 – 5.28 are represents the difference in vapour composition (Δy) for Wilson and NRTL models with 0.3 g/ml concentration of calcium chloride. In addition, the absolute average deviation for vapour composition (AAD) was calculated using equation (5.3)

Table 5.23: Interaction parameter for the Wilson and NRTL models for ethanol (1) – water (2) system at 0.3 g/ml of $CaCl_2$.

Pressure/ kPa	20	40	60	80	100
Wilson					
$(\lambda_{12}- \lambda_{11})$/J.mol^{-1}	526.65	643.66	824.12	1056.78	1146.82
$(\lambda_{21}- \lambda_{22})$/J.mol^{-1}	2188.33	2378.74	2606.65	2772.95	2899.81
AAD	0.203	0.11	0.10	0.174	0.21
NRTL					
$(g_{12}-g_{11})$/J.mol^{-1}	-234.54	-314.87	-290.45	-237.25	170.58
$(g_{21}-g_{22})$/J.mol^{-1}	4384.16	4676.98	4450.16	4344.65	4125.63
α	0.47	0.46	0.45	0.46	0.45
AAD	0.258	0.173	0.113	0.64	0.71

Table 5.24: Experimental vapour compositions at 0.3 g/ml of $CaCl_2$ concentration in the ethanol (1) – water (2) system at pressure of 20 kPa.

Experimental		Wilson	NRTL
x_1	y_1	Δy	Δy
0.000	0.000		
0.083	0.322	0.001	0.013
0.164	0.422	0.021	0.043
0.237	0.540	0.007	0.014
0.345	0.602	0.039	0.007
0.417	0.637	0.024	0.004
0.552	0.689	0.012	0.001
0.653	0.756	0.025	0.002
0.807	0.869	0.009	0.000
0.907	0.940	0.003	0.001
1.000	1.000		

$\Delta y = \left| y_{\exp} - y_{calc} \right|$

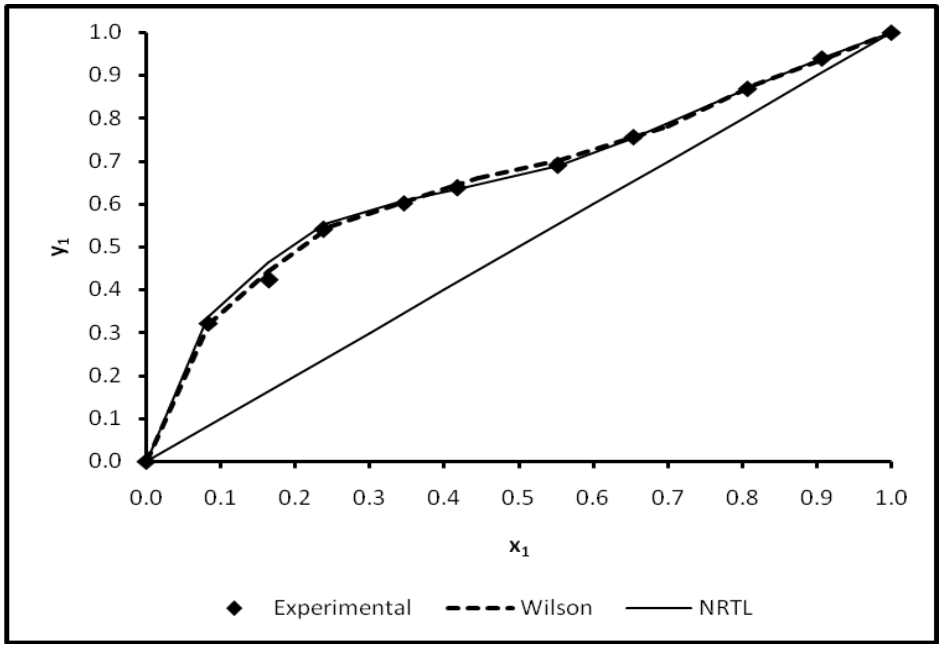

Figure 5.22: NRTL and Wilson model fit for the ethanol (1) – water (2) system at 0.3 g/ml $CaCl_2$ concentration at 20 kPa.

Table 5.25: Experimental vapour compositions at 0.3 g/ml of $CaCl_2$ concentration in the ethanol (1) – water (2) system at pressure of 40 kPa.

Experimental		Wilson	NRTL
x_1	y_1	Δy	Δy
0.000	0.000		
0.077	0.330	0.002	0.022
0.160	0.459	0.003	0.004
0.225	0.559	0.007	0.024
0.378	0.631	0.020	0.011
0.436	0.663	0.026	0.005
0.565	0.721	0.017	0.013
0.681	0.793	0.015	0.006
0.807	0.879	0.016	0.006
0.909	0.945	0.000	0.002
1.000	1.000		

$\Delta y = \left| y_{\exp} - y_{calc} \right|$

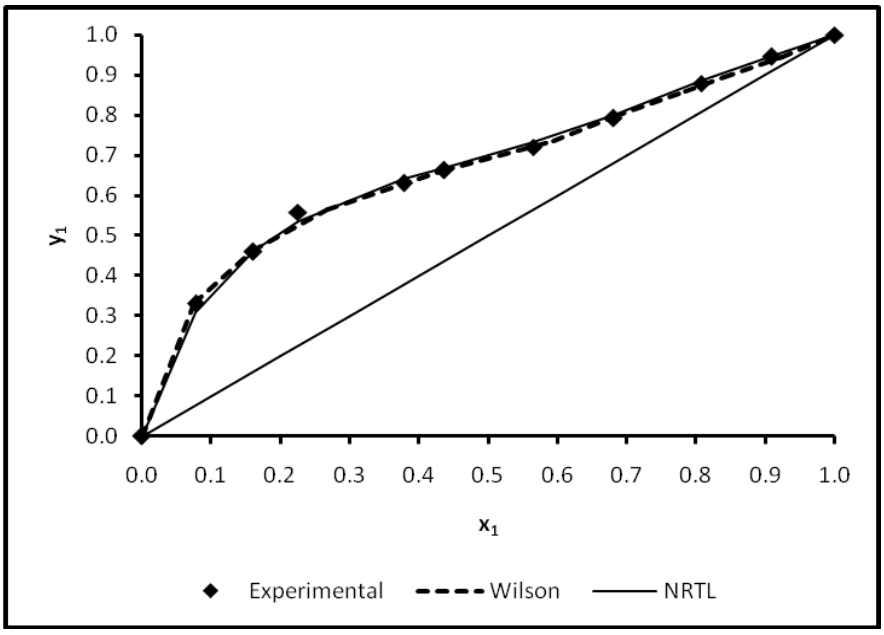

Figure 5.23: NRTL and Wilson model fit for the ethanol (1) – water (2) system at 0.3 g/ml $CaCl_2$ concentration at 40 kPa.

Table 5.26: Experimental vapour compositions at 0.3 g/ml of $CaCl_2$ concentration in the ethanol (1) – water (2) system at pressure of 60 kPa.

Experimental		Wilson	NRTL
x_1	y_1	Δy	Δy
0.000	0.000		
0.071	0.337	0.005	0.006
0.145	0.480	0.006	0.024
0.219	0.573	0.005	0.009
0.382	0.662	0.017	0.007
0.449	0.679	0.018	0.000
0.578	0.732	0.027	0.005
0.715	0.819	0.026	0.021
0.826	0.893	0.019	0.021
0.923	0.952	0.004	0.010
1.000	1.000		

$\Delta y = \left| y_{\exp} - y_{calc} \right|$

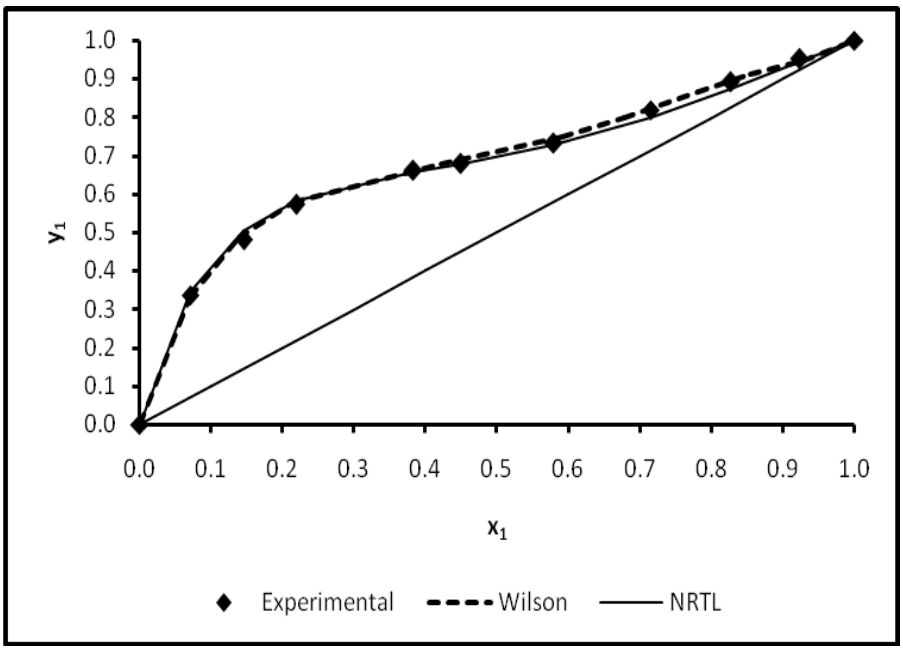

Figure 5.24: NRTL and Wilson model fit for the ethanol (1) – water (2) system at 0.3 g/ml $CaCl_2$ concentration at 60 kPa.

Table 5.27: Experimental vapour compositions at 0.3 g/ml of $CaCl_2$ concentration in the ethanol (1) – water (2) system at pressure of 80 kPa.

Experimental		Wilson	NRTL
x_1	y_1	Δy	Δy
0.000	0.000		
0.064	0.379	0.004	0.011
0.144	0.508	0.020	0.007
0.222	0.591	0.005	0.018
0.395	0.687	0.004	0.012
0.460	0.704	0.043	0.016
0.592	0.760	0.022	0.005
0.743	0.853	0.009	0.018
0.832	0.908	0.005	0.019
0.924	0.958	0.006	0.014
1.000	1.000		

$\Delta y = \left| y_{\exp} - y_{calc} \right|$

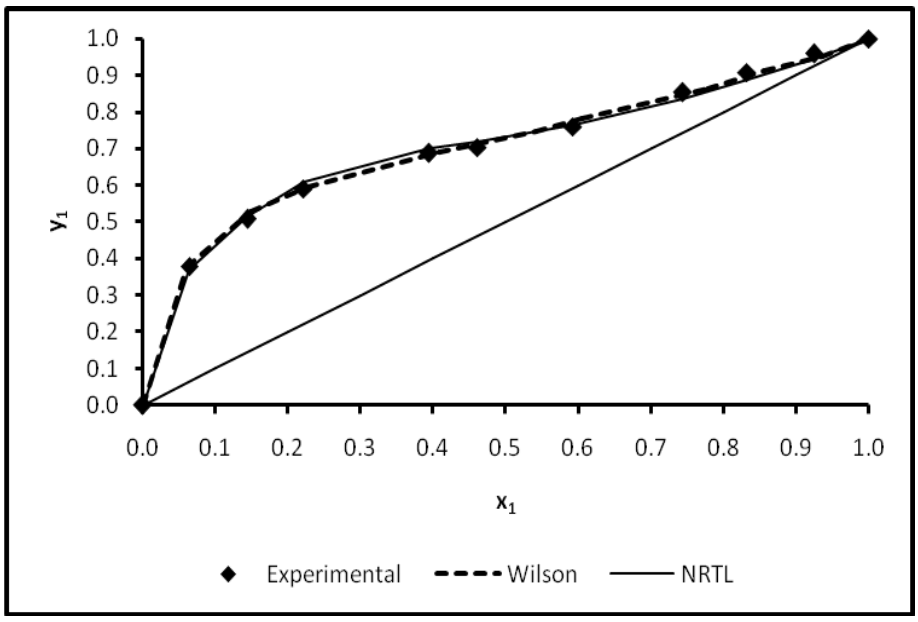

Figure 5.25: NRTL and Wilson model fit for the ethanol (1) – water (2) system at 0.3 g/ml $CaCl_2$ concentration at 80 kPa.

Table 5.28: Experimental vapour compositions at 0.3 g/ml of $CaCl_2$ concentration in the ethanol (1) – water (2) system at pressure of 100 kPa.

Experimental		Wilson	NRTL
x_1	y_1	Δy	Δy
0.000	0.000		
0.049	0.411	0.019	0.007
0.131	0.539	0.008	0.011
0.221	0.628	0.006	0.006
0.400	0.704	0.047	0.010
0.491	0.729	0.015	0.016
0.627	0.797	0.004	0.002
0.760	0.869	0.013	0.011
0.854	0.923	0.005	0.006
1.000	1.000		

$\Delta y = \left| y_{\exp} - y_{calc} \right|$

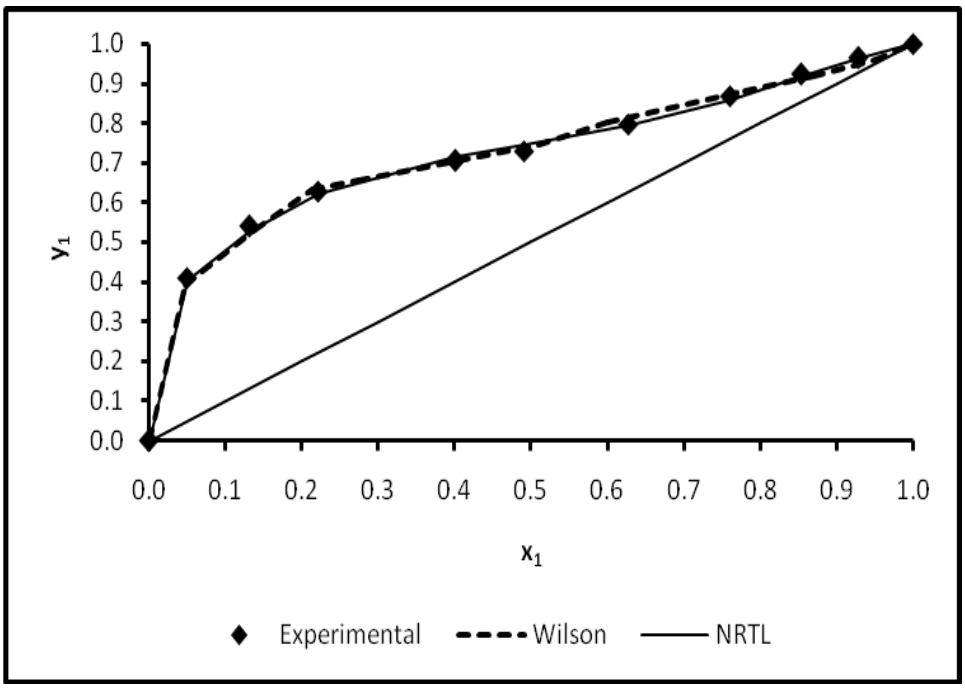

Figure 5.26: NRTL and Wilson model fit for the ethanol (1) – water (2) system at 0.3 g/ml $CaCl_2$ concentration at 100 kPa.

5.10 Reduction of low pressure VLE data

The two most well-known techniques employed in the reduction of VLE data (the combined method and the direct method) were discussed extensively in chapter 3. Based on previous research, the combined method (gamma/phi) was applied in the data reduction of the experimental VLE data measured in this study. Narasigadu (2006) used the models of Pitzer and Curl (1957) and Tsonopoulos (1974) in the combined method to determine the second Virial coefficients, which were then used for the calculation of the vapour phase correction factor. Two local compositions models based on the liquid phase activity coefficient models (Wilson and NRTL correlations) were used for the liquid phase correction. The Antoine equation was used to evaluate the saturated pressures/temperatures in the modeling of the VLE data. The Antoine equation was chosen as it offers a lower degree of complexity that allows for ease of computation, especially for isobaric VLE modeling where the complexity is evident in the calculation of the saturated temperatures.

In this study, the salt containing liquid mixture was treated as pseudo-binary system with Wilson and NRTL correlation. Tables 5.11, 5.17 and 5.23 were shows interaction parameters of the Wilson and NRTL models for the ethanol-water-$CaCl_2$ systemat different pressures and different concentrations. The MATLAB program was used to determine the interaction parameters. The data regression program was written in MATLAB, which offered a variety of built-in optimisation functions. For this work the *fminsearch* function was chosen, which finds the minimum of an unconstrained multivariable function. These models were used at different pressures of 20 kPa to 100 kPa and at the different concentrations of 0.1 g/ml to 0.3 g/ml of calcium chloride salt. The successful use of these two models is shown from Figures 5.12 – 5.26. Figures 5.12 – 5.16 were shows the result of the models at low concentration of 0.1 g/ml, and from figure 5.17 to figure 5.21 shows the result of the models at medium concentration of 0.2 g/ml and final from figure 5.22 to figure 5.26 shows the result of the models at high concentration of 0.3 g/ml.

5.11 PERVAPORATION RESULTS

The cylindrical pervaporation cell was constructed, commission and used to perform the separation of the ethanol-water system at different temperature and different pressures to produce high purity ethanol. The pervaporation membrane has the advantage for the direct separation and it does not need the third component to shift or break the azoetrope. The pervaporation cell produced the following results confirming that the composite flat sheet membrane can be used for the production of high purity ethanol. The optimum temperature and pressure was found.

Ethanol purity

Ethanol purity was tested on the retentate stream for the refractive index after it was diluted with distilled water. This was done at different temperatures and compared with literature values taken from Weast (1983-1984). The water was collected from the permeate tank and the refractive index was tested and compared with literature values from Weast (1983-1984). The desired product (ethanol) was found at retentate stream,

and it was very important to measure the refractive index of the ethanol. Tables 5.29 – 5.31 represent the refractive index of the ethanol product in the permeate stream which provides the purity of ethanol and water.

Table 5.29: Refractive index at different temperatures (99 ethanol vol/vol%).

		Temperature (K)			
	Literature[a]	313.14	323.15	333.15	343.15
Ethanol	1.3612	1.3601	1.3609	1.3611	1.3612
Water	1.336	1.336	1.337	1.337	1.336

[a]Literature values (Weast, 1983-1984) at 293.15 K

Table 5.30: Refractive index at different temperature for 95 wt% ethanol.

		Temperature (K)			
	Literature[a]	313.14	323.15	333.15	343.15
Ethanol	1.3612	1.356	1.358	1.359	1.360
Water	1.336	1.334	1.335	1.337	1.336

[a]Literature values (Weast, 1983-1984) at 293.15 K

Table 5.31: Refractive index at different temperature for 90 wt% ethanol.

		Temperature (K)			
	Literature[a]	313.14	323.15	333.15	343.15
Ethanol	1.3612	1.345	1.352	1.359	1.3611
Water	1.336	1.335	1.335	1.335	1.336

[a]Literature values (Weast, 1983-1984) at 293.15 K

The water flux was measured by collecting a certain volume in the permeate tank. The flux was calculated using equation (3.110). Figures 5.27 – 5.28 represent the water flux at different temperature and pressure.

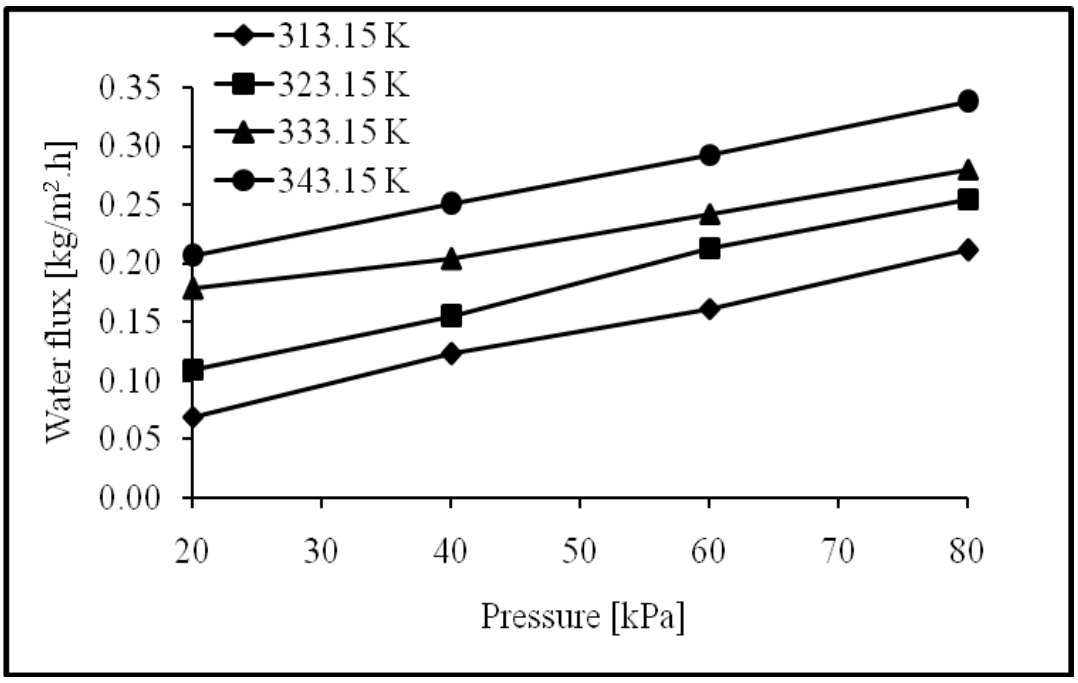

Figure 5.27: Water flux at different temperatures.

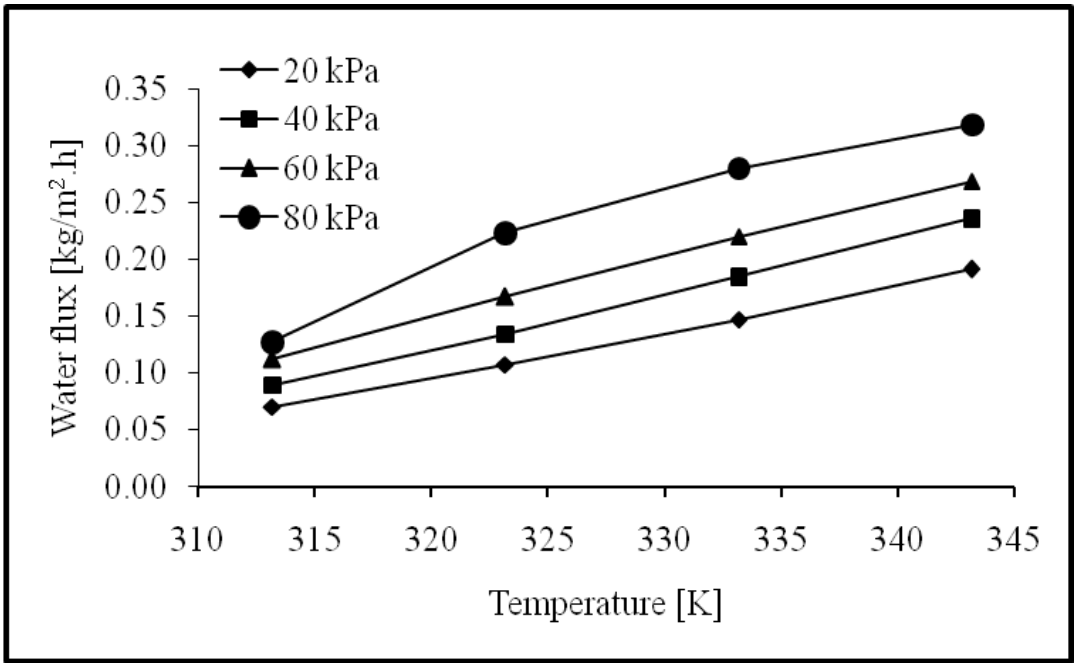

Figure 5.28: Water flux at different pressures.

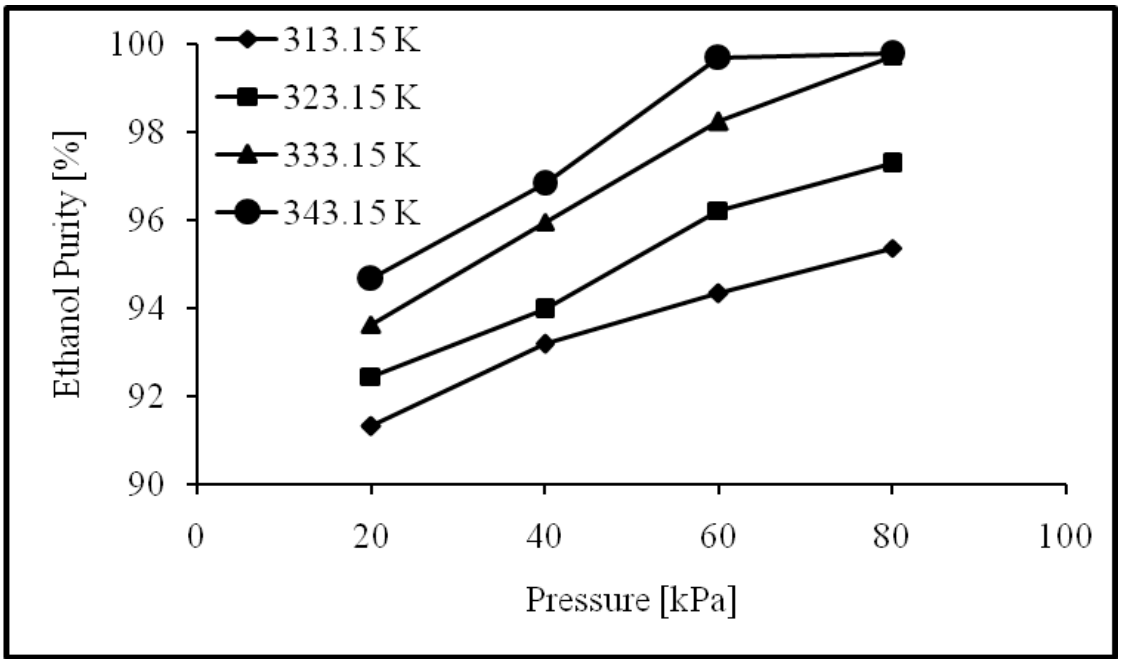

Figure 5.29: Product purity for feed composition of 10% water and 90% ethanol.

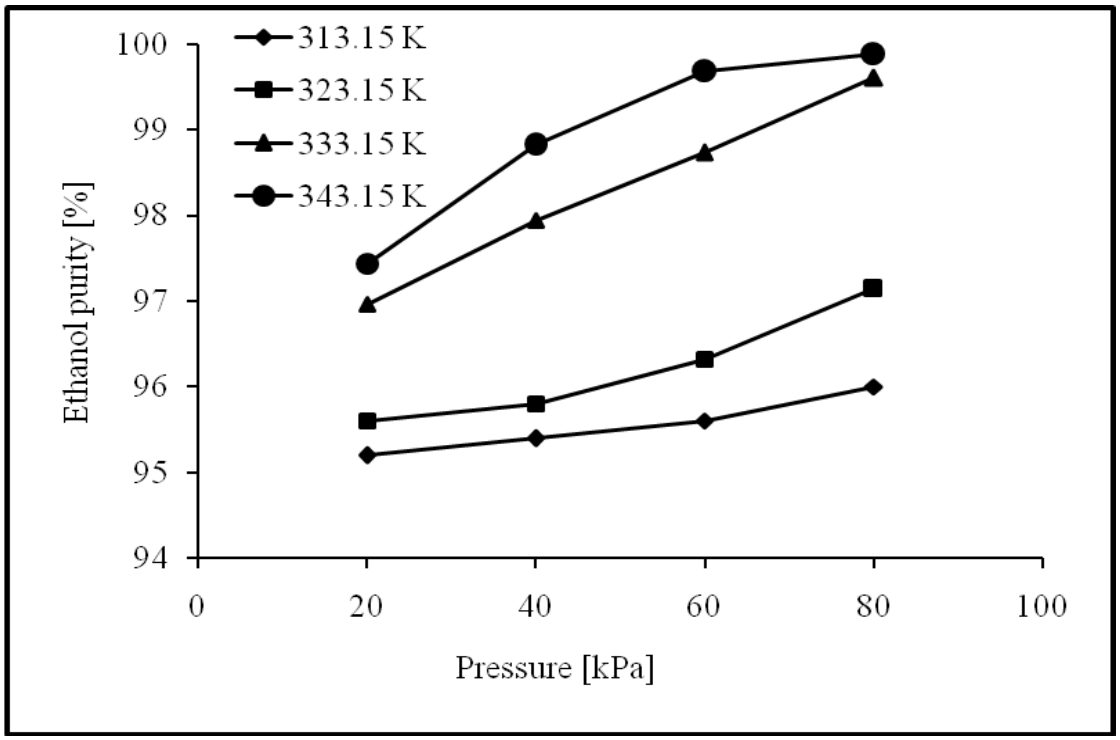

Figure 5.30: Product purity for feed composition of 5% water and 95% ethanol.

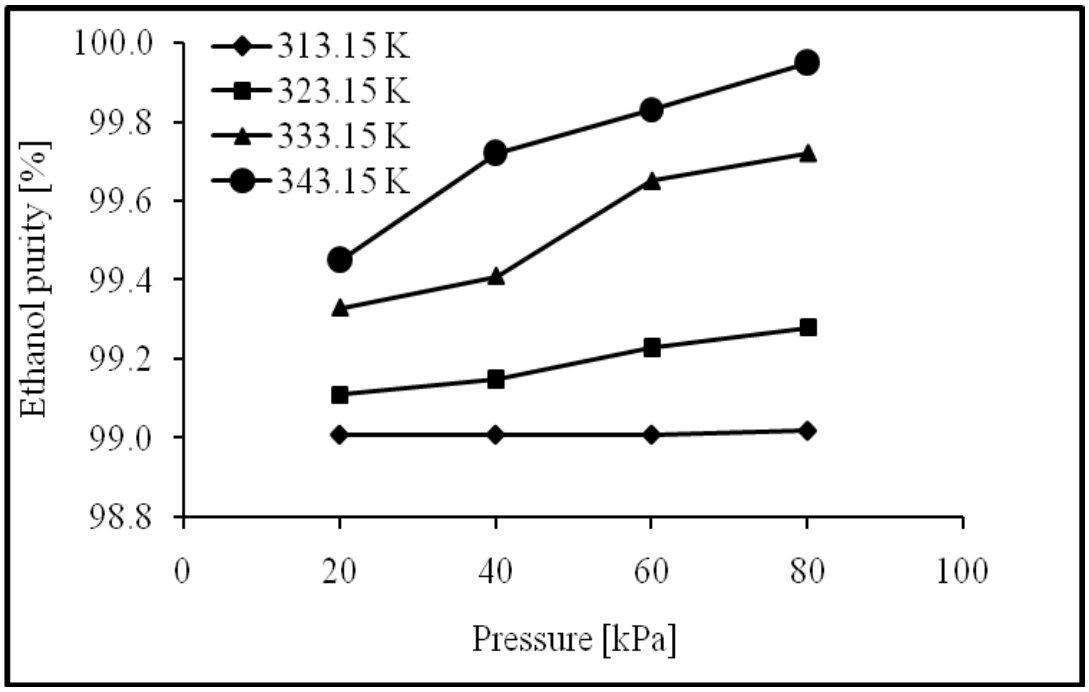

Figure 5.31: Product purity for feed composition of 1% water and 99% ethanol.

Separation factor for pervaporation membrane in ethanol/water mixture

The separation factor is defined as the ratio of the components in the permeate vapour to the ratio of the components in the feed vapour. The separation factor for the separation of ethanol and water was calculated at different temperatures (313.15, 323.15, 333.15 and 343.15) K, where the feed composition of ethanol-water mixture changed from 90% (vol/vol) ethanol and 10% (vol/vol) water to 99% (vol/vol) ethanol and 1% (vol/vol) water. Tables 5.32 – 5.14 represent the separation factor. Figure 5.32 – 5.35 represent the graphical separation factor at different temperatures.

Table 5.32: Separation factor at feed composition of 1% water and 99% ethanol.

Separation factor (α) at 313.15 K		Separation factor (α) at 323.15 K		Separation factor (α) at 333.15 K		Separation factor (α) at 343.15 K	
Ethanol mass %	α	Ethanol mass %	α	Ethanol mass %	α	Ethanol mass %	α
0.9901	1420.134	0.9911	1581.295	0.993	1835.725	0.994	1930.836
0.9902	1435.818	0.9915	1619.519	0.994	1883.028	0.997	1986.424
0.9902	1454.824	0.9923	1759.594	0.996	1915.531	0.998	2066.256
0.9903	1527.187	0.9928	1819.312	0.997	1987.387	0.999	2174.763

Table 5.33: Separation factor at feed composition of 5% water and 95% ethanol.

Separation factor (α) at 313.15 K		Separation factor (α) at 323.15 K		Separation factor (α) at 333.15 K		Separation factor (α) at 343.15 K	
Ethanol mass %	α	Ethanol mass %	α	Ethanol mass %	α	Ethanol mass %	α
0.952	878.690	0.956	1178.674	0.969	1340.591	0.974	1513.354
0.954	952.153	0.958	1203.508	0.979	1559.363	0.988	1728.285
0.956	1035.970	0.9632	1351.401	0.987	1896.925	0.996	1953.479
0.960	1184.246	0.9714	1735.047	0.996	2136.576	0.998	2123.280

Table 5.34: Separation factor at feed composition of 5% water and 95% ethanol.

Separation factor (α) at 313.15 K		Separation factor (α) at 323.15 K		Separation factor (α) at 333.15 K		Separation factor (α) at 343.15 K	
Ethanol mass %	α	Ethanol mass %	α	Ethanol mass %	α	Ethanol mass %	α
0.913	569.298	0.924	662.377	0.936	794.712	0.946	959.744
0.9367	780.782	0.939	820.803	0.959	896.567	0.968	1238.756
0.9432	857.375	0.962	1310.679	0.982	1414.176	0.996	1945.488
0.9535	1047.483	0.972	1826.980	0.997	1930.604	0.997	2177.870

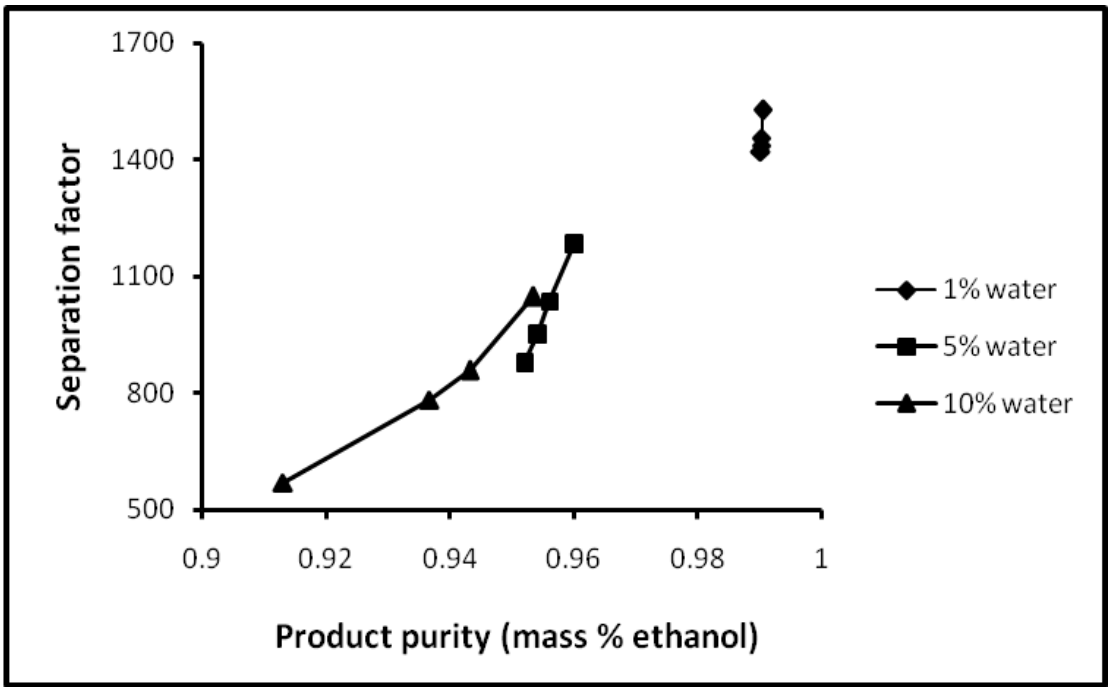

Figure 5.32: Separation factor achieved for ethanol-water at feed composition of 1%, 5% and 10% water at 313.15 K.

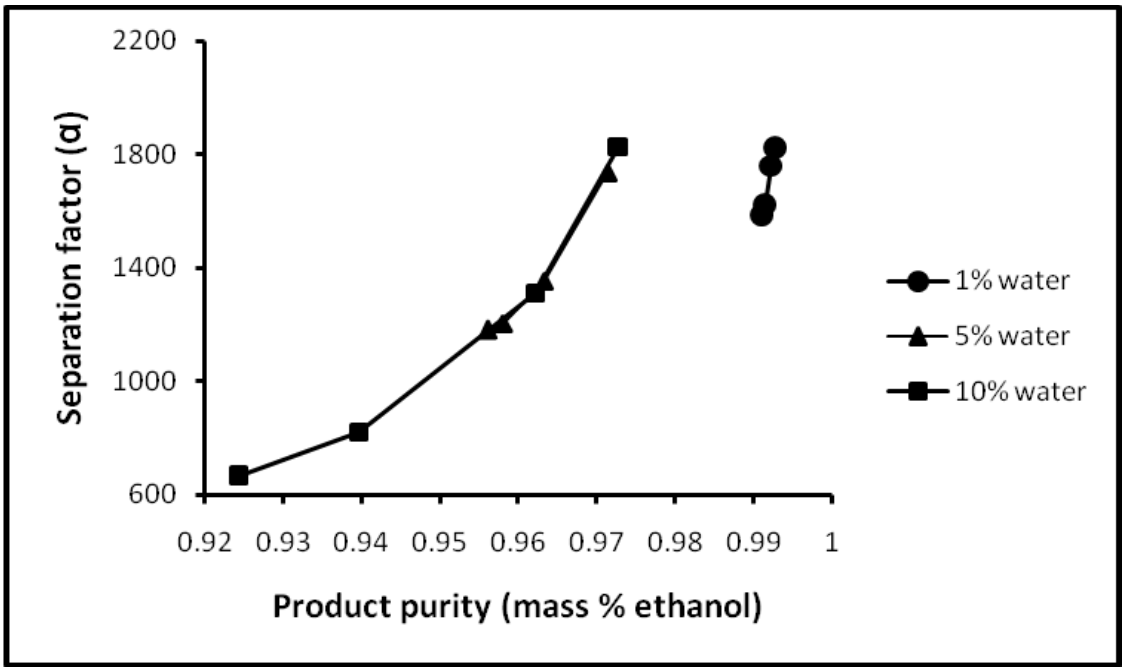

Figure 5.33: Separation factor achieved for ethanol-water at feed composition of 1%, 5% and 10% water at 323.15 K.

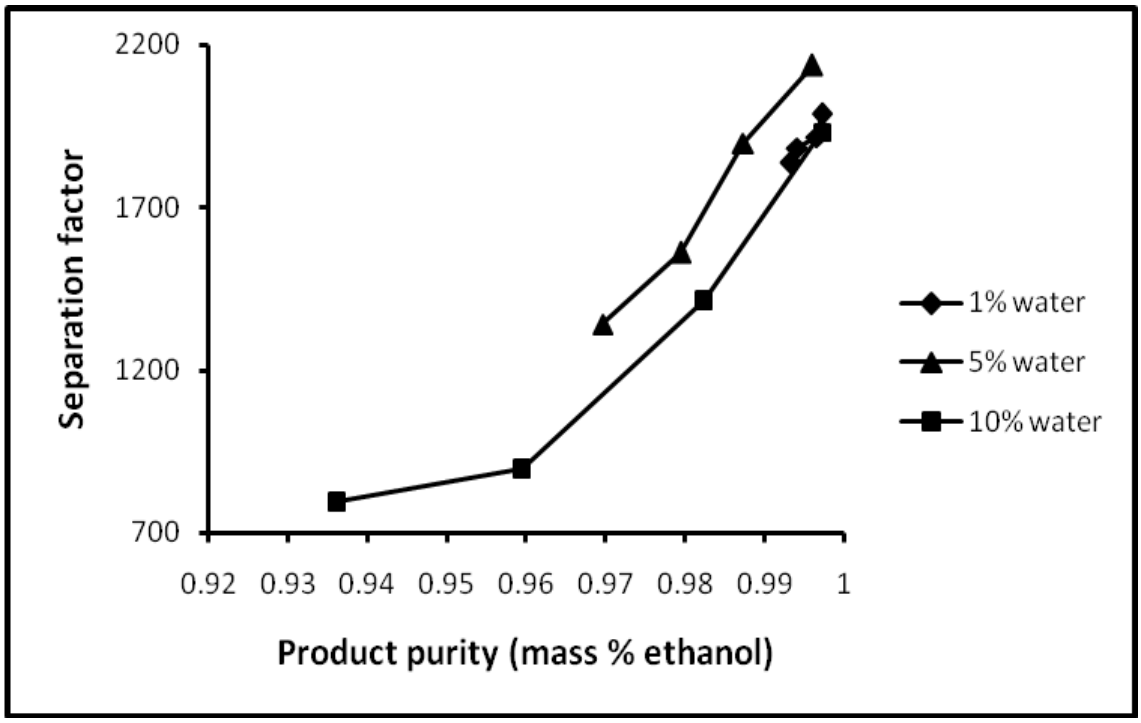

Figure 5.34: Separation factor achieved for ethanol-water at feed composition of 1%, 5% and 10% water at 333.15 K.

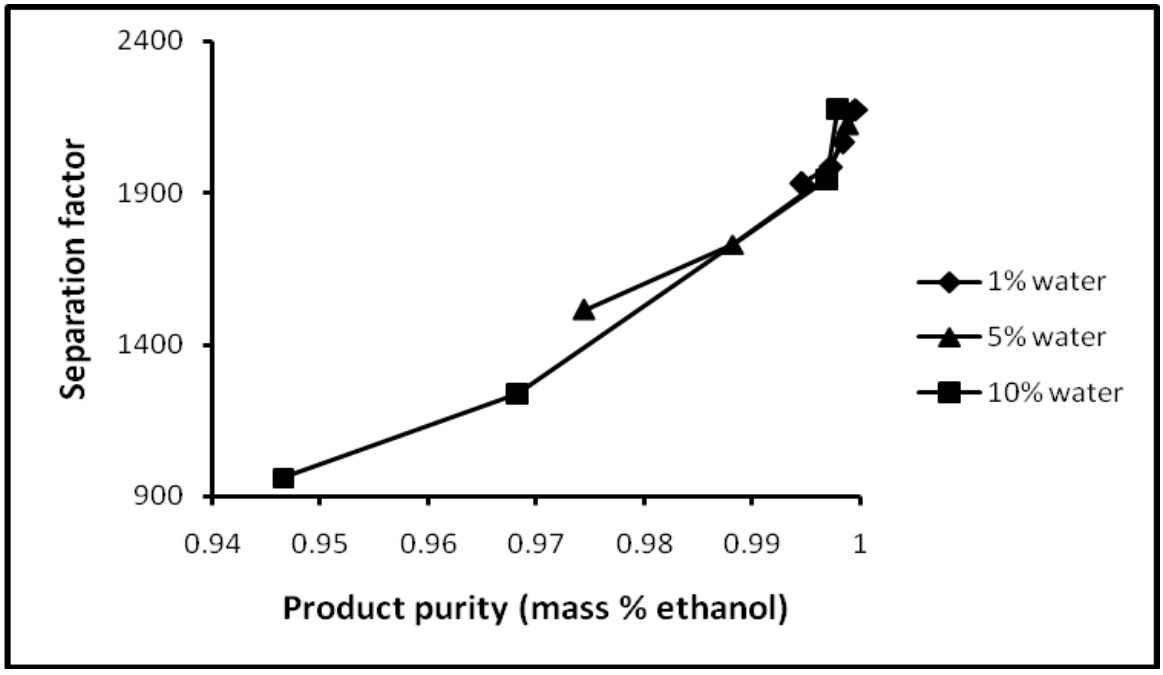

Figure 5.35: Separation factor achieved for ethanol-water at feed composition of 1%, 5% and 10% water at 343.15 K.

5.12 DISCUSSION OF THE PERVAPORATION RESULTS

Pervaporation membrane

Pervaporation has the added advantage in that it facilitates the direct separation of the azeotrope without the addition of other chemicals. Hence, this study was undertaken to explore **the effect of temperature and pressure** using the pervaporation process for the recovery of the high purity ethanol production. In this study the separation of the ethanol-water system was investigated at the concentrations of 90% ethanol and 10% water (vol/vol) to 99% ethanol to 1% water (vol/vol) using pervaporation membrane at different operating pressures from 20 kPa to 100 kPa and changing the feed temperatures from 313.15 K to 343.15 K.

Product (ethanol) in pervaporation process

In pervaporation process, the desired product was found in the retentate stream, which was the ethanol with some water. Pure water was collected in the permeate stream. The special type of composite flat sheet membrane allowed only water to pass through the membrane. This type of membrane was called hydrophilic membrane. It was found that the separation of the ethanol/water mixture was affected at a high flow rate of 50 L/hr in the pervaporation cell. Therefore, it was difficult to achieve a permeate. It is not advisable to operate at very low flow rates below 20 L/hr, because the ethanol/water mixture will stay in the pervaporation cell at the top of a composite flat sheet membrane, which will then become swollen, although some permeate is obtained. It was found that the suitable flow rate for this particular pervaporation cell was 35 to 40 L/hr for all operating pressures. From literature the boiling point of ethanol is 351.15 K, the temperature in the heater storage feed tank was set so that it would not exceed 343.15 K, because ethanol would evaporate. It was found that by applying a low pressure through membrane, it pulls only water vapours, because the type of membrane allows only water to pass through. Almost 50 ml of water was recovered in 2 hours. At a low pressure, less volume was collected compare at a higher pressure of 80 kPa.

Effect of temperature and pressure

The results in Figures 5.29 – 5.31 indicate the repeatability and consistency of the effect of temperature and pressure in the recovering high purity ethanol. The ethanol purity is a function of the temperature, because it shows that as the operating temperature increases from 313.15 K to 343.15 K, the ethanol purity increases. The water flux increased with an increase of temperature and pressure as indicated in Figures 5.27 and 5.28. Tables 5.29 – 5.31 indicate the refractive index at 1%, 5% and 10% ethanol purity at the different temperatures. The refractive indices obtained in the experiment were compared with the refractive index in the literature. It was found that only water was obtained in the permeate stream as the values of refractive index of water was very close to the literature value of Perry and Green (1997).

In addition, the increase thermal motions of the permeating molecules also promote their diffusion. This effect brings about the rapid increase in permeation water, as a result increases ethanol purity. With increases in temperature there is a corresponding increase in the permeate rate, water flux increases. Lund (1995) found that an increase in temperature follows an Arrhenius pattern, confirming the predictions obtained from the conceptual model.

It was found that at the lower temperature of 313.15 K less water was removed in system. Although the system operates at high pressure of 80 kPa and at high concentration of ethanol (99%), it was difficult to remove water at low temperature as shown in Figure 5.31. At high temperature of 333.15 K and 343.15 K and high pressure of 60 kPa and 80 kPa the permeate (water) rate increased per hour as shows in Figures 5.29 and 5.30 as a result of increase in flux as well as the high purity ethanol production increased. These findings indicate that the composite flat sheet pervaporation membrane performed much better at higher temperature and high pressure. The best operating temperature was found at 333.15 K and the pressure of 80 kPa, because at high temperature of 343.15 K some vapours of ethanol was lost in the system. This was found from the calculation of the mass balances on ethanol. Figures 5.29 – 5.31 indicate that as the temperature increases and pressure increases, the ethanol purity increased in the retentate stream. Therefore, the

effect of pressure and temperature increases the performance of the pervaporation using the hydrophilic membrane.

Figure 5.32 – 5.35 shows the separation factor at 99% ethanol and 1% water (vol/vol), 95% ethanol and 5% water (vol/vol), 90% ethanol and 10% water (vol/vol). The increase in temperature from 313.15 K to 343.15 K led to the increased of the separation factors. Results for the separation are tabulated from Tables 5.32 – 5.34. The pervaporation system operating at low flow rate of 35 l/hr leads to high separation factor but lower flux as confirmed by Huang *et al*. (2001).

5.13 Comparison of pervaporation and extractive distillation

When comparing the pervaporation process and extractive distillation, one finds that in the extractive distillation a third component must be added to the system as a separating agent, either salt or liquid. In extractive distillation, salt is more effective because it increases the relative volatility of the ethanol and increases the boiling point of water. Therefore, calcium chloride salt could be used in the extractive distillation to eliminate the azeotrope of the ethanol-water system and the high purity ethanol production could be achieved. These could be achieved using the concentration of 0.3 g/ml of $CaCl_2$ at higher temperature and pressure. The advantage of extractive distillation using salt is that it does not need the second column to remove the salt. Alternatively, the pervaporation process has the advantage of facilitating the direct separation of ethanol-water system as a result of shifting or eliminating the azeotrope completely from the ethanol-water mixture without adding the third component as a separating agent. The elimination of the azeotrope from ethanol-water mixture leads to the recovery of high purity ethanol production. In addition, pervaporation membrane separation could be considered as one effective method and energy-saving process for this azeotropic system.

CHAPTER 6

CONCLUSIONS AND RECOMMEMDATIONS

6.1 Conclusions

Effect of salt in extractive distillation

A vapour-liquid equilibrium recirculation still was used for the measurement of VLE data. In this study calcium chloride was chosen because it provides the largest salting out effect on ethanol. VLE experimentation was performed to assess the ability of calcium chloride as a separating agent in the extractive distillation. The success of calcium chloride salt as a separating agent to eliminate or remove the ethanol-water azeotrope, was achieved at the concentration of 0.2 g/ml and 0.3 g/ml. It shows that at these concentrations an increase in the relative volatility, results in the recovery of the high purity ethanol production at the top of the column. The low concentration of 0.1 g/ml did not eliminate the azeotrope in the ethanol-water system. The interaction parameters were determined for the excess Gibbs energy models: Wilson and NRTL. The fit of these models to the experimental data gave low deviations between the calculated and experimental data. Salt became saturated at the high concentration of 0.4 g/ml.

Pervaporation

This study has shown that the composite flat sheet pervaporation membrane could separate ethanol and water. The increase of water flow rate in the permeate increased the water flux, as a results of increasing the concentration of the ethanol in the retentate stream, this leads to the high purity ethanol production. The effects of temperature and pressure on the pervaporation process increased the performance of the pervaporation membrane. In additional, pervaporation membrane separation could be considered as one effective method and energy-saving process for the separation of the azeotropic system. The pervaporation membrane facilitates the direct separation of ethanol-water system.

6.2 Recommendations

The following recommendations are suggested for use of salt (calcium chloride) in the extractive distillation process and pervaporation process for the ethanol-water system in order to achieve high purity ethanol.

Salt in extractive distillation

Further research could be conducted to assess the potential use of the calcium chloride salt in separation of the ethanol/water system in the extractive distillation above atmospheric pressure with the concentrations below 0.4 g/ml. It is recommended that calcium chloride could be recovered at the bottom of the extractive distillation because it could be used for another purpose. Most researchers presented the experimental VLE data with no attempt to develop correlations for the binary systems or ternary system. It is recommended to use the Wilson, NRTL and UNIQUAC models to regress the systems with salts.

Pervaporation

The pervaporation technique can be considered for commercial applications as it is clear more investigation need to be done on this particular system as it not applicable for large

scale. It is recommended that other processes be employed in the separation of ethanol and water in the industrial separation. An improvement in developing the mathematical model is also recommended, as the existing solution procedure involves the fitting of fluxes. It is suggested to develop a model so that the fluxes and selectivities may be predicted simultaneously. In addition, it is recommended that the cooling system must be at least 268.15 K, so that all vapours would condense resulting in more permeate collected. A hydrophobic membrane could be evaluated with the addition of salt.

References

Abbott, M. M., 1986. *Low-pressure phase equilibria: Measurement of VLE*. Fluid Phase Equilibria, Vol. 29, (193 – 207)

Abrams, D. S., and Prausnitz, J. M., 1975. *Statistical thermodynamics of liquid mixtures: a new expression for the excess Gibbs energy of partly or completely miscible systems*, American Institute of Chemical Engineers Journal, Vol. 21, p. (116 – 128)

Abu Al-Rub, F. A., Banat, F. A., and Simandl, J., 1999. *Isothermal vapour-liquid equilibria of 1-propanol-water mixtures*, Chemical Engineering Journal, Vol. 74, p. (205 – 210)

Anderson, T. F., Prausnitz, J. M., 1978. *Application of the UNIQUAC equation to calculation of multicomponent phase equilibria. 1: VLE; 2. LLE*, Industrial and Engineering Chemistry, Process Design and Development, Vol. 17, p. (552 – 567)

Baker, R. W., 2004. *Membrane Technology and Applications*, 2nd Edition, Chichester, England, Wiley

Belyaev, A. S., Trifonov S. A., and Mushtaev V. I., 2003. *Separation of a Propanol-Water mixture by Membrane Pervaporation*, Chemical and Petroleum Engineering, Vol. 39, p. (583 – 587).

Binning, R. C., Lee, R. J., Jennings, J. F., Martin, E. C., 1961. *Separation of liquid mixtures by permeation*, Industrial and Engineering Chemistry, Vol. 53, No.1, p. (45 – 50)

Boddeker, K. W., Bengston, G., Pingel, H., 1990. *Pervaporation of isomeric butanols*, Journal of Membrane Science, Vol. 54, p. (1 – 12)

Bowen, T. C., Meier, R. G., Vane, L. M., 2007. *Stability of MFI zeolite-filled PDMS membranes during pervaporative ethanol recovery from aqueous mixtures containing acetic acid*, Journal of Membrane Science, Vol. 298, p. (117 – 125)

Brubaker, D. W., and Kammermeyer, K., 1954. *Separation of gases by plastic membrane: Permeation rates and extent of separation,* Industrial and Engineering Chemistry, Vol. 46, No.4, p. (733 – 742)

Busca, G., Berardinelli, S., Resini, C., Arriighi, L., 2008. *Technologies for the removal of phenol from fluid streams: A short review of recent development*, Journal of Hazardous Material, Vol. 113, p. (1 – 24)

Calvar, N., Gonzalez, B., Gomez, E., Dominguez, A., 2006. *Vapor−liquid equilibria for the ternary system ethanol + water + 1-butyl-3-methylimidazolium chloride and the corresponding binary systems at 101.3 kPa*, Journal of Chemical Engineering Data, Vol 51, p. (2178 – 2181)

Calvar, N., Gonzalez, B., Gomez, E., Dominguez, A., 2007. *Study of the behavior of the azeotrope ethanol and water with imidazolium based ionic liquids*, Fluid Phase Equilibria, Vol. 259, p. (51 – 56)

Chen, B. H., Lei, Z. G., and Li, J. W., 2003. *Effect of salt in the extractive distillation,* Journal Chemical Engineering, Vol. 36, p. (20 – 24)

Chou, T. J., and Tanioka., 1999. *Predicting the effect of dissolved salt on the vapour-liquid equilibria for alcohol-water-salt systems*, Trans IChemE, Vol. 77, Part A, p. (329 – 334)

Danner, R. P., and Gess, M. A., 1990. *A data base standard for the evaluation of Vapour-liquid equilibrium models*, Fluid Phase Equilibria, Vol. 56, p. (285 – 301)

Dekker, M., 1999. *Alcohol/Ether separation by pervaporation. High performance membrane design*, Separation Science and Technology, Vol. 34, No. 3, p. (369 – 390)

Doghier, F., Nardella, A., Sarti, G. C., Valentini, C., 1994. *Pervaporation of methanol MTBE mixtures through modified poly(phenylene oxide) membrane*, Journal of Membrane Science, Vol. 91, p. (283 – 291)

Dong, Y. Q., Zhang, L., Shen, J. N., Song, M. Y., Chen, H. L., 2006. *Preparation of poly(vinyl alcohol) sodium algimat hollow-fiber composite membranes and pervaporation dehydration characterization of aqueous alcohol mixture*, Desalination, Vol. 193, p. (202 – 210)

Driolli, E., 1992. *Emerging membrane processes*, Recent Progress En Genie Des Proceeds, Vol. 6, No. 21, p.(339 – 348)

Driolli, E., Zhang, S., and Basile A., 1993. *On the coupling effect in pervaporation*, Journal of Membrane Science, Vol. 81, p. (43 – 55)

Duan, Z. T., Lei, L. H., Zhou, R. Q., 1980. *Salt effect on vapour-liquid equlibria for binary systems of propanol/$CaCl_2$ and butanol/$CaCl_2$,* Petrochemical Technology (China), Vol. 9, p. (350 – 353)

Dutta, B. K., and Sikdar, S. K., 1991. *Separation of azeotropic organic liquid mixtures by pervaporation,* AICHE, Vol. 37, No. 4, p. (581 – 588)

Fahmi, A., Abu, A-R., Fawzi, A. B., Rami, J., 1999. *Vapour-Liquid Equilibrium of ethanol-water system in the presence of molecular sieves*, Separation Science and Technology, Vol. 34, No. 12, p. (2355 – 2368)

Farve, E., and Vallieres, C., 2004. *Pressure versus sweeping gas operation for binary mixtures separation by dense membrane processes*, Journal of Membrane Science, Vol. 244, p. (17 – 23)

Field, R. W., and Lipniziki, F., 2001. *Integration of pressure and sweep gas pervaporation to recover organic compounds from wastewater*, Separation and Purification Technology, Vol. 22 – 23, p. (347 – 360)

Fileti, E. E., Chaudhuri, P., Canuto, S., 2004. *Relative strength of hydrogen bond interaction in alcohol and water complexes*, Chemical Physics Letters, Vol. 400, p. (494 - 499)

Fleming, H. L., 1992. *Consider membrane pervaporation*, Chemical Engineering Progress, Vol. 5, p. (46 – 52)

Fredunslund, A., Gmehling, J., Rasmussen, P., 1977. *Vapour-Liquid Equilibrium using UNIFAC,* Elsevier, Amsterdam

Furter, W. F., 1992. *Extractive distillation by salt effect*, Chemical Engineering Communication, Vol. 116, p. (35 – 40)

Furter, W. F., 1993. *Production of fuel-grade ethanol by extractive distillation employing the salt effect,* Separation and Purification Technology, Vol. 22, No. 1, p. (1 – 21)

Gao, Z., Wang, S., Sun, Q., and Zhang, F., 2003. *Isobaric phase equilibria of the system 1-butanol + water containing penicillin G potassium salt at low pressures,* Fluid Phase Equilibria, Vol. 214, p. (137 – 149)

Gess, M. A., Danner, R. P., Nagvekar, M., 1991. *Thermodynamics analysis of vapour-liquid equilibria: Recommended models and a standard data base,* Design Institute for Physical Property Data, American Institute of Chemical Engineers

Gil, I. D., Uyazan, A. M., Aguilar, J. L., Rodriguez, G., Caicedo, L. A., 1996. *Dehydration of azeotrope ethanol by extractive distillation with salt and solvent as an entrainer,* Chemical Engineering Science, Vol. 51, p. (11 – 20)

Gmehling, J and Oken, U., 1977-1982. *Vapour-liquid equilibrium data collection,* DECHEMA Chemistry data series, Frankfurt/Main

Gmehling, J., Oken, U., Arlt, W., 1984. *Vapour-liquid equilibrium data collection*: Chemistry data series, Vol. 1, Part 8, DECHEMA

Gu, F and Hou, Y., 2000. *Salt effects on the Isobaric vapour-liquid equilibrium for four binary systems,* Journal of Chemical Engineering Data, Vol. 45, p. (467 – 470)

Guerreri, G., 1992. *Membrane alcohol separation process: Integrated pervaporation and fractional distillation*, Transaction of Institute Chemical Electronics, Part A, Vol. 70, p. (501 – 508)

Haggin, J., 1988. *New generation of membranes developed for industrial separations,* Chemical and Engineering News, Vol. 66, p. (7 – 16)

Harris, R. A., 2004. *Monoethanolamine: Suitability as an Extraction Solvent,* Master of Science in Engineering (Chemical Engineering) Thesis, University of KwaZulu-Natal, South Africa

Hayden, J. D., and O'Connell, J. P., 1975. Generalized *Method for Predicting Second Virial Coefficients*, Industrial and Engineering Chemistry. Process Design and Development, Vol.14, p. (209 – 216).

Herington, E. F. G., 1947. *A Thermodynamic consistency test for the internal consistency of experimental data of volatility ratios,* Nature, Vol. 160, p. (610 – 611)

Hilal, N., Yousef, G., Anabtawi, M. Z., 2002. *Operating parameters effect on methanol-acetone separation by extractive distillation,* Separation Science Technology, Vol. 37, p. (3291 – 3303)

Hilmen, E.-K., 2000. *Separation of Azeotropic Mixtures: Tools for Analysis and Studies on Batch Distillation Operation*, Phd Thesis (Chemical Engineering) University of Science and Technology, Norwegian

Hirata, M. S., Ohe, S., Nagahama, K., 1975. *Computer aided data book of vapour-liquid equilibria,* Kodansha Elsevier, Tokyo

Hollein, M. E., Hammond, M., Slater, C. S., 1993. *Concentration of dilute acetone-water solutions using pervaporation,* Separation Science and Technology, Vol. 28, No. 4, p. (1043 – 1061)

Hoshi, M., Kogure, M., Saitoh, T., Nakagawa, T., 1997. *Separation of aqueous phenol through polyurethane membranes by pervaporation,* Journal Applied Polymer Science, Vol. 65, p. (469 – 479)

Howell, D., Coutinho, P., Macedo, E. A., 1989. *Infinite-dilution activity coefficients by comparative ebulliometry. Binary systems containing chloroform and diethylamine*, Fluid Phase Equilibria, *Vol. 95* , p. (149 – 162)

Huang, H-J., Ramaswamy, S., Tshirner, U.W., Ramardo, B.V., 2008. *A review of separation technologies in current and future biorefiners, Separation and purification Technology*, Vol 62, p.(1 – 21)

Huang, R. Y. M., 1991. *Pervaporation membrane separation processes*, Membrane Science and Technology Series, Elsevier

Huang, R. Y. M., and Jarvis, N. R., 1970.*Separation of liquid mixtures by using polymer membrane II. Permeation of aqueous alcohol solutions through cellophane and poly (vinyl alcohol)*, Journal of Applied Polymer Science, vol. 14, p. (2341 – 2356)

Izadifar, M., and Baik, O. D., 2008. *An optimum ethanol-water solvent system for extraction of podophyllotoxin: Experimental study, diffusivity determination and modeling*, Separation and Purification Technology, Vol. 63, No. 1, pp. (53 – 60)

Joseph, A. M., 2001. *Computer-aided Measurement of Vapour Liquid Equilibria in a Dynamic Still at Sub-Atmospheric Pressures*, Master of Science in Engineering (Chemical Engineering) Thesis, University of KwaZulu-Natal, South Africa

Kato, M., Sato, T., Hirata, M., 1971. *Measurement of salt effect on vapour-liquid equilibria by bubble and condensation point method*, Journal of Chemical Engineering of Japan, Vol. 4, p. (308 – 311)

Knight, K. F., Duggal, A., Shelden, R. A., Thompson, E. V., 1986. *Dependence of diffusive permeation rates and selectivities on upstream and downstream pressures, Part V. Experimental results for the hexane/heptanes (ideal) and toluene/ethanol (non-ideal) system*, Journal of Membrane Science, Vol. 26, p.(31 – 50)

Kujawski, W., Pozniak, G., 2004. *Swelling properties of ion-exchange membranes in contact with water-alcohol mixtures,* Separation Science and Technology, Vol. 39, p. (2137 – 3154)

Kumar, A., 1993. *Salt effect on vapour-liquid equilibria: A review of correlations and predictive models,* Separation Science and Technology, Vol. 10, No. 10, p. (1799 – 1818)

Kondo, M., and Sato, H., 1994. *Treatment of wastewater from phenolic resin process by pervaporation,* Desalination, Vol. 98, p. (147 – 154)

Koops, G. H., and Smolders, C. A., 1991. *Estimation and evaluation of polymeric materials for pervaporation membranes,* Elsevier Science Publishers, p. (253 – 278)

Koretsky, D. M., 2003. *Engineering and Chemical Thermodynamics,* New York, Wiley

Krafczyk, J., Fischer, K, Gmehling. J., Menke, J., 2004. *Azeotropic Data*, Second, Completely Revised and Extended Edition, Part 1, Weinheim, Wiley-VCH

Kreiter, R., Wolfs, D. P., Engelen, C. W. R., van Veen, H. M., Vente, J. F., 2008. *High-temperature pervaporation performance of ceramic-supported polyimide membranes in the dehydration of alcohols,* Journal of Membrane Science, Vol. 29, p.(13 – 20)

Letcher, T. M., 2004. *Chemical Thermodynamics for Industry,* Cambridge, Royal Society of Chemistry

Lee, L-S., and Huang, M-Y., 2000. *The vapour-liquid equilibrium of ethanol-water mixture in the presence of benzyltriethylammonium chloride salt at atmospheric pressure,* Chemical Engineering Communication, Vol. 180, No. 1, p. (19 – 38)

Lee, K-R., Liu, M-J., Lai, J-Y., 1994. *Pervaporation separation of aqueous alcohol solution through asymmetric polycarbonate membrane,* Separation Science and Technology, Vol. 29. No. 1, p. (119 – 134)

Lei, Z., Wang, H., Zhou, R., Duan, Z., 2002. *Solvent improvement for separating C4 with ACN* , Separation Science and Technology, Vol 26, p. (1213 – 1221)

Lei, Z., Wang, H., Zhou, R., Duan, Z., 2002.*Influence of salt added to solvent on extractive distillation,* Chemical Engineering Journal, Vol. 87, p. (149 – 156)

Lei, Z., Li, C., Chen, B., 2003. *Extractive distillation: A review,* Separation and Purification reviews, Vol. 32, No. 2, p. (121 – 213)

Lightning Africa, May 2005. *Chemical Technology*, Features: Design and Construction of Chemical Plant, Water treatment, Material and Chemical product design and Solids Handling

Lipnizik, F., Field, R. W., 2001. *Integration of pressure and sweep gas pervaporation to recover organic compounds from wastewater,* Separation and Purification technology, Vol. 22-23, p. (347 – 360)

Liu, X., Sun, Y., Deng, X., 2008. *Studies on the pervaporation membrane of permeation water from methanol/water mixture,* Journal of membrane Science, Vol. 325, p. (192 – 198)

Loeb, Y. C., 1958. *Study of the asymmetric pervaporation membrane,* Journal of Membrane Science, Vol. 343, p. (176 – 179)

Lund, J. G., 1995. *Pervaporative separation of oleinic/oxygenate hydrocarbon mixtures*, Master of Science in Engineering (Chemical Engineering) Thesis, University of KwaZulu-Natal, South Africa

Ma, Y., Wang, J., Tsuru, T., 2009. *Pervaporation of water/ethanol mixtures through microporous silica membranes,* Separation and Purification Technology, Vol. 42, p. (33 – 39)

Malanowski, S., Anderko, A., 1992. *Modelling phase equilibria – Thermodynamic background and practical tools,* Wiley Series in Chemical Engineering, John Wiley & Sons, New York, Chichester,

Malasinksi, W., 1965. *Azeotropy and other theoretical problems of vapour-liquid equilibrium*, Interscience, New York

Mariah, L., 2006. *Membrane distillation of concentrated brines*, Phd Thesis (Chemical Engineering), University of KwaZulu-Natal, South Africa

Mario, L-R., and Jamie, A-A., 2003. *Modeling and simulation of saline extractive distillation columns for the production of absolute ethanol,* Computer & Chemical Engineering, Vol. 27, Issue 12, p. (527 – 549)

Marsh, K. N., 1989. *New methods for vapor-liquid-equilibria measurements,* Fluid Phase Equilibria, Vol. 52, p. (169 – 184)

Marquardt, D. W., 1963. *An algorithm for least-squares estimation of non-linear parameters,* Journal. Society of Industrial and Applied Mathematics, Vol. 11, p. (431 – 441)

Marzal, P., Monton, J. B., Rodrigo, A., 1996. *Isobaric vapour –liquid equilibria of the water + 2-propanol system at 30, 60 and 100 kPa,* Journal of Chemical Engineering Data, Vol. 41, p. (608 – 611)

McCandless, F. P., Alzheimer, D. P., Hartman, R. B., 1974. *Solvent membrane separation of benzene and cyclohexane,* Process Design and development, Vol. 12, No. 3, p. (310 – 312)

Mohammad, S., and Taghi, Z-A., 1996. *A modified solution-diffusion model for separation of ethanol-water azeotrope mixtures in pervaporation,* Chemical Engineering Communication, Vol.152, p. (405 – 412)

Mulder, M. H. V., Franken, T., Smolders, C. A., 1985. *Preferential sorption versus preferential permeability in pervaporation,* Journal of Membrane Science, Vol. 22, p. (155 – 173)

Nakane, T., and Yanagishita, H., 1992. *Preparation of asymmetric polyimide membranes by the phase inversion process,* Koubunshi Ronbunshu, Vol. 49, p. (1015 – 1021)

Namboodiri, V. V., Bowen, T. C., Vane, L. M., 2006. *Selective of Ethanol from water by pervaporation: Zeolite-silicone rubber mixed matrix membranes*, Separation and Purification Technology, Vol. 125, p. (305-308)

Narasigadu, C., 2006. *Phase equilibrium investigation of the water and acetonitrile solvent with heavy hydrocarbons*, Master of Science in Engineering (Chemical Engineering) Thesis, University of KwaZulu-Natal, South Africa

Neel, J., 1991. *Introduction to pervaporation, In: "Pervaporation membrane separation processes"* Elsevier Science Publishers, p. (1 – 109)

Nomura, M., Bin, T., Nakao, S. I., 2002. *Selective ethanol extraction from fermentation broth using a silicate membrane*, Separation Science and Technology, Vol. 27, p. (59 – 66)

O'Brien, D. J. and Craig, J. C., 1996. *Ethanol production in a continuous fermentation/membrane pervaporation system*, Applied Microbiology Biotechnology, Vol. 44, p. (699 – 704)

Ohe, S., 1979. *Correlation and prediction of salt effects on vapor–liquid equilibrium in alcohol–water–salt systems,* Advances in Chemistry Series, No. 155

Ohe, S., 1991. *Computer Aided Data book of vapour pressure* (Liquid-Vapour Equilibrium in Binary Systems), Tokyo, Kodansha

Ohe, S., 1998. *Prediction of salt effect on vapour-liquid equilibria*, Fluid Phase Equilibria, Vol. 144, p. (119 – 129)

Ophardt, P., 2003. *Chemistry of hydrogen bond,* Journal of Applied Chemisrty, Vol. 73, p. (18 – 24)

Orye, R. V., and Prausnitz, J. M., 1965. *Multicomponent equilibria with the Wilson equation*, Industrial and Engineering Chemistry, Vol. 57, p. (18 – 26)

Palmer, D. A., 2000. *Handbook of Applied Thermodynamics*, 2nd Edition, McGraw-Hill.

Parke, S. A., and Birch, G. G., 1999. *Solution properties of ethanol in water*, Food Chemistry, Vol. 67, p. (241 – 246)

Paulsen, V. S., 2002. *Use a spreadsheet to fit vapour-liquid equilibrium data*, Chemical Engineering, No. 3, p. (78 – 81)

Peinemann, K. V. and Nunes, S. P., 2001. *Membrane Technology in the chemical industry*, Weinheim, New York, Wiley-VCH

Pereiro, A. B., Rodriguez, A., 2007. *Mixing properties of binary mixture presenting azeotropes at several temperatures,* Chemical Engineering Journal, Vol 39, p. (1219 – 1230)

Peng, M., Vane, L. M., Liu, S. X., 2003. *Recent advances in VOCs removal from water by pervaporation*, Journal of Hazardous Material, B98 p. (69 – 90)

Perry, R. H., and Green, D. W., 2004. *Perry's Chemical Engineers Handbook*, McGraw Hill Handbook, New York

Pitzer, K. S., and Curl., R. F., 1957. *Emperical Equation for the Second Virial Coefficient*, Journal of the American Chemical Society, Vol. 79, p. (2369 – 2370).

Pitzer, K. S., Lippmann, D. Z., Curl, R. F., Huggins, C. M., Petersen, D. E., 1955, *The Volumetric and Thermodynamic Properties of Fluids. II. Compressibility Factor, Vapour Pressure and Entropy of Vapourization,* Journal of the American Chemical Society, Vol. 77, p. (3433 – 3440)

Prausnitz, J. M., Lichtenthaler, R. N., de Azevedo, E. G., 1978. *Molecular Thermodynamics of Fluid – Phase Equilibria*, 3rd Edition, Prentice-Hall, Upper Saddle River, New Jersey

Prausnitz, J. M., Lichtenthaler, R. N .,and de Azevedo, E. G., 1999. *Molecular Thermodynamics of Fluid-Phase Equilibria*, 3rd Edition, Prentice-Hall, Upper Saddle River, New Jersey

Poling, B. E., Prausnitz, J. M., O'Connel, J. P., 2001. *The Properties of Gas and Liquids*, 5th Edition, McGraw-Hill

Raal, J. D., Mühlbauer A. L., 1998. *Phase Equilibria: Measurement and Computation*, Taylor & Francis, Briston PA

Raghunath, B., Hwang, S. T., 1992. *Effect of boundary layer mass transfer resistance in the pervaporation of dilute organics,* Journal of Membrane Science, Vol. 65, p. (147 – 161)

Rakshit, S. K., Ghosh, P., Bisaria, V. S., 1993. *Ethanol separation by selective adsorption of water*, Bioprocess Engineering,Vol. 8, pp. (279 – 282)

Rath, P., Naik, S. C., 2004. *Prediction of salt effect in vapour-liquid equilibria of system ethyl acetate-ethanol at atmospheric pressure*, Vol. 84, p. (71 – 76)

Rautenbach, R., Albrecht, R., 1980. *Separation of organic binary mixtures by pervaporation*, Journal of Membrane Science, Vol. 7, p. (203 – 223)

Rautenbach, R., Albrecht, R., 1984. *On the behavior of asymmetric membranes in pervaporation*, Journal of Membrane Science, Vol. 19, p. (1 – 22)

Rautenbach, R., Herion, C., Franke, M., Asfour, A-F. A., Bemquerer-Costa, A., 1988. *Investigation of mass transport in asymmetric pervaporation membranes*, Journal of Membrane Science, Vol. 36, p. (445 – 462)

Reddy, P., 2006. *Development of a novel apparatus for VLE measurement at moderate pressures*, Phd Thesis (Chemical Engineering) University of KwaZulu-Natal, South Africa

Redlich, O., Kister, A. T., 1948. Algebraic Representation of Thermodynamic Properties and the Classification of Solutions, *Industrial and Engineering Chemistry*, Vol. 40, p. (345 – 348)

Redman, J., 1990. *Pervaporation heading for new horizons*, Chemical Engineer, Vol. 469, p. (46 – 49)

Renon, H., and Prausnitz, J. M., 1968. *Local Compositions in Thermodynamic Excess Functions for Liquid Mixtures,* American Institute of Chemical Engineers Journal, Vol. 14, p. (135 – 144)

Roizard, D., Jonquieres, A., Leger, C., Noezar, I., and Nee, J., 1999. *Alcohol/Ether Separation by pervaporation: High Performance Membrane Design,* Separation Science and Technology, Vol. 34, No. 3, p. (369 – 390)

Rongqi, Z., and Zhanting, D., 1998. *Extractive Distillation with salt in solvent*, Journal of Chemical Engineering of Japan, Vol. 22, p. (1 – 6)

Sada, E., Morisue, T., and Yamaji, H., 1975. *Salt effect on isobaric vapour-liquid equilibrium of isopropanol-water system,* The Canadian of Chemical Engineering, Vol. 53, p. (350 – 353)

Sandler, S.I., 1999. *Chemical and Engineering Thermodynamics*, third ed., John Wiley and Sons, New York

Seiler, M., Jork, C., Kavarnon, A., Arlt, W., Hiresh, R., 2001. *Separation azeotorpic mixtures using ionic liquids,* AIChE Journal, Vol. 50, No. 10, p. (2439 – 2454)

Sevgili, L. M and Senol, A., 2006. *Isobaric (vapour + liquid) equilibrium for (2-propanol + water + ammonium thiocyanate): Fitting the data by an empirical,* Journal Chemical Thermodynamics, Vol. 38, p. (1539 – 1545)

Shao, P., and Huang, R.Y.M., 2006. *Review of polymeric membrane pervaporation,* Journal of Membrane Science, Vol. 143, P. (1 – 18)

Slusher, J. T., Decker, K. J., Liu, H., Vega, C. A., Cummings, P. T., O'Connell, J. P., 1994. *Vapour-liquid equilibria and salt apparent molar volumes of the water + 2-*

propanol + tetrabutylammonium bromide system, Journal of Chemical Engineering Data, Vol. 39, p. (506 – 509)

Smith, R., 1995. *Chemical Process Design*, McGraw-Hill, Inc

Smith, J. M., Van Ness, H. C., Abbott, M. M.**,** 2001. *Introduction to Chemical Engineering Thermodynamics*, Sixth Edition, McGraw-Hill International Edition

Sommer, S., Melin, T., 2000. *Zeolite membranes in chemical industry*, in the 2000 18th Annual Membrane Technology/Separation Planning Conference, Boston, Massachusetts, USA.

Sun, R. Y., 1999. *Molecular thermodynamics of salt effect in vapour-liquid equilibrium of ethanol-water system,* Fluid Phase Equilibria, Vol. 157, p. (29 – 40)

Sun, T., Bullock, K. R., and Teja, A. S., 2004. *Correlation and prediction of salt effects on vapour-liquid equilibrium in alcohol-salt-salt systems,* Fluid Phase Equilibria, Vol. 219, p. (257 – 264)

Swietoslawski, W., 1963. *Azeotropy and polyazeotropy*, Oxford Pergamon Press

Tan, T. C., 1987. *Model for predicting the effect of dissolved salt on the vapour liquid equilibrium of solvent mixtures,* Chemical Engineering Residence Desilation, Vol. 65, p. (355 – 367)

Tarakad, R. R., Danner, R. P., 1977. *An improved corresponding states method for polar fluids: Correlations of Second Virial Coefficients,* American Institute of Chemical Engineers Journal, Vol. 23, p. (685 – 695)

Teplyakov, V.,1991. *Membrane gas separation in petrochemistry: Problem of the polymeric membrane selection*, In: "Effective Industrial membrane Processes: Benefits and Opportunities" Elsevier Science Publishers, p. (401 – 415)

Teng, M-Y., Lee, K-R., Liaw, D-J., Lai, J-Y., 2000. *Preparation and pervaporation performance of poly(3-alkylthiophene) membrane,* Polymer, Vol. 41, p. (2047 – 2052)

Thoma, S., Resch, A., Voelz., 1998. *Pervaporation:* Case Study, p. (1 – 11)

Thongsukmak, A., Sirkar, K. K., 2008. *Extractive pervaporation to separate ethanol from its dilute aqueous solutions characteristics of ethanol-producing fermentation processes,* Journal of Membrane Science, Vol. 28, p. (1 – 44)

Tsonopoulos, C., 1974. *An Emperical Correlation of Second Virial Coefficients,* American Institute of Chemical Engineers Journal, Vol. 20, p. (263 – 272)

Tsuboka, T., Katayama, T., 1975. *Modified Wilson Equation for Vapour-Liquid and Liquid-Liquid Equilibria,* Journal of Chemical Engineering of Japan, Vol. 8, p. (181 – 187)

Vane, L. M., 2005a. *Pervaporation-Membrane process for bioethanol recovery, solvent dehydration and contaminant removal,* Case study, p. (1 – 5)

Vane, L. M., 2005b. *A review of pervaporation for product recovery from recovery from biomass fermentation processes,* Journal Chemical Technology. Biotechnology, Vol. 80, p. (603 – 629)

Van Ness, H. C., 1959. *Exact forms of the coexistence equation for binary vapour-liquid equilibrium,* American Institute of Chemical Engineers. Journal, Vol. 16, p. (18 – 22)

Van Ness, H. C., 1995. *Thermodynamics in the treatment of vapour/liquid equilibrium (VLE) data,* Pure and Applied Chemistry, Vol. 67, p. (859 – 872)

Van Ness, H. C., Abbott, M. M, 1982. *Classical Thermodynamics of nonelectrolyte solutions: With Applications to Phase Equilibria,* McGraw-Hill, New York.

Van Ness, H. C., Byer, S. M., Gibbs, R. E., 1973. *Vapour-liquid equilibrium: Part I. An appraisal of data reduction methods,* American Institute of Chemical Engineers Journal, Vol. 19, p. (238 – 244)

Verhoef, A., Figoli, A., Leen, B., Bettens, B., Drioli, E., Van der Bruggen, B., 2008. *Perfomance of a nanofiltration membrane for removal of ethanol from aqueous solutions by pervapoaration*, Separation and Purification Technology, Vol. 60, p. (54 – 63)

Volkov, V. V., 1994. *Reviews separation of liquids by pervaporation through polymeric membranes*, Russian Chemical Bulletin, Vol. 43, No. 2, p. (208 – 219)

Walas, S. M., 1985. *Phase Equilibrium in Chemical Engineering*, Butterworth, Boston

Wang, X-P., Feng, Y-F., Shen, Z-Q., 2000. *Pervaporation properties of a three-layer structure composite membrane*, Journal of Applied Polymer Science, Vol. 75, No. 6, p. (740 – 745)

Wang, L., Li, J., Lin, Y., Chen, C 2007. *Separation of dimethyl carbonate/methanol mixtures by pervaporation with poly(acrylic acid)/poly (vinyl alcohol) blend membranes*, Journal of Membrane Science, Vol. 305, p. (283 – 246)

Watson, J. M., and Payne, P. A., 1990. *A study of organic compound pervaporation through silicone rubber*, Journal of Membrane Science, Vol. 49, p. (171 – 205)

Weast, R. C., 1983-1984. *CRC Handbook of chemistry and physics*, CRC Press

Wesslein, M., Heintz, A., Lichtenthaler, R. N., 1990. *Pervaporation of liquid mixtures through poly (vinyl alcohol) (PVA) membranes II. The binary systems methanol/1-propanol and methanol/dioxane and the ternary system water/methanol/1-propanol*, Journal of Membrane Science, Vol. 51, p. (181 – 188)

Wessling, M., Werner U., Hwang, S-T., 1991. *Pervaporation of aromatic C_8- isomers*, Journal of Membrane Science, Vol. 57, p. (257 – 270)

Wilson, G. M., 1964. *Vapour-Liquid Equilibrium. XI: A New Expression for the Excess Free Energy of Mixing*, Journal of the American Chemical Society, Vol. 86, p. (127 – 130)

Wisniak, J., Tamir, A., 1978. *Mixing and excess thermodynamic properties.* A literature source book, Elsevier Scientific Publishing Company, Amsterdam

Xu, y., Chen, C., Zhang, P., Sun, B., Li, J., 2006. *Pervaporation properties of polyimide membranes for separation of ethanol + water mixtures*, Journal of Chemical Engineering data, Vol. 51, p. (1841 – 1845)

Yampolskii, Y. P., Volkov, V. V., 1991. *Studies in gas permeability and membrane gas separation in the Soviet Union*, Journal of Membrane Science, Vol. 64, p. (191 – 228)

Yuzhong, Z., Keda, Z., Jiping, X., 1993. *Preferential sorption of modified PVA membrane in pervaporation,* Journal of Membrane Science, Vol. 80, p. (297 – 308)

Zhigang, L., Biaohua, C., Zhongwei, D., 2005. *Special distillation process*, British Library, ELSEVIER

Zhigang, L., Chengyne, L., Biashua, C., 2003. *Extractive distillation: A review,* Separation and Purification reviews, Vol. 32, No. 2, p. (121 – 213)

Zhigang, L., Hongyou, W., Rongqi, Z., Zhanting, D., 2002.*Influence of salt added to solvent on extractive distillation,* Chemical Engineering Journal, Vol. 87, p. (149 – 156)

Appendix A

LOW PRESSURE VLE CALCULATION METHODS

Ideal system or ideal solution

The assumption of ideal systems i.e. ideal gas and ideal solution provide useful models that serve as a standard to which real systems can be compared. Ideal solution is a solution that obeys Raoult's law. An ideal gas is a model gas comprising imaginary molecules of zero volume that were not interact. Consider at a low pressure (pressure below 1 bar) all the intermolecular forces are approximately the same. Treat the vapour as an ideal gas and liquid as an ideal solution. The fugacity coefficient in the liquid phase is approximately equal to the fugacity coefficient in the vapour phase, from the Lewis/Randall reference state;

$$\hat{\varphi}_i = \varphi_i^o \tag{A.1}$$

and as the vapour is treated as ideal the Poynting factor $\left[\exp\left(\frac{1}{RT}\int v_i^l dP\right)\right]$ is approximately unity at lower pressure and the equation can be simplified as:

$$y_i P = x_i f_i \tag{A.2}$$

Applying equation for the pure species fugacity, it becomes:

$$y_i P = x_i P_i^{sat} \tag{A.3}$$

this equation is known as Raoult's law

Non ideal system or liquids

Real system follow Raoult's law, if there is form of chemical interaction between the component a and b (e.g., a-ethanol and b-water). Since it unlikely that a-a interaction is identical to the a-b interaction. Consider the behavior of some real binary systems for low pressure for the vapour phase to be ideal gas. The case where the like (a-a and b-b)

interaction is stronger than the unlike (a-d) interaction ($\gamma_i > 1$) as well as when the like interaction is weaker ($\gamma_i < 1$). If the vapour phase is non ideal then use fugacity coefficient and if the liquid phase is nonideal then use activity coefficient. The following equation applies:

$$y_i \hat{\varphi}_i^v P = x_i \gamma_i^l f_i^o \tag{A.4}$$

and, from the Lewis/Randall reference state;

$$f_i^o = f_i \tag{A.5}$$

Assume that the vapour phase can be represented as an ideal gas and the fugacity of the pure liquid is given by P_i^{sat}. Therefore, the VLE behavior for weakly associating systems can be described with the required accuracy by the following simplified equation:

$$x_i \gamma_i P_i^{sat} = y_i P \tag{A.6}$$

The vapour pressure of pure component i at the system is calculated from Antoine equation which is:

$$\log P^{sat}(kPa) = A - \frac{B}{C + T(^0C)} \tag{A.7}$$

The binary system that has low volatile is known as azeotropic mixture and the composition are reversible. Azeotropic occurs where the composition of vapour and liquid are equal. The relationship for the partition coefficient, K_j or VLE ratio is defined by: $K_i = \frac{y_i}{x_i} = \frac{\gamma_i P_i^{sat}}{P}$ (A.8)

The separation factor or the ratio of the K-value of two species is called the relative volatility, α_{ij}. It can be derived by:

$$\alpha_{ij} = \frac{K_i}{K_j} = \frac{\gamma_i P_i^{sat}}{\gamma_j P_j^{sat}} \tag{A.9}$$

In the case of azeotropic system, no separation of ethanol/water could be achieved therefore $\alpha_{ij} = 1$. The systems where the difference $\alpha_{ij} - 1$ the separation factor is close to unity, then a large number of theoretical stages are required and a special distillation process has to be used.

Liquid mixture

For liquid mixture in equilibrium with its vapour, the following three conditions must be met:

- The temperature of liquid and vapour must be equal for there to be thermal equilibrium
- The pressure must be equal for there to be mechanical equilibrium.
- The Gibbs free energy must be at a minimum with respect to a transfer of any component from liquid to gas or gas to liquid.

Phase rule

The conditions for there to be equilibrium between two or more phases are the pressure P, the temperature T, and chemical potential or fugacity of each substance $:_i$ shall have the same value in every phase or the intensive state of PVT system is established when its temperature, pressure and the compositions of all phases are fixed. However, for equilibrium state these variables are not all independent and fixing a limited number of them automatically establishes the others. This number of independent variable is given by phase rule and its called the number of degrees of freedom of the system. It is the number of variable which may be arbitrarily specified and which must be specified in order to fix the intensive state of a system at equilibrium. This number is the difference between the number of variables needed to characterize the system and the number of equations that may be written connecting these variables. For a system containing N chemical species distributed at equilibrium among π phases. The phase rule variable are temperature, pressure, presumed uniform throughtout the system and N – 1 mole fractions in each phase. The number of these variables is $2 + (N - 1)\pi$**.** The masses of the

phase are not phase rule variable because they have nothing to do with the intensive state of the system. The Duhem's theorem is another rule similar to the phase rule, but less celebrated. It applies to closed systems at equilibrium for which the extensive state as well as the intensive state of the system is fixed. Duhem's theorem is stated as follows: for any closed system formed initially from given masses of prescribed chemical species, the equilibrium state is completely determined when any two independent variables are fixed. The equations that may be written connecting the phase rule variables are:

$$\mu_i^{\alpha} = \mu_i^{\beta} .....\mu_i^{\pi} \tag{A.10}$$

for each species, *i* giving $(\pi - 1)N$ phase equilibrium state

$$\sum_i \mu_i dn_i = 0 \tag{A.11}$$

for each independent chemical reaction, giving r equations. The total number if independent equations are therefore $(\pi - 1)N + r$. In their fundamental forms these equations relate chemical potentials which are functions of temperature, pressure and composition of the phase rule variable. Since the degree of freedom of the system, F is the difference between the number of variable and the number of equations:

$$F = 2 + (N - 1)\pi - (\pi - 1)N - r \tag{A.12}$$

or

$$F = 2 - \pi + N - r \tag{A.13}$$

The number of independent chemical reactions r can be determined as follows:

- Write formation reactions from the elements for each chemical compound present in the system.
- Combine these reaction equations so as to eliminate from the set all elements not present as elements in the system.

The Phase Equilibrium Computation

The fundamental principles of phase equilibrium so far discussed can be applied in some important VLE calculations. These can be applied to both ideal and nonideal chemical system involving binary or multi-component mixture. The basic equation for VLE:

$$\left(\frac{f}{P}\right)_i . P . y_i = P_i x_i \gamma_i \qquad \text{(A.14)}$$

These are applicable to in all case.

Ideal system

Ideal systems have both fugacity and activity coefficient equal to unity or equal to 1, $\left(\frac{f}{P}\right)_i = \gamma_i = 1$. The general expression for VLE simplifies down to: $Py_i = P_i x_i$, this is known as Raoult's Law. This relationship is used in the calculation of bubble point and dew point.

The Bubble Point Calculations

Bubble point calculations were performed when the liquid phase composition (all the x_i's) is known and the vapour composition (the y_i's) are required to calculate as well as bubble point temperature or pressure. The steps in the trial and error procedure are as follows according to Smith and Van Ness (1987). There are two types of bubble point calculations

- Bubble point temperature calculations: when the liquid composition and system pressure (P) are known.
- The bubble point pressure calculations: when the liquid composition and system temperature (T) are known

The bubble point temperature calculations: for an ideal system of known liquid composition (the x_i's) and at given pressure, P, the bubble point temperature (T_B) can be determined graphically from T-x-y diagram (T_B is read off the T vs x curve at the specified P) or analytically by using the equation: $Py_i = P_i x_i$

Rearranging equation to: $y_i = \left(\frac{P_i}{P}\right) x_i$ (A.15)

Since the sum of the P_i^{sat} entire component in the vapour phase is unity or equal to 1.

$$\sum_{i=1}^{N} y_i = \sum_{i=1}^{N} \left(\frac{P_i}{P}\right) x_i = 1 \quad \text{(A.16)}$$

where: N = number of components

P = pressure being constant

$$P = \sum_{i=1}^{N} P_i x_i \quad \text{(A.17)}$$

This equation has only one unknown parameter and that one is the temperature – since the vapour pressure of pure component are functions only of temperatures (T). These equations equation can be solved analytically for T provided and the Antoine type expression correlating vapour pressure with temperature.

The routine calculation follows the steps outlined belows by Smith *et al*. (2001):

- Assume a suitable temperature (T).
- Calculate the vapour pressure P_i of each component at the assumed temperature (T) or look up at the vapour pressure vs temperature plot to find the Pj of each component.
- Calculate the total pressure: $P^{cal} = \sum_{i=1}^{NC} P_i x_i$ which depends only on temperature.
- Check whether the calculated value of total pressure (P^{cal}) is sufficiently close to the actual system pressure. If the margin is small enough then assume another temperature is the acceptable. If P^{cal} is greater than P, then a second set of approximation (with lower value of T) is required and the procedure is to repeat.

The Dew Point Calculations

- The dew point temperature calculations: when the vapour composition (the y_i's) and system pressure (P) are known.
- The dew point pressure calculations: when the vapour composition (the y_i's) and system temperature (T) are known

Both calculations are based on the equation: $x_i = \left(\frac{P}{P_i}\right) y_i$. Since sum of all mole fraction term is liquid phase is unity or equal to 1.

$$\sum_{i=1}^{N} x_i = \sum_{i=1}^{N}\left(\frac{P}{P_i}\right) y_i = 1 = P\sum_{i=1}^{N}\left(\frac{y_i}{P_i}\right) \qquad \text{(A.18)}$$

Therefore $$P = \frac{1}{\sum_{i=1}^{N}\left(\frac{y_i}{P_i}\right)} \qquad \text{(A.19)}$$

This equation has only one unknown variable and that one is either pressure (if the system temperature is given) or temperature (if the system pressure is given). Dew point temperature calculations: this is to be done by trail and error method converging on the correct temperature. The system pressure, P, is given and all the y_j's are known.

The working procedure follows

Assume a suitable temperature value of temperature.

Determine the vapour pressure of the components at this temperature.

Put these vapour pressure data in the $P = \frac{1}{\sum_{i=1}^{N}\left(\frac{y_i}{P_i}\right)}$ to calculate the total pressure, P^{cal}

Check whether P^{cal} is sufficient close to P. if the P^{cal} is too far from P, switch over to second set of approximation, assume T again and repeat the process all over again.

Nonideal System

The equation: $Py_i = P_i x_i$ does not work well for nonideal systems, as they do not obey Raoult's Law. The equation $\left(\frac{f}{P}\right)_i . P . y_i = P_i x_i \gamma_i$ can still be use for bubble point and dew point calculations, provided the activity coefficients are available.

Bubble Point Calculations

The above equation can be rearranged to: $y_i\left(\frac{f}{P}\right)_i = \left(\frac{P_i}{P}\right) x_i \gamma_i$. Assuming the gas phase behavior is close to ideality $|f/P|_j = 1$ and hence the equation becomes $y_i = \left(\frac{x_i P_i}{P}\right)\gamma_i$. The values of activity coefficient of individual components must be available. The working procedure for bubble point calculation for nonideal system is similar to that used in the ideal case.

$$\text{Since} \sum_{i=1}^{N} y_i = 1, \quad and \quad \sum_{i=1}^{N}\left(\frac{x_i P_i}{P}\right)\gamma_i = 1 \tag{A.20}$$

$$\text{Therefore } P = \sum_{i=1}^{N} P_i x_i \gamma_i \tag{A.21}$$

The working procedure follows

- Assume a suitable temperature (T).
- Calculate the vapour pressure P_i of each component at the assumed temperature (T) from Antoine type equation or look up at the vapour pressure vs temperature plot.
- Calculate the total pressure: $P^{calc} = \sum_{i=1}^{N} P_i x_i \gamma_i$ (A.22)
- Check whether the calculated value of total pressure (P^{cal}) is sufficiently close to the actual system pressure. If not, then assume another temperature unit converged.

If K – values are used the bubble point calculation can be made on basis of following equation: $y_i = K_i x_i$

Therefore: $\sum_{i=1}^{N} y_i = \sum_{i=1}^{N} K_i x_i = 1$ (A.23)

Where K_i = distribution coefficient for component i

It is function of temperature, pressure and compositions

Working Procedure as follows

- Assume a suitable temperature (T).
- Determine the K – values of all component (De Priest chart)
- Check whether the $\sum_{i=1}^{N} K_i x_i = 1$. If sum of $K_i x_i$ term is unity or 1, the correct temperature has been assumed, if not repeat the procedure by assuming another temperature.

The Dew Point Calculations

The dew point calculation is more difficult than bubble point calculations. It is requires the process of iteration to determine the activity coefficient for the components as much as the liquid compositions of the components are known.

The working procedure follows

- Assume a suitable temperature (T).
- Calculate the vapour pressure P_i of each component at the assumed temperature (T) from Antoine type equation or look up at the vapour pressure vs temperature plot.
- Determines the x_i's
- Use the valves of x_i through the process of iteration to calculate new activity coefficients

Appendix B

B1. Antoine constant, critical values and equations

The vapour pressure of pure component *i* at the system was calculated from Antione equation which is:

$$\log P^{sat}(kPa) = A - \frac{B}{C + T(^0C)} \qquad \text{(B.1)}$$

where: A, B, and C are constant of the component i

T = temperature (^{0}C) of the system

Table B1: Antoine coefficients (Perry and Green, 1997).

Component	**A**	**B**	**C**
Acetone [C_3H_6O]	7.63132	1566.69	273.419
Water	8.01767	1715.70	234.268
Ethanol [C_2H_6O]	8.20417	1642.89	230.3

Table B2: Pure component liquid molar volumes (Poling *et al.*, 2001).

Component	**V^L (cm^3/gmol)**
Water	18.07
Ethanol	58.68

Table B3: Critical values and acentric factors for selected component (Poling *et al.*, 2001).

Component	T_c (K)	P_c (kPa)	V_c (cm^3/gmol)	z_c	ω
Water	647.3	22120	57.1	0.235	0.344
Ethanol	513.9	6140	167.1	0.240	0.644

Where: J_i = is the permeation flux through the membrane

L = is the membrane thickness

P_i^G = is the separation permeability coefficient.

Appendix C

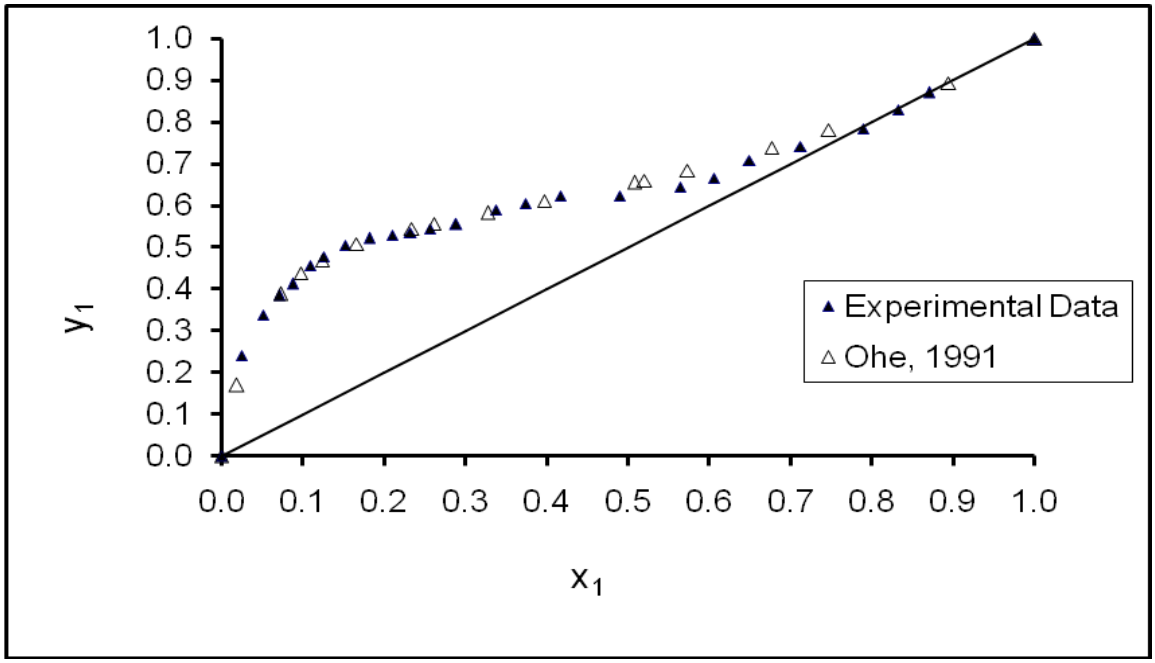

Figure C1: VLE still calibration with ethanol (1) –water (2) system at 100 kPa with no salt.

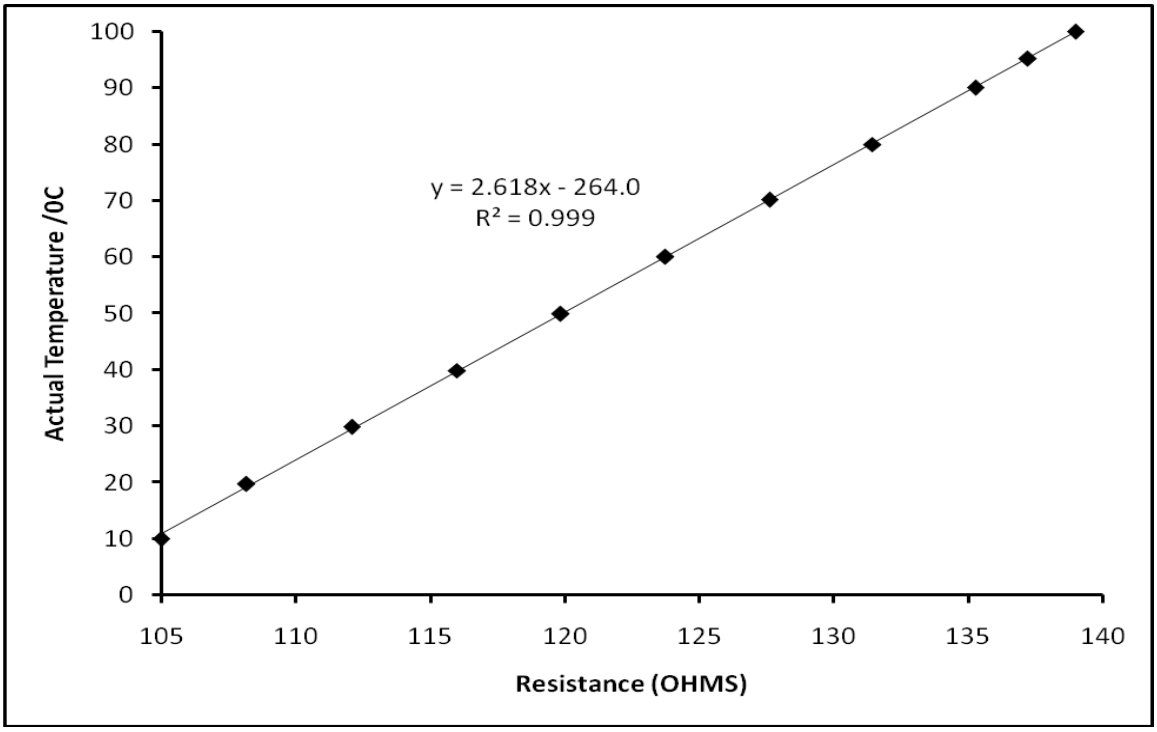

Figure C2: Temperature probe calibration for the VLE still.

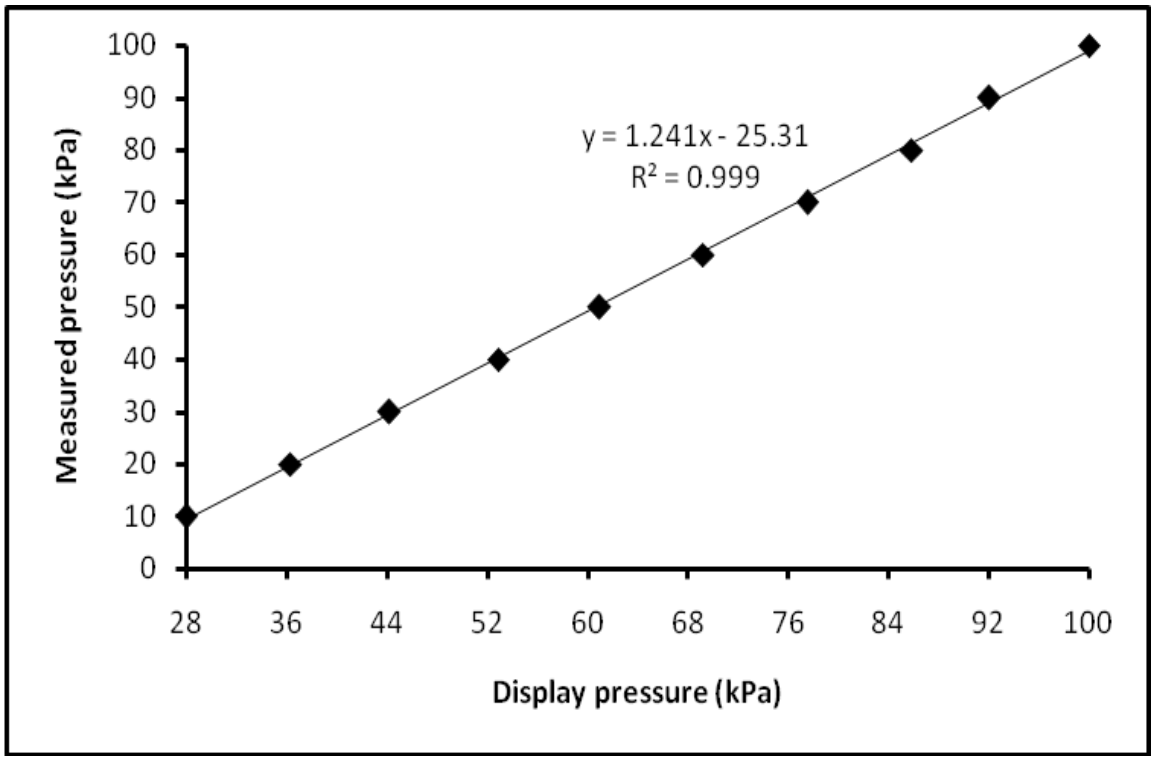

Figure C3: Pressure transducer calibration for the VLE still.

GAS CHROMATOGRAPHY HP 5890 SERIES II CALIBRATION

Table C1: GC HP 5890 SERIES II OPERATING PARAMETERS.

Parameter	**Values**	**Units**
Column Temperature	453.15	K
Injector Temperature	493.15	K
Detector Temperature	493.15	K
Gas Pressure (Helium)	150	kPa

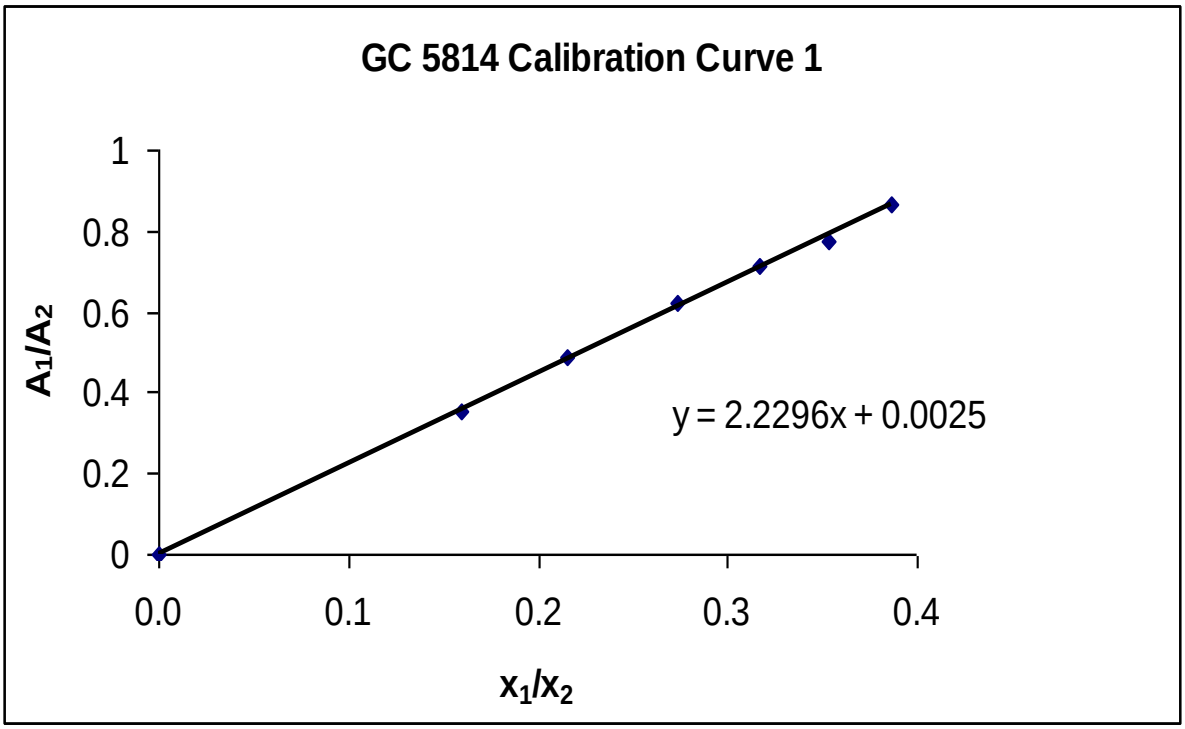

Figure C4: GC HP 5890 series II calibration with ethanol (1) and water (2) (Concentration ethanol).

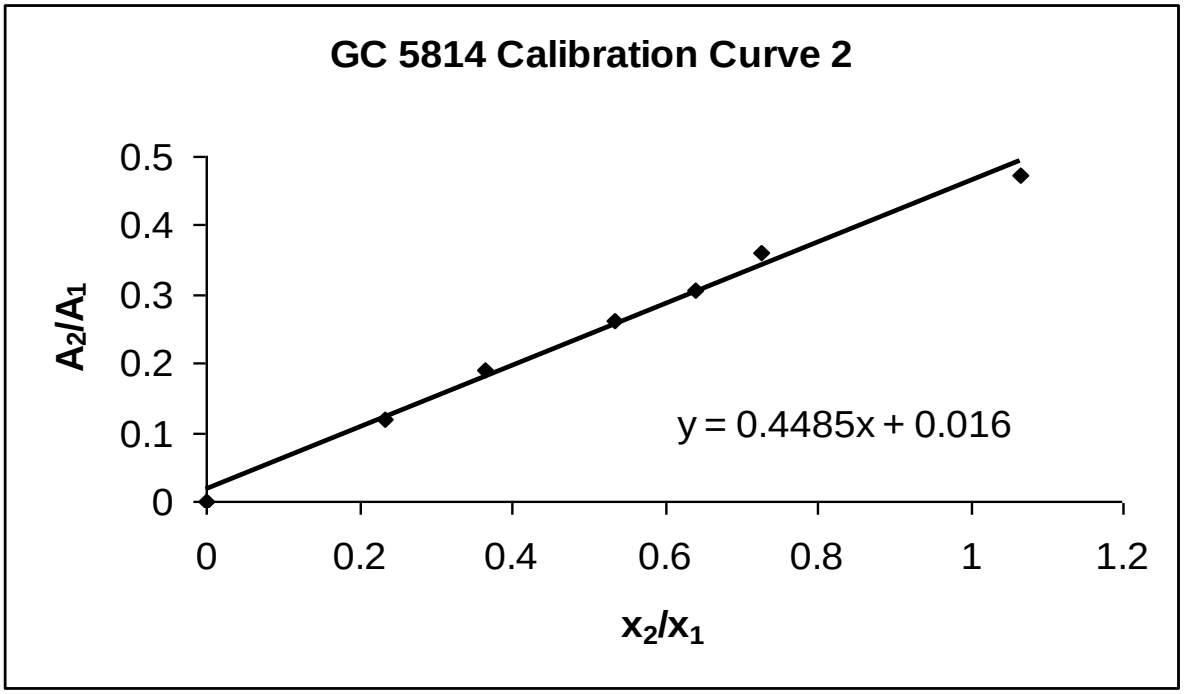

Figure C5: Inverse GC HP 5890 series II calibration with ethanol (1) and water (2) (Diluted ethanol).